

April 2017

Developing a Multiplexing Assay System for the Quality Control of Cell Therapy Products

Amishi Vairagade

Worcester Polytechnic Institute

Julia Michelle Smith

Worcester Polytechnic Institute

Thai Thanh Trinh

Worcester Polytechnic Institute

Follow this and additional works at: <https://digitalcommons.wpi.edu/mqp-all>

Repository Citation

Vairagade, A., Smith, J. M., & Trinh, T. T. (2017). *Developing a Multiplexing Assay System for the Quality Control of Cell Therapy Products*. Retrieved from <https://digitalcommons.wpi.edu/mqp-all/4125>

This Unrestricted is brought to you for free and open access by the Major Qualifying Projects at Digital WPI. It has been accepted for inclusion in Major Qualifying Projects (All Years) by an authorized administrator of Digital WPI. For more information, please contact digitalwpi@wpi.edu.

Developing a Multiplexing Assay System for the Quality Control of Cell Therapy Products

A Major Qualifying Project Report:

Submitted to the Faculty of the Worcester Polytechnic Institute

In partial fulfillment of the requirements of the Degree of Bachelor of Science

By:

Julia Smith

Thai Trinh

Amishi Vairagade

April 27, 2017

Prof. Kristen Billiar, Ph.D., WPI

Prof. Edward Clancy, WPI

This report represents the work of WPI undergraduate students submitted to the faculty as evidence of completion of a degree requirement. WPI routinely publishes these reports on its website without editorial or peer review. For more information about the projects program at WPI, please see <http://www.wpi.edu/academics/ugradstudies/project-learning.html>.



WPI



Abstract

When used for autologous transplant, mesenchymal stem cells require extensive quality control (QC) before being reintroduced into the body. One standard method of QC is biological assays, which are a manually completed laboratory test for determining the concentration of foreign substances in a cell culture solution. Biological assays have a number of limitations including time, cost, and level of manual involvement. With these limitations in mind, a proof-of-concept device was developed to show the potential for an automated multiplexed assay device for QC. This prototype device design can accurately intake and dispense reagent volumes necessary for the completion of two assays, in a range between 50 and 350 μL . The device is also capable of providing the required temperature environment for each step of the assay process, changing between room temperature (24 °C) and 65 °C in under five minutes.

Table of Contents

Abstract	1
Table of Tables	8
Authorship Page.....	9
1 Introduction	11
2 Background	14
2.1 Regenerative Medicine	14
2.2 Stem Cells.....	14
2.2.1 Mesenchymal Stem Cells (MSCs)	14
2.3 Applications of MSCs.....	15
2.3.1 Therapeutic Applications	15
2.3.2 Autologous Transplant Therapy.....	15
2.4 MSC Quality Control for Autologous Transplant	16
2.4.1 Toxin Detection Assays	16
2.4.2 Residual Cell Culture Material Assays	17
2.4.3 Limitations of Quality Control	18
3 Project Strategy.....	20
3.1 Initial Client Statement	20
3.2 Design Requirements	20
3.2.1 Objectives.....	20
3.2.2 Engineering Standards	21
3.3 Revised Client Statement.....	22
3.4 Project Management Approach.....	22
3.4.1 Gantt Chart.....	23
3.4.2 Scrum Methodology: Daily Stand-up Meetings	25
3.4.3 Weekly Client Meetings	25
3.4.4 Trello Board.....	25
4 Design Process	26
4.1 Needs Analysis	26
4.1.1 Clinical/Patient Need	26
4.1.2 Client Need.....	27
4.1.3 Device Requirements	27

4.2	Alternative Designs	28
4.2.1	Ideal System Architecture	28
4.2.2	Assay Plate	29
4.2.3	Microcontroller	30
4.2.4	Fluid Control.....	33
4.2.5	Temperature Control	38
4.2.6	Heat and Fluid Controller Driver	42
4.2.7	Control Mechanism.....	43
4.3	Feasibility Studies and Experimental Modeling	45
4.3.1	Fluidic Control System Modeling	45
4.3.2	Temperature Control System Modelling	47
4.4	Final Design Approach	54
4.4.1	Prototype Architecture	54
4.4.2	Assay Selection.....	54
4.4.3	Fluid Control.....	56
4.4.4	Temperature Control	59
4.5	Pretotype Design.....	61
5	Design Verification	64
5.1	Assay Experimentation	64
5.1.1	Mycoplasma Baseline Assay Experiment	64
5.1.2	BSA Baseline Assay Experiment	67
5.2	Fluidic Control Experimentation	68
5.2.1	Syringe Pump Calibration Curve Determination Experiment	68
5.2.2	Syringe Pump with Manifold: Dead Volumes Experiment.....	70
5.2.3	Syringe Pump with Manifold: Intake Accuracies Experiment	71
5.2.4	Syringe Pump with Manifold and Air Pump: Output Volume Loss Experiment	72
5.2.5	Cross Contamination Experiment	73
5.2.6	BSA Assay Run: Water Trial Experiment	74
5.3	Temperature Control Experimentation	76
5.3.1	Heating from Room Temperature to 65° C Experiment	76
5.3.2	Cooling from 65 °C to Room Temperature (24 °C) Experiment	78
5.3.3	Temperature Control System Cooling Experiment	79

6	Design Validation	81
6.1	Prototype Validation: BSA Assay Run with System.....	81
6.2	Prototype Validation: Mycoplasma Assay Run with System	82
7	Discussion.....	84
7.1	Fluidic Control System Discussion.....	84
7.2	Temperature Control System Discussion.....	85
7.3	Potential Project Impacts.....	86
7.3.1	Economics	86
7.3.2	Environmental Impact.....	86
7.3.3	Societal Influence	86
7.3.4	Political Ramifications	86
7.3.5	Ethical Concerns.....	86
7.3.6	Health and Safety Issues	87
7.3.7	Manufacturability	87
7.3.8	Sustainability.....	87
8	Conclusions and Recommendations	88
9	References	90
	Appendices.....	93
	Appendix A: Potential Pretotype Brochure.....	93
	Appendix B: R&D Systems Mycoprobe Mycoplasma Detection Assay Kit Procedure	96
	Appendix C: MyBioSource BSA Detection Assay Procedure	101
	Appendix D: Syringe Pump Calibration Curve Determination Experiment (Full)	108
	Appendix E: Syringe Pump with Manifold: Dead Volumes Experiment (Full)	116
	Appendix F: Syringe Pump with Manifold: Intake Inaccuracies Experiment (Full)	128
	Appendix G: Syringe Pump with Manifold and Air Pump: Output Volume Loss Experiment (Full).....	130
	Appendix H: BSA Water Trial Experiment: Full	133
	Appendix I: System BSA Assay Experiment Data	135
	Appendix J: System Mycoplasma Experiment Data.....	136

Table of Figures

FIGURE 1 PROJECT GANTT CHART	24
FIGURE 2 ARCHITECTURE DRAWING OF IDEAL SYSTEM BREAKDOWN	29
FIGURE 3 ARDUINO MEGA 2560 MICROCONTROLLER BOARD	31
FIGURE 4 TEXAS INSTRUMENTS 16-BIT MICROCONTROLLER BOARD	32
FIGURE 5 PERISTALTIC PUMPING MECHANISM.	33
FIGURE 6 TORQUE-ACTUATED PUMP	34
FIGURE 7 TYPICAL OTS AUTOMATED SYRINGE PUMP.	35
FIGURE 8 ACTUONIX P16 LINEAR ACTUATOR CHOSEN FOR SYRINGE PUMP RETRIEVED FROM HTTPS://S3.AMAZONAWS.COM/ACTUONIX/ACTUONIX+P16+DATASHEET.PDF	36
FIGURE 9 NRESEARCH SOLENOID VALVE MANIFOLD	37
FIGURE 10 COOLDRIE ONE SINGLE VALVE DRIVERS	38
FIGURE 11 KAPTON HEATER	39
FIGURE 12 POTENTIAL HEATING SYSTEM CREATED BY TRT TEAM	39
FIGURE 13 PELTIER TEC MODULE	40
FIGURE 14 TEMPERATURE SENSOR RETRIEVED FROM WWW.GOOGLE.COM/SEARCH?Q=LM35&RLZ=1C1CHFX_ENUS608US608&SOURCE=LNMS&TBM=ISCH&SA=X &VED=0AHUKEWIZVCR70ZRTAHVM2SYKHTGXDFQAQ_AUIBIGB&BIW=1270&BIH=633#IMGRC=DCXCZGTS1ZYA MM:	41
FIGURE 15 MC33926 MOTOR DRIVER SHIELD FOR ARDUINO MICROCONTROLLER BOARD	43
FIGURE 16 PID CONTROL LOOP	44
FIGURE 17 NRESEARCH VALVE MANIFOLD TECHNICAL DRAWING	46
FIGURE 18 TRANSIENT RESPONSE: HEAT INPUT AND CONVECTION OF ALUMINUM VS. COPPER	49
FIGURE 19 TRANSIENT COOLING RESPONSE OF ALUMINUM VERSUS COPPER	50
FIGURE 20 THERMAL CIRCUIT OF ALUMINUM SHEET WITH POLYSTYRENE WELL	51
FIGURE 21 THERMAL CIRCUIT OF A MACHINED ALUMINUM BAR AND POLYSTYRENE WELL	52
FIGURE 22 PROTOTYPE ARCHITECTURE	54
FIGURE 23 FLUID CONTROL SYSTEM CONSISTING OF SYRINGE PUMP AND SOLENOID VALVE MANIFOLD	56
FIGURE 24 SCHEMATIC SHOWING CONTROL OF SYRINGE PUMP AND VALVE MANIFOLD SYSTEM	57
FIGURE 25 FLUIDIC CONTROL SUBSYSTEM DETAILED SCHEMATIC	58
FIGURE 26 PROTOTYPE TEMPERATURE CONTROL SYSTEM ARCHITECTURE DRAWING	59
FIGURE 27 IMAGE OF ENTIRE TEMPERATURE CONTROL SYSTEM	59
FIGURE 28 TEMPERATURE CONTROL SYSTEM SCHEMATIC	60
FIGURE 29 TEMPERATURE CONTROL SUBSYSTEM DETAILED SCHEMATIC	61
FIGURE 30 SOLIDWORKS DRAWING OF POTENTIAL ASSAY DEVICE (LEFT) AND POTENTIAL ASSAY DEVICE INTEGRATED INTO A LAB BENCH SETTING (RIGHT)	62
FIGURE 31 MYCOPLASMA ASSAY INITIAL RUN RESULT WELLS.	65
FIGURE 32 MYCOPLASMA ASSAY SECONDAY RUN RESULT WELLS.	66
FIGURE 33 INITIAL BSA ASSAY STANDARD DILUTION CURVE COMPARE TO MANUFACTURER EXAMPLE	67
FIGURE 34 INITIAL BSA ASSAY RESULT WELLS. DESCENDING CONCENTRATION FROM	68
FIGURE 35 BASELINE BSA ASSAY STANDARD DILUTION CURVE (LEFT) AND BSA RESULTANT WELLS (RIGHT) WITH CONCENTRATION DESCENDING FROM TOP RIGHT WELL (30,000 NG/ML) TO BOTTOM RIGHT (0NG/ML)	68
FIGURE 36 GRAPH OF OUTPUT VOLUME VS. LINEAR ACTUATOR DISTANCE DATA FROM ALL EXPERIMENTAL ITERATIONS WITHOUT OUTLIERS (LEFT). GENERATED CALIBRATION CURVE FROM ALL ITERATION DATA WITH OUTLIERS REMOVED (RIGHT)	70

FIGURE 37 VOLUME OUTPUT COMPARISON BETWEEN SYSTEM WITH AND WITHOUT MANIFOLD	71
FIGURE 38 RESULTS OF SYSTEM INTAKE EXPERIMENT: GOAL INTAKE VS. ACTUAL INTAKE (LEFT). CHANGE IN INTAKE VOLUME VS. GOAL VOLUME INTAKE (RIGHT)	72
FIGURE 39 DISTRIBUTION OF VOLUME LOST WITH AIR PUMP INTEGRATION (LEFT) AND DISTRIBUTION OF VOLUME LOST WITH NO AIR PUMP (RIGHT).....	73
FIGURE 40 TOP VIEW OF CONTAMINATED WELLS (LEFT). SIDE VIEW OF CONTAMINATED WELLS (RIGHT)	74
FIGURE 41 DISTRIBUTION OF VOLUMES REQUESTED VS. ACTUAL VOLUME OUTPUT FOR FOUR VOLUMES	75
FIGURE 42 HEATING FROM RT TO 65°C WITH 80X80MM ATTACHED HEAT SINK	77
FIGURE 43 SIMULATED AND EMPIRICAL DATA FOR TRANSIENT HEATING OF THE SYSTEM	77
FIGURE 44 COOLING FROM 65°C TO ROOM TEMPERATURE WITH 80X80MM HEAT SINK (LEFT) AND SYSTEM COOL FROM 65°C TO ROOM TEMPERATURE WITH 60X60MM HEAT SINK (RIGHT).....	79
FIGURE 45 COOLING STABILITY GRAPH OF COOLING THE SYSTEM FROM 60 °C TO 24 °C.....	79
FIGURE 46 COMPARISON OF BASELINE ASSAY TEST RESULTS AND SYSTEM ASSAY TEST RESULTS	82
FIGURE 47 COMPARISON OF BASELINE MYCOPLASMA ASSAY RESULTS (TOP) TO SYSTEM MYCOPLASMA ASSAY RESULTS (BOTTOM). POSITIVE CONTROLS INDICATED BY DARKER RED COLOR: LEFT WELLS. NEGATIVE CONTROLS INDICATED BY TRANSPARENT COLOR: RIGHT WELLS.	83

Table of Tables

TABLE 1 PROJECT GANTT CHART BREAKDOWN	23
TABLE 2 OTS BSA ASSAY TRADEOFF ANALYSIS	55
TABLE 3 OTS MYCOPLASMA TRADEOFF ANALYSIS	55
TABLE 4 MANUFACTURER INCLUDED OD RESULT COMPARISON (LEFT) EXPERIMENTAL OD AND RESULTS (RIGHT) 65	
TABLE 5 MANUFACTURER INCLUDED O.D. RESULT COMPARISON (LEFT) EXPERIMENTAL O.D. AND RESULTS.....	66
TABLE 6 MANUFACTURER SPECIFICATIONS FOR ASSAY RESULTS (LEFT).	83

Authorship Page

Section	Main Author	Main Editor
Abstract	Julia Smith	Julia Smith
1 Introduction	Amishi Vairagade/Thai Trinh	Amishi Vairagade/Julia Smith
2 Background		
2.1 Regenerative Medicine	Amishi Vairagade	Amishi Vairagade/Julia Smith
2.2 Stem Cells	Julia Smith	Julia Smith
2.3 Application of MSCs	Julia Smith	Julia Smith
2.4 MSC Quality for Autologous Transplant	Julia Smith/Amishi Vairagade	Amishi Vairagade/Julia Smith
3 Project Strategy		
3.1 Initial Client Statement	Julia Smith	Julia Smith
3.2 Design Requirements	Julia Smith	Julia Smith
3.3 Revised Client Statement	Julia Smith	Julia Smith
3.4 Project Management Approach	Julia Smith	Julia Smith
4 Design Process		
4.1 Needs Analysis	Julia Smith	Julia Smith
4.2 Alternative Designs	Thai Trinh/Amishi Vairagade	Thai Trinh/Julia Smith
4.3 Feasibility Studies and Experimental Modeling	Thai Trinh/Amishi Vairagade	Thai Trinh/Amishi Vairagade
4.4 Final Design Approach	Thai Trinh	Thai Trinh/Julia Smith
5 Design Verification		
5.1 Assay Experimentation	Julia Smith	Julia Smith
5.2 Fluid Control Experimentation	Julia Smith/Amishi Vairagade	Julia Smith
5.3 Temperature Control Experimentation	Thai Trinh	Thai Trinh/Julia Smith
6 Design Validation		
6.1 Prototype Validation: BSA Assay Run with System	Julia Smith	Julia Smith
6.2 Prototype Validation: Mycoplasma Assay Run with System	Julia Smith	Julia Smith
7 Discussion		
7.1 Fluidic Control System Discussion	Julia Smith	Julia Smith
7.2 Temperature Control System Discussion	Julia Smith	Julia Smith
8 Conclusions and Recommendations	Julia Smith/Amishi Vairagade	Julia Smith
Appendix A: Potential Pretotype Brochure	Amishi Vairagade	Julia Smith/Amishi Vairagade
Appendix B: R&D Systems Mycoprobe Mycoplasma Detection Assay Kit Procedure	N/A	
Appendix C: MyBioSource BSA Detection Assay Procedure	N/A	
Appendix D: Syringe Pump Calibration Curve Determination (Full)	Amishi Vairagade	Julia Smith/Amishi Vairagade

Appendix E: Syringe Pump with Manifold: Dead Volumes Experiment (Full)	Amishi Vairagade	Julia Smith/Amishi Vairagade
Appendix F: Syringe Pump with Manifold: Intake Inaccuracies Experiment (Full)	Amishi Vairagade	Julia Smith/Amishi Vairagade
Appendix G: Syringe Pump with Manifold and Air Pump: Output Volume Loss Experiment (Full)	Amishi Vairagade	Julia Smith/Amishi Vairagade
Appendix H: BSA Water Trial Experiment: Full	Amishi Vairagade	Julia Smith/Amishi Vairagade
Appendix I: System BSA Assay Experiment Data	Amishi Vairagade	Julia Smith/Amishi Vairagade
Appendix J: System Mycoplasma Experiment Data	Amishi Vairagade	Julia Smith/Amishi Vairagade

1 Introduction

With current medical treatments, it is often difficult to target the source as well as the symptoms of chronic diseases, which are due to malfunctioning or aging cells. This results in inefficient and high cost medical treatment for patients. One possible solution is regenerative medicine. This area of medicine focuses on treating the fundamental causes of the diseases rather than only the symptoms. Specifically, regenerative medicine aims to improve, repair, or regenerate damaged tissues by replacing them with healthy tissues or cells (Alliance for Regenerative Medicine, 2013). For example, when diagnosed with Type 1 Diabetes Mellitus, a patient is most often treated by continuously introducing insulin to body due to the malfunctioning of the pancreas. However, using regenerative medicine strategies, scientists are researching how to recover pancreatic cells and return them to a healthy, insulin-producing condition. The patient's body can then naturally produce insulin without life-long treatment (United State Government Accountability Office, 2015).

Currently, there are many important regenerative medicine technologies used in the healthcare industry, including cell-based therapy, gene therapy, and tissue engineering. Among these technologies, cell-based therapy is the most prominent, as it is currently involved in more than 1,900 clinical trials worldwide (Alliance for Regenerative Medicine, 2013). Cell-based therapy is a subsection of regenerative medicine that involves harvesting stem cells and progenitor cells such as mesenchymal stem cells or neural stem cells. This therapy also includes isolating differentiated adult cells from human body such as fibroblasts, osteoblasts, and myocytes. These healthy cells are then introduced into a patient's body in order to replace non-functioning and damaged cells (Alliance for Regenerative Medicine, 2014).

Cell-based therapy is a promising area in the medical field and can be used to treat many conditions and diseases, such as heart failure, cancer, and spinal cord injuries. Cell-based technologies have contributed to the treatment of more than 160,000 patients. From 2008 to 2013, 12 cell therapy products have received approval by various regulatory agencies (Alliance for Regenerative Medicine, 2013). Some cell therapy products that have been approved by the U.S. Food & Drug Administration (FDA) are Fibroblasts from Fibrocell Technologies, Inc. and Clevecord, which is HPC (Hematopoietic Progenitor Cell) Cord Blood from the Cleveland Cord Blood Center (U.S. Food & Drug Administration, 2017).

These cell-based technologies usually use three major types of cells: autologous, allogeneic, and pluripotent cells (National Cell Manufacturing Consortium, 2016). Autologous cells are the patient's own cells, which are used as a personalized treatment. These can be used to recover the patient's ability to produce blood cells after chemotherapy in order to help treat blood cancers such as leukemia and myeloma. Moreover, using the patient's own cells reduces the risk of cellular incompatibility and graft vs. host conditions. Allogeneic cells are stem cells that harvested from a compatible donor. These cells can also help the patient to recover blood cell production after chemotherapy but has a high risk for immune rejection (Cancer Treatment Centers of America, 2017). Pluripotent cells can differentiate themselves into any of three basic body layer cell groups: ectoderm, endoderm, and mesoderm. As a result, pluripotent stem cell can produce any cell or tissue, which is useful for cell replacement for damaged organs or tissues (Boston Children's Hospital, 2017).

Though cell manufacturing has the potential to greatly benefit patients, the cells used in the cell-based products require intense maintenance and quality control to ensure their viability and safety. It is very crucial to ensure that the cells injected into the patient's body are safe and uncontaminated. Current methods of stem cell quality control include models, assays, and sensors to gauge the quality of the cells. These methods can be not only be expensive but also time consuming. There are other challenges associated with the current quality control methods such as difficulty with obtaining reproducibly accurate results, which can lead to potentially harmful errors. Inaccurate results not only compromise the quality of the cells but can also be dangerous and even life threatening for the patient (National Cell Manufacturing Consortium, 2016).

The purpose of our project is to overcome these quality control challenges by designing and creating a proof-of-concept device to demonstrate the ability of multiplexing assays used for testing mesenchymal stem cells (MSCs), which will be used for autologous transplant. The current quality control of MSCs has several challenges associated with it. The current quality control tests using assays are performed manually by a laboratory technician and involve steps such as pipetting, transferring, and incubating. Because of the cost of the off-the-shelf assay kits as well as the manual labor involved in these tests, the cost of quality control is very high and one of the most expensive aspects of the cell therapy process. Furthermore, running these assays can be time consuming as each assay can take up to seven hours to complete, resulting in higher labor costs and extensive time spent on this area. Another limitation of running these assays manually is that it may result in human errors like reproducibility, false negatives and false positives. False negatives are particularly dangerous because if contaminated cells are reintroduced into the body, severe side effects can take place for the patient and health could

be compromised. False positives can result in viable cells being discarded leading to a waste of cells, time, and cost associated with the tests. Thus, it is important to build and design a device that can multiplex these assays while reducing the costs involved in the quality control and reducing the time involved in running these tests.

For this project, our MQP team created a proof-of-concept device to show the potential for an automated, multiplexing assay device that our client, Triple Ring Technologies, could further develop in the future. Because of the early stage of this project, the prototype was unable to reach all goals laid out due to time constraints but we see this device being capable of solving many of the aforementioned problems after future development and implementation. This device ideally would be able to simultaneously perform key quality control assays on a single patient's MSC sample to ensure that the cells are healthy and viable before reintroduction into the body. The device would require little manual involvement and would consequently result in lower labor costs, reduced time spent on quality control, and higher reproducibility and accuracy. This product could eventually be a marketable device that can greatly assist with the quality control of cell therapy products.

2 Background

2.1 Regenerative Medicine

The medical field has advanced through the years and has seen innovation in treating various diseases. One such important advancement in the medical field is regenerative medicine. Regenerative medicines are used for the treatment of a part of the body that has damage due to a health condition or aging. Regenerative medicine is focused on treating the root of the health condition in order to address it. Though still a growing field with much room for improvement, regenerative medicine is an important innovation in the healthcare industry as it has led to effective health care treatment. Regenerative medicines include a wide spectrum of approaches involving cell-based therapies, gene therapy, biologics and small molecules, tissue engineering, stem cells, and biobanking to treat many serious conditions. (Alliance for Regenerative Medicine, 2013).

Cell-based therapies are a subset of regenerative medicine in which healthy cells are used to heal the impaired part of the body. This method of treatment promotes and strengthens the body's immune system by redeveloping and renewing the body's cells. Cell based therapies usually use hematopoietic stem cells and mesenchymal stems cells which are undifferentiated adult stem cells. These cells differentiate to form other cell types such as intestinal cells, muscle cells, and blood cells. Because of the variety of cells that MSCs are able to differentiate into, they are very versatile and have almost unlimited potential for applications in a wide range of diseases (Bender, 2016)

2.2 Stem Cells

Stem cells are undifferentiated cells that are found throughout most tissues in the body. These cells are capable of differentiating into a large variety of different cell types depending on their location and the function of the surrounding tissues. Because of their renewable properties, stem cells can repair themselves and are often responsible for the repair of the surrounding tissue by differentiating into the appropriate type of cell, depending on the tissue's needs. (NIH, 2016).

2.2.1 Mesenchymal Stem Cells (MSCs)

This project focuses on mesenchymal stem cells and their potential applications in research and the treatment of a variety of diseases. Mesenchymal stem cells are valuable because of their ability to differentiate into a large range of cell types. The applications for these cells and their potential to treat a variety of different diseases and disorders make them very valuable to the scientific research community. Some current applications research include the treatment of cardiovascular diseases, neurodegenerative disorders such as Parkinson's and Alzheimer's, and autoimmune diseases including rheumatoid arthritis and type 1 diabetes. However, these cells become less capable of differentiating

quickly with increasing cell culture passages, therefore all cells collected must be put to use because it is difficult to ensure a constant supply of viable cells. (Ullah, et al, 2015).

The particular stem cells that are the focus of this project are mesenchymal stem cells (MSCs). These stem cells are derived from an adult human and were originally thought to be found only in bone marrow (NIH, 2016). However, more recently, scientists have shown that they are found in virtually every tissue in the body including adipose tissue, amniotic fluid, and even umbilical cords. Depending on their location, MSCs have the potential to differentiate into a range of other cell types, in particular, bone, cartilage, fat, and even occasionally neural cells (Ullah, et al, 2015). Additionally, they can also differentiate into stromal cells which are assistive in the support of blood production (NIH, 2016).

2.3 Applications of MSCs

2.3.1 Therapeutic Applications

Stem cell therapy is a relatively new area of medicine and its possible applications are seemingly limitless, though most areas of research have not been advanced past clinical trial stages of treatment. Research conducted in recent years has shown that cell therapy treatments can assist with healing of bone and cartilage diseases; this process required infusion of MSC rich bone marrow into the affected area to help combat both osteogenesis imperfecta and hypophosphatasia. This therapy can also be used to address various cardiovascular diseases which is highly beneficial given the non-regenerative nature of cardiovascular cells. Infusion of MSCs in the affected region can assist in recovering from heart disease, heart failure, and myocardial infarction. Autoimmune disease such as Crohn's disease and Rheumatoid arthritis can also benefit from the anti-inflammatory properties of the MSCs. (Kim, Cho, 2013).

2.3.2 Autologous Transplant Therapy

The application of MSCs for this project is in autologous MSC transplant therapy. Autologous transplant therapy is a method of cell therapy in which a patient's own cells are harvested, preserved, and reinjected into the body after a period of time. This therapy is most often used as a treatment for blood conditions or cancers like lymphoma or leukemia. Because the chemotherapy required to treat these condition destroys cancer cells as well as blood forming cells found in bone marrow, it is helpful to resupply the body with healthy and unaffected stem cells to quicken the time it takes for the body to regenerate the lost blood cells.

The process for autologous transplant consists of multiple steps: harvesting, preservation, quality control, and reinjection into the body. MSCs are collected from the bone marrow when the patient is relatively healthy or just prior to chemotherapy or radiation treatment (Leukemia &

Lymphoma Society, 2017). Stem cells are typically collected using apheresis, where they are isolated from the bone marrow. The collected stem cells are then either cryogenically preserved until needed or cultured to expand the number of cells available and then cryogenically preserved until required. If the stem cells are cultured, they must undergo extensive quality control to ensure purity before reintroduction to the body.

Once the cells are required, generally after cancer treatment has been completed, the stem cells are reinfused into the body, typically through a central venous catheter. Once the cells have been reintroduced, there is a period of time necessary for the engraftment of the saved cells in which they are required to replace all cells that had died during treatment. After this period of time has passed, the cells are able to regrow and regenerate as required. (Memorial Sloan Kettering Cancer Center, 2017).

2.4 MSC Quality Control for Autologous Transplant

In the biotechnology field, when biomedical products such as MSCs are to be used in human or animal therapeutics, they need to be appropriately purified from contaminants to prevent health risks. Contamination in the final product can come from outside sources or excess amounts of residual substances used during the cell culture process. Therefore, it is important to ensure that the concentration of residual substances or contaminants in the final product are within FDA approved limits. Biological assays are one method used to identify presence of specific contaminants in a cell solution.

2.4.1 Toxin Detection Assays

During the cell culture process, it is possible for the cultures to be contaminated by certain toxins, such as bacteria. These toxins can be very harmful and can fully compromise the culture and all cells being grown because of the potentially harmful effects they could have on the cells and on the patient who would be receiving the cells. Therefore, it is very important that the MSCs used for autologous transplant are rigorously tested for these toxins to ensure maximum safety for the patient.

2.4.1.1 Toxin Detection Assays: *Mycoplasma*

One of the most common biological contaminants is mycoplasma. Mycoplasma is a microorganism that has the capacity to modify certain properties of the cell it infects, including its development patterns. It is also capable of inducing the spread of viruses and yield in the infected cell culture. (Ryan, 2008).

Mycoplasma is a dangerous contaminant because its microscopic size allows it to easily infect cultures and remain potentially undetected. Additionally, these small microorganisms have the ability to replicate themselves and, because they lack cell walls, can quickly reproduce and infect the cell culture.

Mycoplasma colonies are hearty and difficult to destroy which enables them to grow rapidly in a healthy cell culture environment. Because of these characteristics and the potential for health risks for patients, it is very important that cells be tested for mycoplasma before they are reintroduced into the body. (Ryan, 2008).

2.4.1.2 Toxin Detection Assays: Endotoxin

Another toxin that is important to test MSCs for is endotoxin. Endotoxin is a complex lipopolysaccharide found in gram negative bacteria and is released upon both cell death and reproduction of the bacteria. Endotoxin infection can cause a number of problems in both *in vitro* and *in vivo* environments, making it very important to identify its presence as soon as possible. In an *in vitro* environment, endotoxin can cause a multitude of problems with cell cultures as it affects production of macrophages and can inhibit colony formation of the desired cell type. *In vivo*, endotoxin infection can result in inflammatory and pyrogenic responses, beginning with fever and chills and sometimes worsening to potentially fatal septic shock. (Sigma Aldrich, 2017). Endotoxin is carried on laboratory equipment because of its affinity for hydrophobic surfaces such as cell culture plates. This toxin is particularly problematic because of its high stability and resistance to heat, which makes it difficult to eradicate using normal sterilization methods, particularly autoclaving. (Sigma Aldrich, 2017).

2.4.2 Residual Cell Culture Material Assays

In order to ensure the purity of the cells, it is important to test for residual cell culture materials. Some cell cultures may involve use of residual cell culture material derived from animal sources, particularly bovine or porcine. These may cause contamination of the cells with adventitious agents. Thus, it is important to test for residual cell culture materials to confirm the viability and purity of the cells. (Bioreliance, 2017).

2.4.2.1 Residual Cell Culture Material Assays: Bovine Serum Albumin (BSA)

One such substance cell culture is tested for is Bovine Serum Albumin (BSA). Serum is an important part in tissue engineering and cell culture as it is used to supply nourishment to the culture. It also acts as a carrier for essential compounds like hormones, growth factors, and nutrients. (Francis, 2010).

It has been observed that BSA infusion can have ill-effects on health. It has been observed that albumin can result in increased capillary permeability, excessive circulation, and pulmonary edema. (Drummond & Ludlam, 1999). Additionally, it is important to be cautious with the use of any animal based products when culturing cells that will be reintroduced to the human body, as this can also have ill effects. In general, animal derived serums can lead to many problems with human MSC culture

including introducing variability in the culture, changing cell growth patterns, and contaminating the culture with cytotoxic factors found in the serum. It can also be a risk for introducing viruses, bacteria, prions, bacteria, and other contaminants into the cell solutions. These contaminants can compromise the health of the cells and the patient if the cells are reintroduced into the blood stream. Finally, the use of animal based serum can disrupt the adhesion of the cells and cause hindrance of the cell growth. This disruption may result in disturbing the stability of the cells and further interfere cell growth and function (Tekkotte, et al., 2011).

2.4.2.2 Residual Cell Culture Material Assays: Trypsin

Trypsin is a material that is formed in the pancreas and is very commonly used in adherent cell culture (Sigma Aldrich, 2017). Its main purpose is to cleave peptides on lysine and arginine side chains which effectively breaks the bonds between adherent cells and the cell culture plate in which they grew (Worthington Biochemical Corporation, 2017).

Trypsin is typically taken from either bovine or porcine sources when used in cell culture. This is an important material to test for as residual material because of its non-human source. It is risk-inducing to reintroduce cells into the body that have been exposed to an animal based material. Trypsin can carry viruses that are prevalent and difficult to eradicate in the porcine population. It can additionally be contaminated with other adventitious agents that can cause changes in cell cultures and difficulties with creating a suitable biological product. (European Medicines Agency, 2014).

2.4.3 Limitations of Quality Control

Biological assays are some of the most popular laboratory methods for detecting potentially hazardous substances in cell solutions. They are used in hospitals, laboratories, industry and research to identify the presence and concentration of particular substances in a cell solution including proteins, antibodies, and hormones. These tests perform based on the principles of the binding ability of antibodies, which are proteins generated by the immune system in response to the presence of foreign agents like bacteria. Due to their high specificity to bind to certain molecular structures, antibodies are used in some assays to detect certain biological molecules. (ImmunoChemistry Technologies, 2017). However, these assays have significant room for improvement. The main concerns with these assays are the high cost, time commitment, and possibility for human error involved.

Off-the-shelf (OTS) assay kits are expensive and vary greatly in cost range. For example, the R&D Systems' Proteome Profiler Human Kidney Biomarker Array price per kit is \$495, which breaks down to \$125 per sample and \$3.28 for each data point. R&D Systems' Fluorokine® MAP Multiplex Human Inflammation 12-plex kit costs \$2,390, which breaks down to \$30 per sample and \$2.5 for each data

point (Biocompare, 2011). In addition to these examples, there are hundreds of other assay kits on the market with costs that range from hundreds to thousands of dollars. These OTS assay kits are also very time consuming to perform. For example, the MycoProbe® Mycoplasma Detection Kit from R&D Systems requires five hours to run the whole assay (R&D Systems, 2016), not including sample and reagent preparation time. Another example is the MyBioSource BSA Detection Assay kit, which takes up to two hours to complete, with additional time again required for preparation (MyBioSource, 2016). Finally, a considerable amount of manual work is involved in executing assays, which involves manual procedures like pipetting, washing, and transferring of solutions. Moreover, running the assay procedures manually may introduce risk for human error and difficulties in reproducibility. An experienced operator is required to ensure that the assays are correctly executed. It is crucial to ensure the assay procedure is performed correctly since the therapeutic applications rely on the stable and accurate data.

With consideration of the above limitations, an automated system to perform all the aforementioned assay procedures would be extremely beneficial to help reduce expenses and increase confidence in results. This device could be used to execute assays by utilizing automated fluid and temperature control, reducing manual involvement. Additionally, more accurate and consistent results could be accomplished by testing the repeatability of such a device. Furthermore, the device can decrease costs related to instruments required to run the assay. Finally, by scaling reactions to use smaller volumes of reagents can be used to further reduce the costs involved in QC.

3 Project Strategy

3.1 Initial Client Statement

The client for this project was Triple Ring Technologies (TRT), a research and development firm that specializes in medical devices, in vitro diagnostics, and imaging. TRT created this project as a continuation of previous work done within the In Vitro Technologies department. The original client statement for this MQP is as follows.

“The goal of this project is to develop a concept and prototype device that demonstrates multiplexed assays used in the quality control (QC) testing of stem cells manufactured for autologous transplant. Because these QC tests are currently performed manually with separate technologies, they are one of the more expensive components of the stem cell manufacturing process. We would like to significantly reduce the cost of QC by developing a system that bundles a number of tests into a compact, automated cartridge.”

Using this client description, the project team was able to initiate background research to become familiar with the field of quality control testing and potential solutions to the problem at hand.

3.2 Design Requirements

3.2.1 Objectives

At the project outset, TRT provided a number of design requirements for the device. These objectives were necessary to guide the group through the brainstorming and design process to ensure that the eventual prototype addressed the client’s needs for the product. Though this project is one that will be continued after the completion of our work, our group worked to incorporate as many of the constraints and specifications as possible so that the continuing work would proceed toward final product success.

The assay instrument or device should be capable of multiplexing assays simultaneously in one device. The design and system architecture of the device should consider proper temperature control for incubation areas and time. It should also consider reagent mixing and fluid motion to ensure all assays run in the device are completed correctly and without contamination with each other. The instrument should possess proper fluidics control and be able to manage temperatures within the device. For this project, a proof-of-concept prototype device should be created to show that this potential design could be possible in the future.

The pretotype portion of the project should be a product concept of the product as it could be far in the future. This pretotype should have all objectives met by the device in order to show how the product could be a useful and necessary addition in labs. Additionally, it can include drawings in order to

illustrate product concept and workflow or potentially 3D mockups of the system. Therefore, potential clients and buyers can better visualize and see the need for this product and realize its future advantages over the gold standard QC methods on the market now.

3.2.2 Engineering Standards

During the engineering design process, it is vital to consider the industry and engineering standards that are relevant to the system at hand. Because this system is meant to prove that cells are useable in the human body, there are strict guidelines that it must conform to in order to be considered safe and effective. For this project, it was necessary to look at standards regarding sterility, testing, electrical limitations as well as other areas. The group did research to determine the standards in these areas according to ISO standards, FDA requirements, ASTM standards, and IEC standards.

One of the standards used to ensure the quality and the safety of the device is ISO (International Organization for Standardization) 11737-2:2009- Sterilization of medical devices. This standard states important testing required to avoid any contaminants on the medical device thus ensuring patients' safety (ISO 11737, 2009).

IEC 60601-1 is a standard covering electrical equipment for medical use. This standard regulates safety requirements for electrical connections like plug insulation and flexibility of power cords. Moreover, there is a subsection describing constraints for medical electrical equipment including risk management, testing methods, and classification. With this standard, we have a guideline for how to prevent potential harm like electrical shock to users (IEC 60601-1, 2015).

IEC 60083 provides information about plugs system and socket-outlets in several countries around the world. For example, it gives information about pole numbers, shape, alignment, voltage and current for sockets in Australia, Austria, and other countries. Knowing this data, it is helpful for us to specify the compatibility of our product's power usage with the power system in different countries.

IEC 60252-1 provides information about safety requirements for AC motor capacitors, which includes performance, testing and rating. Some details can be mentioned are the phase system, frequency specifications and capacitor types. Since our project involves pumping, which may result in usage of motors, it is important to consider these constraint to the product so as to prevent possible damage (IEC 60252, 2010).

ISO 9001: International Organization for Standardization (ISO) specifies ISO 9001:2015, which incorporates/includes quality management system in any field in over 170 countries. This standard helps in customer satisfaction by ensuring the quality of the products (ISO 9000, 2017).

ISO 13485: It is very essential to bind to medical device standards in order to ensure safety of the patients. Another very important standard is ISO 13485, which ensures the quality management of the system. This standard is applicable for organizations which are involved in design, manufacturing/production, distribution, installation or servicing of medical devices or anything similar or related (ISO 13485, 2016).

ISO 14001: 2015 is an environment management ISO standard. The standard identifies the impact of the medical device on the environment. It recognizes the effects of manufacturing the device and its parts on the environment. This helps ensure a safety environment for the company and its employees as well (ISO 14000, 2015).

3.3 Revised Client Statement

During the initial research period, our MQP team was able narrow our project focus by working with TRT to ensure that client needs would be met by our design. The revised client statement below was a result of this work.

“The goal of this project is to develop a concept and prototype device that demonstrates semi-automated fluidic and temperature control to show potential for a multiplexed assay device to be used in the quality control (QC) testing of mesenchymal stem cells (MSCs) manufactured for autologous transplant. The assays of concern in this project test for mycoplasma and bovine serum albumin (BSA). We would like to significantly reduce the cost of QC by developing a system that bundles these tests into a compact, automated system with easy-to-read, absorbance based results. Additionally, this automated device would be required to meet the minimum requirements for FDA level sensitivities for the results of these performed assays.”

3.4 Project Management Approach

This project was a three term project conducted both on campus at WPI and onsite at the client’s facility in Newark, CA. It consisted of a preparation period (seven weeks prior to arrival), an implementation period (eight weeks onsite) and concluded with a completion and documentation period (seven weeks after the project duration). A number of methods were employed to ensure good planning and time management for the duration of the project.

During the preparation term, the team worked to develop an understanding of the project background and be more prepared for the onsite portion of the project. The team had weekly meetings with our TRT project liaisons: Director of In Vitro Technologies (Roger Tang), Practice Lead of In Vitro Technologies (Ryan McGuinness), and a Senior Scientist (Optical Technologies) and WPI alumnus (Jen Keating). These meetings were meant for the team to present progress and pose questions to our

liaisons for the coming week's research. Additionally, the TRT team provided a number of resources to expedite the process, including documentation of current research and the current state of the project. TRT also provided documents regarding the motivation behind the project, namely reports on regenerative medicine, the market potential for this field, and discussion on its future developments.

In the future, it would be beneficial for the project to incorporate a Pre-Qualifying Project (PQP) official course registration in order to ensure that the students are prepared for the background research and preparation that needs to be completed before arriving onsite at the company. Because this project was the first of its kind, there was not a registered PQP and despite weekly meetings and information sharing with TRT liaisons, our group was unable to complete the required preparation work and research because of time limitations due to academic course load. Therefore, future MQP teams could benefit from a scheduled PQP to ensure that scheduling other academic courses can be balanced with the preparation work for the project.

3.4.1 Gantt Chart

Upon arrival at TRT, the group worked to compile a Gantt chart with a potential outline of the term and the tasks that would be required to complete the project in a timely manner. This chart can be seen in Table 1 and Figure 1 below.

Table 1 Project Gantt Chart Breakdown

Task Name	Start Date	End Date	Duration (Days)
Detailed project plan	1/10/2017	1/11/2017	1
Finalizing assay choices	1/11/2017	1/13/2017	2
Introduction & Project Background*	1/12/2017	1/15/2017	3
Create general cartridge architecture	1/13/2017	1/18/2017	5
Design microfluidic pathways for each assay	1/13/2017	1/18/2017	5
Order Assay Kits	1/16/2017	1/20/2017	4
Project Strategy and Design Process*	1/15/2017	1/20/2017	5
Assay experimentation	1/19/2017	1/25/2017	6
Surface modification	1/19/2017	1/27/2017	8
Finalizing cartridge specifications based on assay	1/25/2017	1/27/2017	2
Create potential cartridge components	1/27/2017	2/2/2017	6
Create general system architecture; temp, valves,	1/28/2017	2/1/2017	4
Final Design Verification & Validation*	1/20/2017	2/10/2017	21
Heat/fluid control design	1/30/2017	2/4/2017	5
Pretotype development	2/6/2017	2/11/2017	5
Experimentation/modification of cartridge compo	2/2/2017	2/17/2017	15
Experimentation of heat control components	2/6/2017	2/20/2017	14
Integration of cartridge components	2/17/2017	2/24/2017	7
Discussion, Conclusions, & Recommendations*	2/10/2017	3/3/2017	21

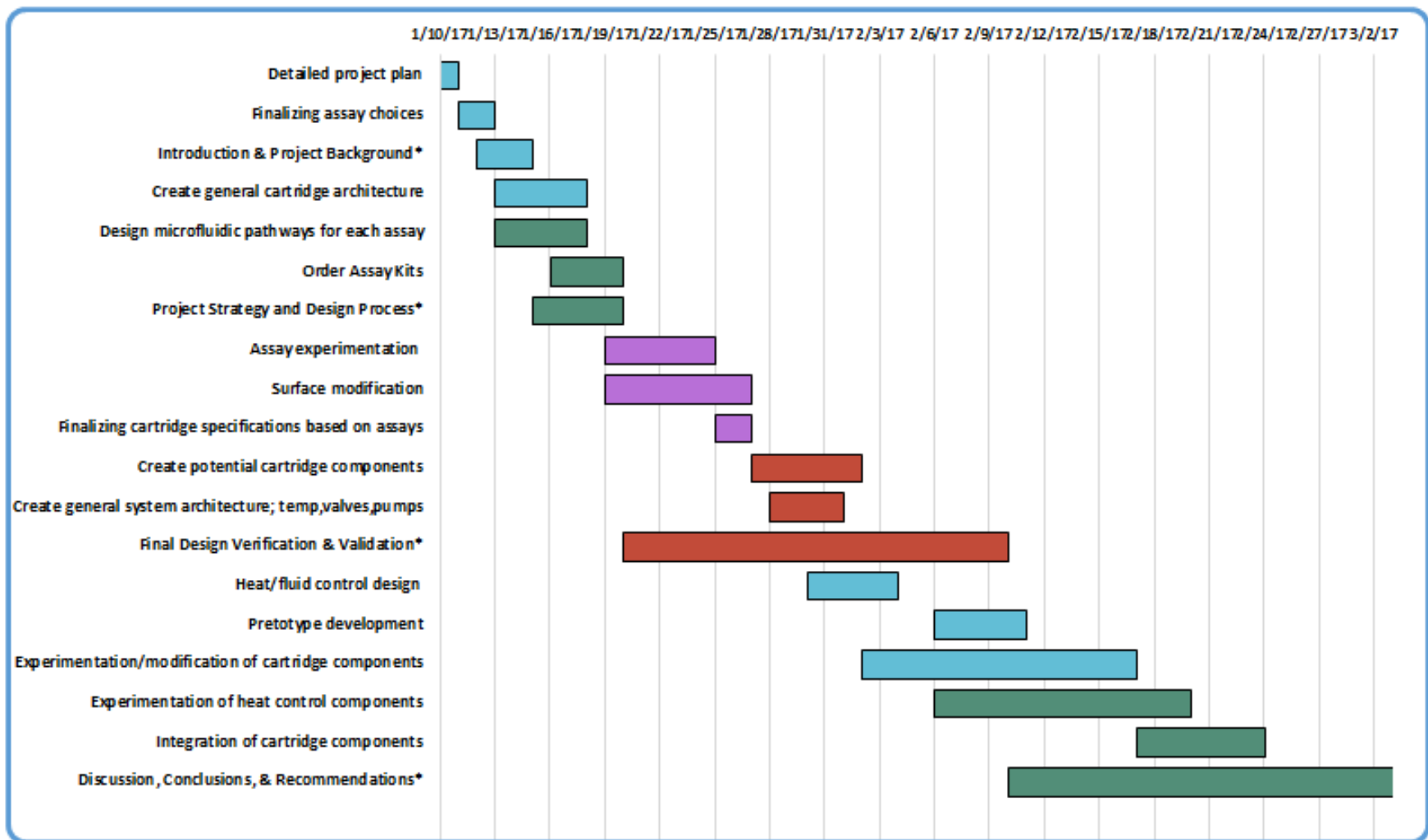


Figure 1 Project Gantt Chart

3.4.2 Scrum Methodology: Daily Stand-up Meetings

Per the suggestion of the TRT team, the team implemented a specific facet of agile development and scrum methodology, mainly the daily stand-up. Scrum methodology refers to the highly iterative process of discussing daily what was achieved the previous day, what the goals for that day are, and what is standing in the way of progress. The MQP team had a short daily meeting with the TRT team to discuss these daily goals and ensure that progress was being made as expected by addressing problems as soon as they arose. These meetings were helpful in more specifically breaking down tasks and creating the agenda for the day's work. This type of organization was necessary because of the short nature of the onsite portion of the project and the need for maximum progress as fast as possible.

3.4.3 Weekly Client Meetings

A weekly meeting, with the TRT team, MQP team, and WPI advisors was also a tool to stay organized and on-track. This project was required to satisfy the WPI MQP requirements for the Biomedical Engineering and Electrical and Computer Engineering departments. Therefore the team had an academic advisor from each department to gauge progress of the project in both areas. These meetings were helpful in showing the progress the team had made over the last week while also allowing the opportunity for feedback and questions on the work done.

3.4.4 Trello Board

For additional organization, the team created a more detailed breakdown of tasks using an online project management tool called Trello. Trello facilitates digital implementation of agile development including the ability to add tasks with detailed checklists, assign tasks to individual team members, upload results, and conduct discussions through comments on tasks.

The use of Trello allowed for easy parallelization of work through distribution of work to all team members. Tasks in Trello are easily modifiable and were actively modified to incorporate additional items needed to complete work. The tasks were organized and broken down roughly according to the part of the prototype system that was affected by the task: fluid control, temperature control, and assay experimentation and design. Once specific tasks were completed, they could be checked off and new tasks could be added so that progress could be made and monitored.

4 Design Process

4.1 Needs Analysis

4.1.1 Clinical/Patient Need

Every year, almost 60,000 stem cell transplants are performed all over the world. These transplants are performed for treating disorders like cancer and blood related conditions (Alliance for Regenerative Medicine, 2013). According to the Alliance for Regenerative Medicine Annual Report (ARM), the cell therapy industry generated over \$900 million for bio-therapeutic companies in 2012. The clinical need for this project revolves around the necessity for quality control for the transplanted cells. If this quality control process is ineffective, the patient's health could be compromised, which remains the main concern and motivation behind these tests. Because these biological assays are currently performed by hand, human error can be introduced into the QC process, which can have dangerous side effects for the patient involved. For example, if because of human error a toxin detecting assay comes back with a false negative and the cells are wrongly assumed to be safe for reintroduction into the body, the patient's health could be compromised. In the case of a toxin such as endotoxin, presence of the toxin in an in vivo environment can have serious consequences including fevers, chills, immune responses, and potentially fatal septic shock (Sigma Aldrich, 2017). Therefore it is crucial that these tests be performed reproducibly and without error. Additionally, in a more economic view, false positives can also present issues during QC. If false positives are present, the cells in question would need to be disposed of and would not be approved to be used as a therapy. However, if the contaminant in question was not actually present and the cells were healthy and uninfected, a significant amount of time and cost would be wasted and the patient would lose the opportunity to have the cells reinjected.

These biological assays are also cost and time intensive. Assay kits can be expensive, with cost and amount of included reagents varying greatly from kit to kit. For example, the R&D Systems' Proteome Profiler Human Kidney Biomarker Assay can cost \$495 per kit, while the R&D Systems' Fluorokine MAP Multiplex Human Inflammation 12-plex kit can cost \$2390 per kit (Biocompare, 2011). The time involved is also high, as one of these assay runs typically takes a minimum of three hours of total time with intermittent manual involvement. Some OTS assays like the Mycoprobe Mycoplasma Detection Kit can take up to four and a half hours to complete with additional manual steps that can increase the total time (R&D Systems, 2016). In the case of autologous transplant, each round of QC would have to be performed separately because of the risk of cross-contamination between the cell types. Therefore, because each set of cells would have to be tested separately, the time cost involved in the process is problematic and greatly increases the cost of the process as a whole. The high cost of

these OTS kits coupled with the assay completion time and manual labor costs cause QC to be the most expensive part of autologous cell therapy process. If the time and cost involved with completing these assays was reduced using an automated, multiplexed system, research and QC laboratories could greatly increase throughput, lessen QC total cost, and have greater assurance of the accuracy and reliability of the test results.

4.1.2 Client Need

The client need for this project is motivated by the creation of a new TRT medical device that can be released to the market in the future. In the short term view, TRT looked at this project as the opportunity to progress the device enough ahead to apply for the California regenerative medicine grant to ensure that the research and testing necessary to develop this product could be funded for the foreseeable future. Our client hoped that our MQP team could accomplish a proof-of-concept device that would assist in applying for the grant and showing the potential of this product in the future.

4.1.3 Device Requirements

The requirements for this device were in a way rather non-specific because of the early stage of the project. Because our team was developing a prototype/proof-of-concept device, it was often necessary for the team to create logical specifications that were unspecified by the assay manufacturers or the TRT team.

The first consideration was the necessity for a properly coated surface on which to run the assays inside the device. Because some assays, especially the ELISA (enzyme linked immunosorbent assay) category, require a modified surface that will allow for specific bindings to take place, it was necessary to the device to possess the correct type of plate for these reactions. Additionally, TRT's goal was to have all result collection completed by an absorbance microplate reader, a standard machine in most biological labs, in order to simplify the device slightly. Therefore, it is necessary that whatever surface the assays are conducted on can be moved and fit into a standard reader for data collection.

For the quality control biological assays to be able to be run correctly, the created device would be required to move the manufacturer specified volumes of each reagent around the device, as necessary. These volume specifications can be found in the OTS assay inserts and range from 50-350 μL . The exact volumes for each reagent vary depending on the kit being used, but in general this range of volumes would need to be accurately controlled by the system. There was no specific flow rate or time of output necessary for this subsystem of the device but the team wanted to be able to replicate the flow and time of the reagent through the system to closely resemble those of an actual lab pipette. Additionally, there could be no splashing or cross-contamination between the wells so the team would

also have to ensure that there was enough control over the fluid to limit these areas as much as possible.

The assay kits also have a specified temperatures at which the reagent mixtures must incubate in order for the chemical reactions to be completed successfully. Most kits that our team researched did not have specific tolerances so the group decided that the temperature system should be able to heat to within 2-3 °C of the required temperature to reduce the possibility of error due to the temperature level. The team also had to decide on what length of time was acceptable for the heating system to have to heat up and cool down to the desired temperatures. These specifications were decided based on the incubation time and temperature required by the assay kits. For example, for a temperature of 65 °C that would incubate for one hour, the team decided that the system should take no more than five minutes to heat and cool to and from room temperature to ensure that solutions would be at the appropriate temperature for as close to the required time as possible.

4.2 Alternative Designs

During the project design process, the group came up with a variety of different options and solutions to the problem at hand. Many possible components were considered before final decisions were made and used in the prototype. These options were either researched, discussed, and found to be ill-fitting for the design or were experimented with to determine their potential usefulness to the design. All of these options were considered and contributed to the design process in some way to ensure that the final design had the most appropriate and useful components. The main areas for which different options were considered were in regards to assay plates, fluid control, and temperature control.

4.2.1 Ideal System Architecture

During the brainstorming process, the team decided to create a long-term, end-goal architecture for the system to have a more definite idea of what components were necessary for the prototype. Though this architecture describes a number of subsystems that our team was not able to address, it provided an idea of how our prototype could develop more in the future and what areas would need to be implemented and improved. Figure 2 below shows the whole system architecture and lists the subsystems and components we deemed necessary to have a potentially successful final product.

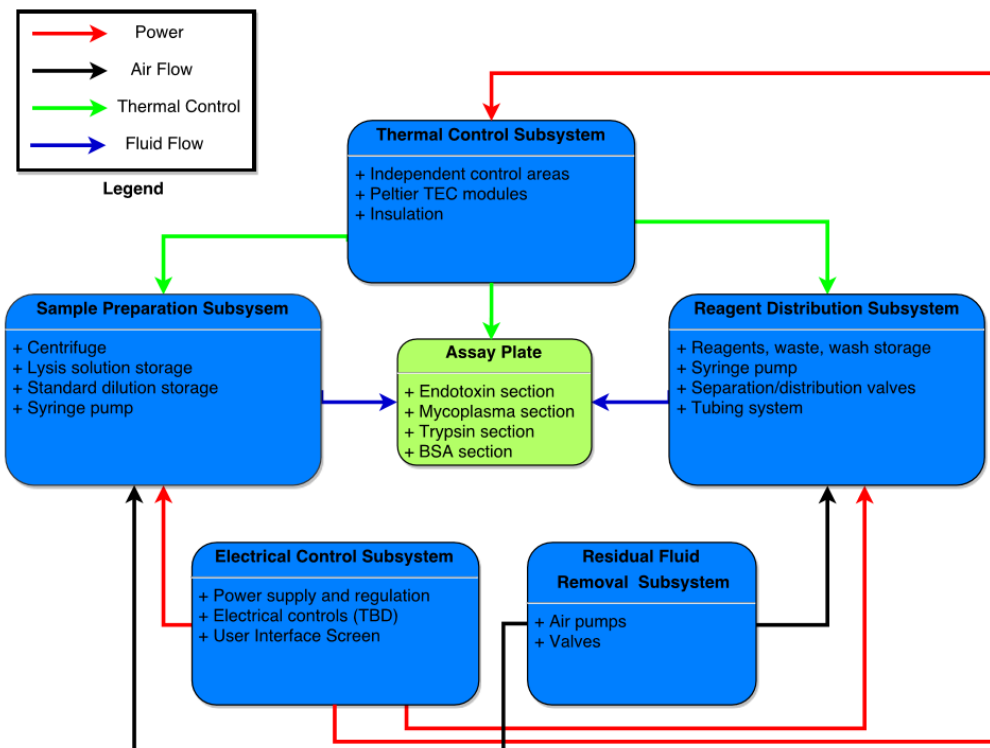


Figure 2 Architecture Drawing of Ideal System Breakdown

4.2.2 Assay Plate

One option that the team considered for the assay plates needed to run these tests was to create a PDMS cartridge using a 3D printed negative mold to form fluidic channels. The assay reagents would be pumped through various parts of the cartridge and heated appropriately when required. However, one major flaw with this potential design was the necessity of duplicating the surface chemistry that is present in OTS kit assay plates. Since the assays of concern are ELISA based assays, they require a specifically coated surface on which the appropriate binding and reactions can take place. Because of the proprietary nature of the assay kits, these surfaces are very difficult to replicate. Attempting to do so would require an extensive amount of time to determine the correct substances while also experimenting to ensure that the correct bindings take place.

To avoid recreating the surface chemistry on the assay plates, the team also looked at using the existing OTS assay plates to see how they could be integrated into a potential device. Using the preexisting plates would allow for correct binding and would remove one potential area for error in the device. The plates included in the kits were also stripwell plates which was another benefit because the assays typically only need 8-16 wells, or 1-2 strips of 8 wells, on which to run the assay. Therefore, the other wells would not have the potential of being contaminated because only the needed number could

be removed. Finally, these plates already fit a standard absorbance plate reader. This would eliminate the need for creating a cartridge that had the proper dimensions to fit in the reader correctly.

4.2.3 Microcontroller

Since the two main blocks of our project, temperature and fluid control, must be automated the heart of the whole system should be something that allows user to give instructions to the system through a friendly interface. Moreover, we also wanted to have data recorded from these systems to facilitate testing protocol. Lastly, the control system should be small enough to fit into a device that would fit comfortably on a standard lab bench. As a result, one device that can satisfy all above requirements is a microcontroller. A microcontroller is a system on chip that has an integrated circuit (IC) built inside. A microcontroller has both input and output port peripherals that allows the device to communicate with several external devices, which in our case would be the temperature and fluid control systems. Moreover, it also has program memory inside that allows the programmer to upload digital instructions to execute commands using common programming languages such as C or C++. In addition, since we were developing a prototype for proof-of-concept rather than a marketable product, we did not want to design our own circuit board or microcontroller to perform aforementioned tasks. As a result, one of the most important features needed was a microcontroller board with a user friendly integrated development environment (IDE). This IDE could save time by introducing powerful and convenient programming functions that allow the team to integrate communication between the microcontroller and the temperature and fluid systems without being concerned about how to setup the communication protocol between these devices.

In this section, the team describes some options for microcontroller development board that are widely available on market and were considered for this project.

4.2.3.1 *Arduino Mega 2560*



Figure 3 Arduino Mega 2560 microcontroller board

Retrieved from: <https://www.arduino.cc/en/Main/arduinoBoardMega>

The Arduino Mega 2560, seen in Figure 3 above, is a development board that has an 8-bit chip ATmega2560 powered by 5 V. This board has 54 digital I/O pins along with 16 analog input pins. This number is very impressive since it has a lot of available pins to allow for additional communication with the temperature and fluidic systems. The board also has 8 KB of RAM memory with maximum clock speed of 16 MHz. Moreover, it has a built-in flash memory of 256 KB that allows user to store the program inside the board, even after disconnecting the power to Arduino board. Therefore, whenever we turn on this device, our automated system will be on without having to reprogram it. Additionally, the Arduino Mega 2560 can be powered through two possible ports of 5 V. One is via USB cable port which is a convenient option because it allows us to study the current draw and power consumption of the system before selecting an appropriate battery. After we are familiar with how much power the system consumes, we can purchase a 5 V battery and connect through Arduino's battery port, which makes the system relatively independent of computer and can become a separate device. Lastly, Arduino LLC has developed its own IDE with the Arduino language. This programming language is a higher level version of C/C++ that combines several C/C++ system instructions to communicate with devices into simpler and more compact commands for the user. For example, Arduino's `digitalRead()` function is actually a combination of several C commands such as configuring register pin data being read from, accessing ram memory, storing data read from digital pin to memory location and so on.

4.2.3.2 MSP430F5529 USB LaunchPad Evaluation Kit

Another option for the system's microcontroller is the MSP430F5529, which is a 16-bit microcontroller board from Texas Instruments (TI) and can be seen in Figure 4 below. It is low power and connects to a PC through a USB 2.0 port. It supports 40 pins to allow communication with external devices. Maximum clock speed 25 MHz with 128 KB flash memory and 8 KB RAM. This board has several built-in external devices such as 12-bit analog to digital converter (ADC) and a temperature sensor, which are necessary for the thermal function of our system. In terms of hardware efficiency, this board is more advanced than the Arduino Mega 2560 since it consumes less power, while supporting powering options between 5 V to 3.3 V. Moreover, the higher clock speed can improve the system execution if there are too many processes required to be competed simultaneously in the final design. The 12-bit ADC also introduces better resolution to the user than the 10-bit ADC of the Arduino Mega 2560, which can result in more precise data collection for temperature values or linear actuator syringe data. Similar to Arduino, this board also has its own IDE called Code Composer Studio. This is similar to a C/C++ program interface that has a built-in driver setup to be compatible with the board. However, this IDE is much more advanced than Arduino since it allows user to trace down value in each pin register, setting a break point and real time operating system design.



Figure 4 Texas Instruments 16-bit microcontroller board

Retrieved from: <http://www.ti.com/tool/msp-exp430f5529lp>

In terms of hardware consideration, the MSP430F5529 definitely has more benefits than the Arduino Mega 2560. It can execute programs faster and it also has more bit range (16 bits) in the core than the 8-bit ATmega2560 chip. With more instruction and data bus, the process of making decisions, accessing memory, and configuring hardware interface with external devices will be faster. MSP430F5529 also has lower price of \$13, compared to \$40 for the Arduino Mega 2560. However, one

significant drawback of MSP430F5529 is that the programming content of TI board is much more complicated. It requires the programmer to access each bit of register ports to turn them on or off in order to setup different modes of that port, which can be the input port, output port and other functions such as internal clock setup. Moreover, to communicate with external devices, the programmer needs to know about the protocol associate with it such as SPI, I2C or UART. Setting up the drivers for these protocol is complicated and time consuming, which was not suitable for the seven week time constrain the team had on the project. Given that time is the most important concern and other hardware or price drawbacks are not as significant, the Arduino Mega 2560 was chosen.

4.2.4 Fluid Control

Usual fluid control involves applying pressure to push or vacuum the fluid inside a fluid path. Therefore, this section discusses what fluid control mechanisms we considered for generating these pressure forces while also being compatible with our system requirements.

4.2.4.1 Pumping Options

One of the first options the team looked at was a peristaltic pump, which consists of a rotating wheel leaning against a tube, as seen in Figure 5 below. These continuous sealing actions against the tube result in a vacuum force, which can draw fluids from one end into interior tubing system. When the sealing releases pinches at the other end, the fluid will be drawn out. As a result, if we put reagents reservoir at one tube end, this pump can deliver them into a microfluidic channel at the other end. In terms of automation, by controlling the rotating speed of the wheel, we can manage the flow rate that is appropriate for the fluidic systems.

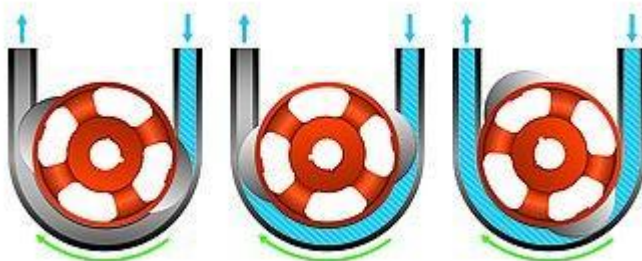


Figure 5 Peristaltic pumping mechanism.

Retrieved from <http://www.verderflex.com/en/how-do-peristaltic-pumps-work/>

Another option is torque-actuated pump. This design, seen in Figure 6, is from the Hong Kong University journal. The system has a screw in red and a base in grey. The base has threads that allow the screw to introduce fluid into the system. When the screw is rotated clockwise, the solution flows from the red section into a microfluidic channel; when the screw is rotated counterclockwise, the fluid in the

microfluidic channel is vacuumed back into the reservoir. One advantage of this system is its compact and simple design. Moreover, this design is suitable for a microfluidic system, which is one of the most challenging feature of our desired system. The main drawback is that since the screw system is manually controlled, we would have to create an external piece that can attach to the screw to automate it. Moreover, since the design is not off-the-shelf it would require selecting appropriate materials to 3D print.

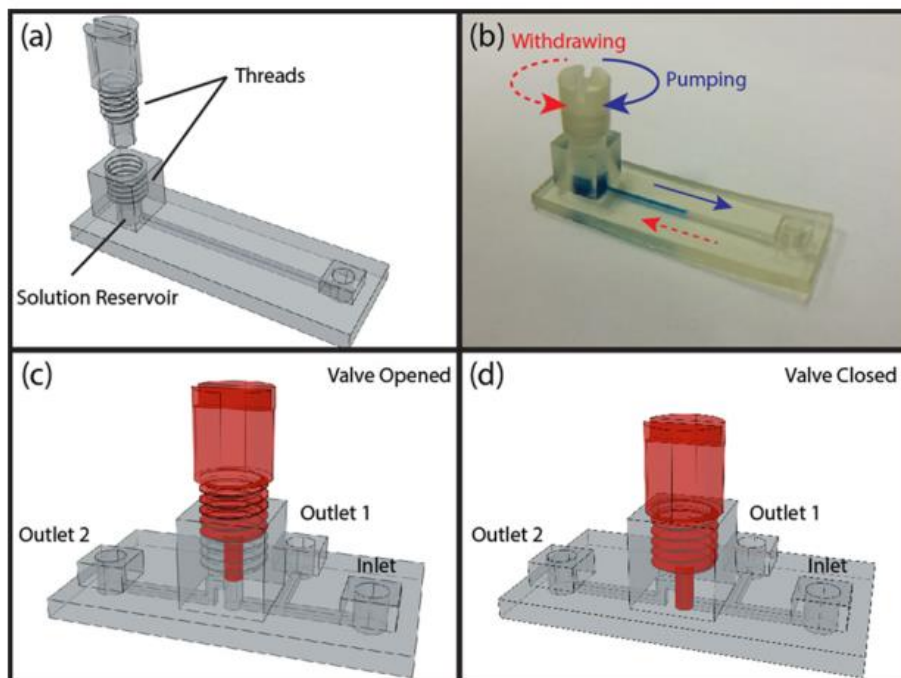


Figure 6 Torque-actuated pump

Retrieved from https://www.researchgate.net/publication/286652883_Simple_Cost-Effective_3D_Printed_Microfluidic_Components_for_Disposable_Point-of-Care_Colorimetric_Analysis

Lastly, the syringe pump is one of the most popular pumping techniques. As seen in Figure 7, the syringe plunger usually attaches to a linear actuator that is capable of shortening and expanding. These actions of compressing and expanding will result in push and pull actions on syringe plunger, thereby allowing for the intake or output fluids from the syringe. The movable linear actuator is usually driven by a motor with controllable pumping or vacuuming speed. One of the advantages of the syringe pump is its friendly interface with the linear actuator, which is available off-the-shelf product. The design is fairly simple, yet can maintain good accuracy of fluid dispensing.

Given the short amount of time and for the sake of the proof-of-concept, the team wanted to choose a design that consists of widely available OTS components. This requirement, however, does not fit well to either the peristaltic or torque actuated pumps. Both of these would require external

mechanical parts to allow for automation of the pumps which would also require many calculations and experiments before the system would become usable. Moreover, for the peristaltic pump, the rotating wheel is not a popular component and therefore the team would most likely have to design and 3D print the appropriate piece. As a result, the syringe pump was chosen. This choice was made because syringes and linear actuators are easily bought OTS and the interface between these components is straight forward and easy to control.



Figure 7 Typical OTS automated syringe pump.

Retrieved from: <http://www.kdscientific.com/products/infusion-syringe-pumps.html>

4.2.4.2 Motor

After careful consideration, the team determined that in order to generate pressure force into the fluidic path, we needed to have an automated push/pull mechanism. These types of automation usually involve the usage of motor control. There are several motor options available on the market and we had to decide on which is our best option. Below are three of the most popular motor options available:

A DC motor is based on continuous shaft rotation motor driven by DC voltage signal through power and ground connection only. This power signal is usually controlled by Pulse Width Modulation (PWM) signal. PWM signal with more duty cycles will result in more power delivered to the motor, increasing the motor's speed and force. This motor is the most simple and easiest to drive with only relays. However, the shaft progression only stops when power is off, which can result in errors.

Servo motors are usually DC motors with external components such as a control circuit and position sensor to facilitate more precise actuating. Servo motors do not rotate freely but are based on a

control input signal. This control signal commands the DC motor when to stop rotating and stay at the desired position. This will prevent any external forces that can push or pull the actuator, thereby preventing possible error during operations. PWM is also used to control the servo motor operations.

Stepper motor uses a base motor that has several toothed electromagnets with a central gear in between. Similar to servomotor, stepper motor has external circuit to control each electromagnet, thereby turning the motor shaft. This electromagnet control is simply switching power on or off to energize and cause rotation from one electromagnet to the adjacent one, which is called a step. Therefore, the precision of motor rotation is higher with separate electromagnets arranged in one full circle. Moreover, this design allows stepper motor to hold position by torque rather than power like the DC motor or servo motor, thereby introducing less error and less energy consumption.

With the purpose for proof-of-concept, which requires control of current draw to the linear actuator as well as control of the linear actuator position, the servo motor is the most ideal one. Servo motors usually include both a position sensor and a current sensor that the DC motor does not have. These sensors record important information that is necessary to select the proper moving range and moving speed for dispensing and inputting reagents into fluidic system. In addition, the simpler rotary mechanism of servo motor comparing to the more complicated mechanism of stepper motors can facilitate our short project time.

4.2.4.3 Syringe Pump Motor

One important requirement for the motor was that it should be compatible with an Arduino motor driver controller board that is available on the market, which means the sensor signal should be within the maximum voltage range of Arduino (5 V). To satisfy this requirement, the team selected an Actuonix P16 linear actuator. The P16 is among the most popular and cost effective devices that combines both linear actuator and servo motor. This product, seen in Figure 8, requires 12 V DC to allow push/pull operations with built-in position feedback. The feedback system consists of a simple potentiometer wiper with 5 V power to a positive reference rail and ground to a negative reference rail.



Figure 8 Actuonix P16 linear actuator chosen for syringe pump Retrieved from <https://s3.amazonaws.com/actuonix/Actuonix+P16+Datasheet.pdf>

The steel bar is an actuator attached to a servo motor. This bar can move in and out, thereby pushing or pulling a syringe plunger if it is attached to the actuator. The electrical wires include power and ground wires. There are also position feedback wires that can feed data into Arduino analog pin to keep track of the position of steel bar. The distance information is sampled through a 10-bit DAC built in the device, which is capable of reporting actuator position in the range from 0 to 2^{10} . These numbers are the values will be reported from sensor to microcontroller and 2^{10} represents the largest distance the P16 can travel, which is 50 mm.

4.2.4.4 Solenoid Valve Manifold

One concern we had when we were working on the prototype was how to reduce the size of the device as much as possible. Therefore, it was undesirable to have a single syringe pump to handle one reagent only. For the assays of concern in this project, there can be up to eight different reagents that need to be dispensed but having eight syringe pumps is undesirable. As a result, we needed to have a mechanical part that can act as an interface between one syringe pump and several reagent reservoirs. After inquiring with TRT employees, we were able to find a part, the NResearch solenoid valve manifold which is available OTS, in an onsite lab and readily available for use.



Figure 9 NResearch Solenoid valve manifold

Retrieved from: <http://www.nresearch.com/>

As we can see from Figure 9 above, this piece is 12 V solenoid valve manifold from NResearch. The manifold consists of four 3-way solenoid valves. Each hole, seen on the front side of the manifold, are input channels which would attach via tubing to reagent reservoirs. There are also input and output holes at the top and bottom of white part that we cannot see in this picture. These solenoid valves are controlled by applying 12 V DC power to two power lines, resulting in an on or off state. As a result, by connecting four reservoirs to four side channels, with the syringe pump connected to the input hole and an assay plate at the output hole, we can utilize only one syringe pump to deliver four reagents to a

well. We were informed that NResearch can customize their products so this piece could be implemented with as many as eight valves in order to control all eight reagents through only one syringe pump. However, that is the goal for future. For our purpose of proof-of-concept, we decided to make use of the available four-way solenoid valves manifold in the TRT lab and justify how well it can work in our system. However, another problem arose since these solenoid valves operate at 12 V, which is too large compared to our Arduino Mega 2560 pin's maximum voltage rate of 5 V. However, NResearch also provides electronic drivers along with the solenoid valves, which are the CoolDrive One Single Valve Drivers.

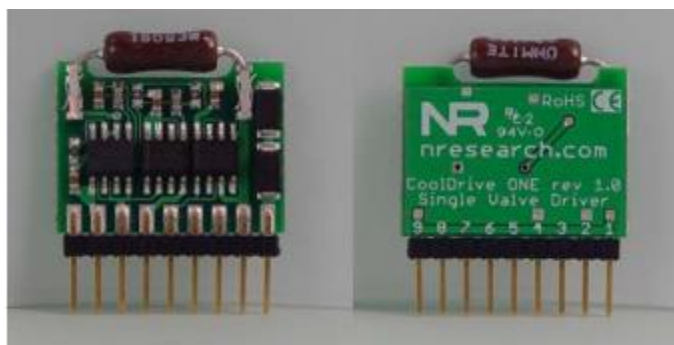


Figure 10 CoolDrive One single valve drivers

Retrieved from: <http://www.nresearch.com/Images/Drivers/CoolDriveONE.pdf>

This driver, seen in Figure 10, is a printed circuit board with IC chips built-in that can regulate 12 V power delivered from power supply to the solenoid valve driver. In the driver, there is logic chip that accepts 5 V digital signal from Arduino pin. The board basically then acts like a switch. If it receives 5 V from digital output of Arduino, it closes the switch and allows 12 V power to pass through. If it receives less than 0.8 V, it disconnects the switch and solenoid valve turns off.

4.2.5 Temperature Control

For the temperature control subsystem of our prototype, the team had to consider a number of different heating and cooling mechanisms to accurately control the incubation environment for the assays. The various options that were considered are discussed in the following sections.

4.2.5.1 Kapton heaters

The first option for temperature control was inherited from previous TRT work on this project, where they chose to use Kapton polyimide film, seen in Figure 11, from OMEGA Engineering Inc., attached to aluminum blocks as a heat source. This was used in parallel with a Minco CT325 microheater controller which utilized a RTD/thermistor sensor to better control the temperature. The operating voltage range is 4.75 V to 60 V DC while RTD input should be from 100 Ω to 1000 Ω and the thermistor input should be 50 k Ω . The power source provides energy to heater up to 240 watts and the RTD sensor

can detect temperature from 2° C to 200° C. The thermistor can detect temperature from 25° C to 75° C. The temperature is read with a voltmeter connecting to the left-most two pins with calibration of 0.010 V/°C.



Figure 11 Kapton heater

Retrieved from: http://www.omega.com/pptst/KHR_KHLV_KH.html

The Minco controller delivers power through red electrical wire to a dark orange thermfoil. These thermofolios are taped to a metal bar, which converts electrical power to heat. By controlling the amount of current delivered to the metal bar, the temperature can be adjusted. The entire temperature control setup can be seen in Figure 12 below.

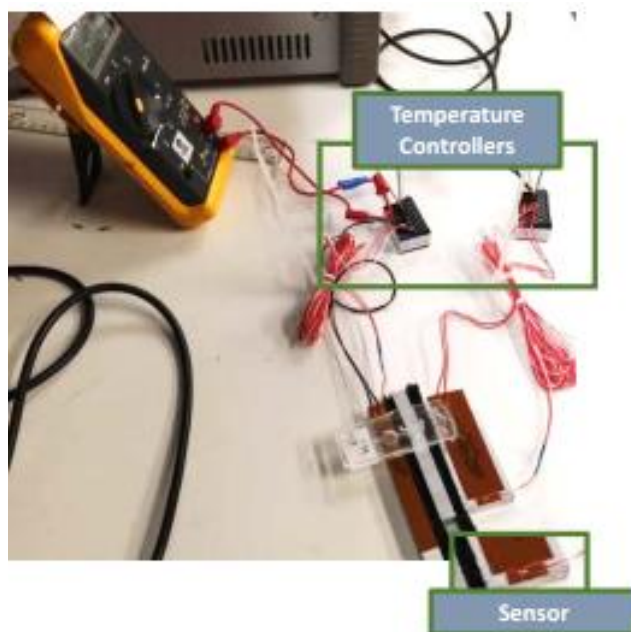


Figure 12 Potential heating system created by TRT team

However, the film has an area of 1 in x 3 in and energy density of 10 W/in² and 115 V power. Since it has such a high voltage requirement, it was expected that it would take a significant amount of time to reach the desired temperature when connected to the 20 V power supply.

4.2.5.2 *Peltier Thermoelectric Heating and Cooling*

One of the most popular heat control method is the Peltier TEC module, seen in Figure 13. The Peltier TEC makes use of the Peltier effect to generate heat flux across a p-n junction. The p-n junction is sandwiched between two ceramic plates, where one plate is bonded to the hot side of Peltier and the other is bonded to the cold side. When the Peltier module is provided with electrical energy, it will heat up one side and cool the other side. Moreover, this hot and cold effect can be opposite if we reverse the polarity of delivered energy. One of the most popular as well as reasonably priced Peltier modules is the TEC1-12706. It has dimensions of 40 x 40 x 3.8 mm and can operate from -30 °C to 83 °C, which includes all temperatures required for this project. The max voltage allowed is 12 V with a corresponding max current draw of 6.1 A.



Figure 13 Peltier TEC module

Retrieved from: <https://www.amazon.com/TEC1-12706-Thermoelectric-Peltier-Cooler-Volt/dp/B002UQQ3Q2>

When used to heat an 82 x 34 x 10 mm aluminum bar, the previously mentioned Kapton heater took almost 20 minutes to heat the block from room temperature (24 °C) to 37 °C. Since we needed the temperature transition to take less than five minutes, the Kapton heater option was discarded because of this long temperature change time. The group then tested the Peltier TEC to determine if the time for temperature change could be less than that of the Kapton heater. By attaching the hot side of the module to the same sized aluminum bars, the Peltier could heat up the aluminum bar from room temperature (24 °C) to 37 °C in two minutes and from room temperature (24 °C) to 65 °C in five minutes. With this

preliminary sample data, we concluded that the Peltier TEC module was appropriate for our design requirements. The TEC can also produce cold in order to stop the heating process and cool down the aluminum block back down to room temperature, which was another requirement for the heating system. This could speed up the cooling process compared to passive cooling that would be the method cooling used if the Kapton polyimide film heaters were selected. Finally, the TEC module is much cheaper than the polyimide film. As a result, with considerations of efficiency, price, and availability, we decided to select the TEC1 12706 Peltier TEC module as the temperature source.

4.2.5.3 Temperature Sensor

The device also required a temperature sensor to show the actual temperature of the heating block during the temperature control process. We wanted a sensor that can operate within the range of our assay temperatures, meaning it would have to maintain good performance at and beyond 65° C. Moreover, the temperature should communicate easily with the Arduino without requiring further implement of a driver setup or other communication protocol. One of the most popular and cost effective temperature sensors is the LM35, which can be seen in Figure 14.

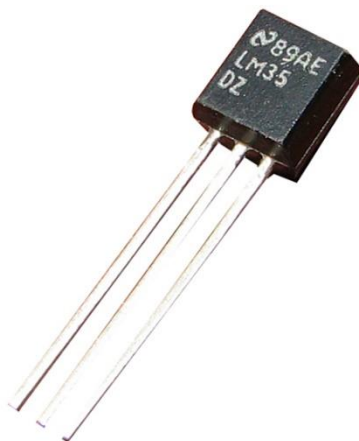


Figure 14 Temperature Sensor Retrieved from

www.google.com/search?q=lm35&rlz=1C1CHFX_enUS608US608&source=lnms&tbm=isch&sa=X&ved=0ahUKEwiZvcr70ZrTAhVM2SYKHTgxDFaQ_AUIBigB&biw=1270&bih=633#imgsrc=dCxcZGTs1zyamM:

This LM35 temperature sensor has an operation range from -55 °C to 150 °C, which is much larger than our maximum temperature requirement of 65° C. It also has a 0.5 °C accuracy at the ambient room temperature of 25 °C, which is adequate for our purpose of proof-of-concept. Moreover, current consumption of this sensor is only 60 µA and operating voltage ranges from 4 V to 30 V. Finally, it has simple communication with the Arduino via the analog input pin.

4.2.6 Heat and Fluid Controller Driver

After consideration and selection, we had chosen the three most important components for the system:

- Arduino Mega 2560 is the brain of the system, carrying out instructions to communicate and gather data from peripheral devices.
- P16 Linear Actuator, which will be attached to a syringe holder that can push or pull the syringe plunger to handle fluidic flow. Position data will feed back to the Arduino serial monitor and will be used to correspond how much volume associates with distance traveled.
- Peltier TEC module is used to generate heat to the metal block. The amount of heat or cold generated will be determined through power magnitude that we provide to the Peltier TEC module.

However, one problem in this design was that P16 Linear actuator requires 12 V power, while the Peltier TEC requires 8 V. Both these values exceed the 5 V limit of the Arduino and if they are connected directly to the Arduino pins, the Arduino will be immediately and irreparably damaged. Therefore, we needed an interface between the Arduino and these devices to regulate the power through the 5 V instructions of the Arduino. Moreover, another common feature between these two devices is that they need to be able to reverse and forward the polarity of voltage applied to them. For the linear actuator, forward drives the steel bar out, vacuuming the reagents into fluidic system, and reverse drives the steel bar in, dispensing the reagents to the 96-well plate. For the Peltier TEC module, forward makes the site facing the metal block heat up, and reverse makes that same site cool down, bringing the metal block back to room temperature (24° C). One of the most common circuitry that allows for this specification is an H-Bridge. Conveniently, we were able to retrieve an OTS motor driver controller board, a Pololu Dual MC33926 Motor Driver Shield for Arduino, from the TRT lab, seen in Figure 15 below.

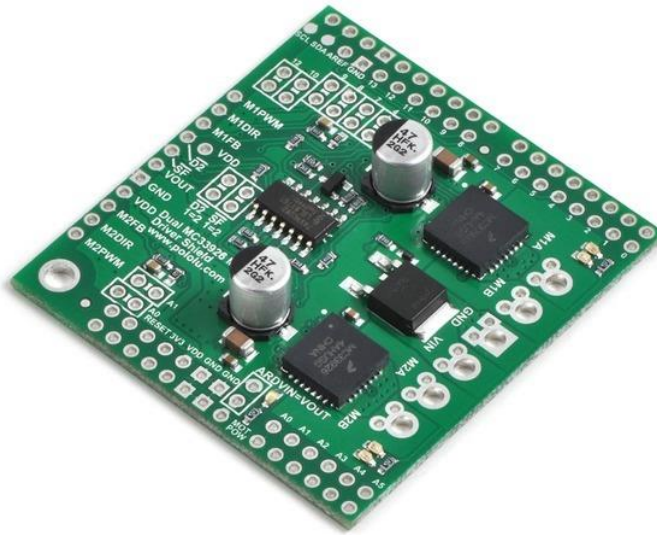


Figure 15 MC33926 Motor driver shield for Arduino microcontroller board

Retrieved from: <https://www.pololu.com/product/2503>

This driver board can handle voltage from 5 V to 28 V delivered to external devices and has a current limit draw of 3 A, while the maximum voltage for the actuator is only 12 V. With this number, we were not afraid of current overload with the 6 A breakdown limit of Peltier TEC module that can damage the Peltier. Moreover, this driver board is compatible with Arduino and therefore the board can be powered through the 5 V pin from the Arduino and receive the Arduino command to increase or decrease current draw to devices, and forward or reverse energy polarity to meet requirements. One of the most significant features of this board is its robust drivers that can limit over current draw, over temperature shutdown, under voltage shutdown, and short circuit protection. All of these power protections are not present in the Arduino, which is why the Arduino is very sensitive to power surge, which can damage the board. Finally, Pololu created a library that simplifies communication protocol between the Arduino and the MC33926 board. The user only needs to call a single line of code to control delivered power and power polarity which saves a significant amount of time in integrating the system using this motor driver board.

4.2.7 Control Mechanism

One problem with the Peltier TEC module was that if it continually received full energy draw from the power supply, it would continue to heat up and will eventually reach its max operating temperature and break. Moreover, we wanted to keep the system to be stable at specific assay temperature of 37 °C and 65 °C. Lastly, it was desirable to not only heat up the metal bar but also cool it down to room temperature (24 °C) or even below for future application of freezing samples. As a result, we needed an automated controlling method that can vary energy delivery to the Peltier module as well as be able to

reverse that power so as to cool down the metal bar. There were two iterations on this part: One was to use power relay. The relay is an electrical component that acts like a toggle switch (turning on and off the power) with more advanced feature: built-in voltage regulation for preventing power surge which can be automated through a microcontroller. It is also one of the most common mechanisms for temperature control in a standard house thermostat: If we use a heater and want to reach 40° C, the thermostat tracks the temperature sensor until it reaches 40° C and switches off power relay. If the temperature is below 40 °C, relay will be switched on. This on-off mechanism, however, does not meet with our product requirement closely. Since we need the temperature to only have a tolerance of ± 1 °C, turning on and off power cannot do it. This is because if we turn off the heater, while being full powered, at 40 °C, the metal block still has internal heat remains that can keep increasing the block temperature far off. Moreover, relay cannot support the function of reversing power polarity but only passive cooling. As a result, we needed to come up with an option that can reverse power polarity and when the block temperature is approaching the desired temperature, lower the current draw from power supply. Therefore, since our goal was to automatically adjust the control value, the team implemented a PID control mechanism.

4.2.7.1 PID explanation

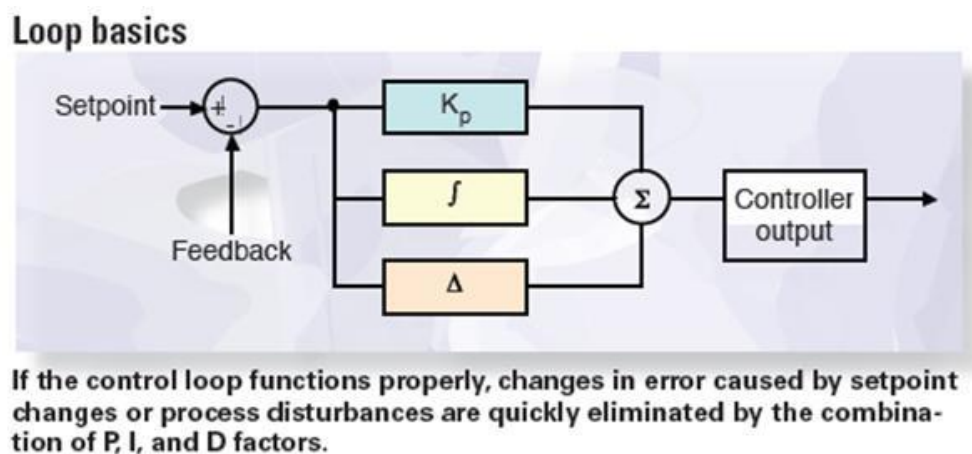


Figure 16 PID Control Loop

Retrieved from: <http://machinedesign.com/sensors/introduction-pid-control>

PID is also known as a Proportional, Integral, and Derivative control loop, which are widely used currently. An example of this control loop can be seen in Figure 16. One popular control loop concept in daily life is driving car. When you are driving your car, if you are reaching your destination, you see your speedometer is at 65 mph and you want to slow down to 30 mph, 20 mph and then 0. The less offset distance you are away from the destination, the less speed you want your car to have and vice versa. As a result, your eyes, speedometer, foot, and gas pedal form a control loop that allows you to adjust the

car speed properly. In a similar way, the PID controller computes the output (speed) to be based on the input error of travel distance. In PID, we can control three parameters:

- **Proportional factor:** This factor controls the regulated output by multiplying the measured input error and a certain gain factor. This control type allows the system, if far away from desired goal, to approach the goal faster. However, one problem is if the gain factor is too large, it can cause overshoot, meaning that the system can go above the desired goal level. In addition, it takes long time for system to stabilize from that oscillation. Moreover, when error is small, the control loop cannot detect it well and barely any output appears. Therefore, for a more accurate control system, using proportional factor alone is not enough.
- **Integral factor:** This factor considers the offset error and duration of offset. From that, the integral factor integrates the error over time and based on that sum, changes output to reduce that error sum of the previous calculation. On the other side, as the 'I' factor takes into consideration of past error, it can result in overshoot to the desired goal.
- **Derivative factor:** This generates a rate of error instantaneously and computes the product of that rate with a certain gain factor. The derivative factor deals with how fast the error is changing over time so it can compensate the stability of the control system. Therefore, we can use this factor for stabilizing the system but not for approaching desired goal fast as proportional system.

Since our heating systems has requirements of reaching assay temperature (37 °C, 65 °C, room temperature (24 °C) with an offset allowance of 2 °C, we only consider proportional factor since it can satisfy above goals while also being the easiest factor to tune.

4.3 Feasibility Studies and Experimental Modeling

4.3.1 Fluidic Control System Modeling

Because of the nature of the requirements for this project, it was difficult to perform a feasibility study on the fluidic control portion of the device. Because of the early stage and proof-of-concept nature of the device, there was no specification for flowrate, time of fluid control, tubing diameter, size constraints, or other such areas of concern. As such, the feasibility of the device had to be determined through empirical and experimental methods. However, the team did analyze the solenoid valve manifold system to determine what effects the internal pathway of the valve manifold used would have on the system by creating spaces for fluid dead volumes and cross contamination. Later in the project, we found through experimentation that this value was not consistent and varied with different

conditions. The architecture of the valve manifold can be seen in Figure 17 and full calculations are below.

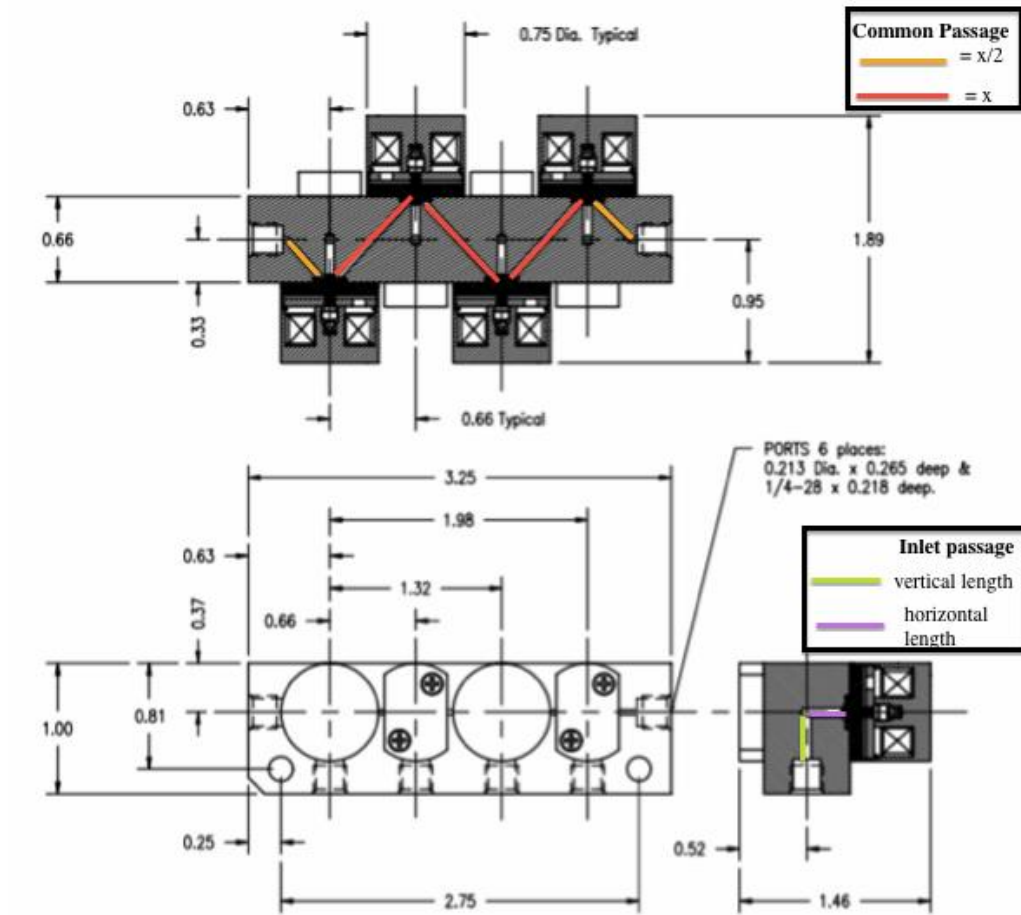


Figure 17 NRResearch valve manifold technical drawing: modified by MQP team to highlight path lengths

Retrieved from <http://www.nresearch.com/>

In order to calculate or analyze the internal pathway in the solenoid valve manifold, the following steps were performed. In order to calculate the total length of the common passage, the length of the common passage consisting of diagonal path was calculated.

Length of common passage (Diagonal paths= x , $x/2$)

$$x = \sqrt{0.66^2 + 0.66^2} = 0.93 \text{ in}$$

$$x/2 = 0.467 \text{ in}$$

Total Length of the common passage can be calculated by using the following equation:

$$= (x*3)+(x/2*2)= (0.93*3)+(0.467*2) \text{ in} = \mathbf{3.72 \text{ in}}$$

Inlet Passages consists of horizontal and vertical lengths. In order to calculate the total length of the inlet Passage, both the horizontal and the vertical lengths were added.

Horizontal length= $0.66/2 = 0.33$ in

Vertical length= $0.81/2 = 0.406$ in

Total Length of the Inlet passage can be calculated by using the following equation:

= (vertical length of each inlet passage + horizontal length of each inlet passage) * 4

= $(0.406 + 0.33) * 4 = 2.944$ in

Internal Volume for the common passage = 91 uL (Given in the drawing)

Internal Volume each inlet port = 32.5 uL (Given in the drawing)

The area of the common passage can be calculated by dividing total volume by total length. The following equation was used to calculate the area of common passage:

Area of the common passage (A_1) = Total Volume / Total Length = 91 uL / 3.72 in

= $0.00556 \text{ in}^3 / 3.72 \text{ in} = 0.00149 \text{ in}^2$

The diameter of the common passage was calculated by using the area of the common passage.

Diameter of the common passage

= $\sqrt{(4 * A_1) / \pi} = \sqrt{(4 * 0.00149) / \pi} = 0.042$ in

Similarly, the area and diameter of the inlet passage was calculated using the following equations:

Area of each inlet (A_2) = Volume in each inlet passage / Length of each inlet passage

= $32.5 \text{ uL} / 0.736 \text{ in} = 0.0198 \text{ in}^3 / 0.736 \text{ in} = 0.0269 \text{ in}^2$

Diameter of each inlet = $\sqrt{(4 * A_2) / \pi} = \sqrt{(4 * 0.0269) / \pi} = 0.185$ in

Since resistance of the flow is directly proportional to length, the team tried to reduce the length of the wire tube connecting the manifold. The team used 1/32 in diameter tube. In order to lower the resistance of the flow, the smaller diameter tube can be used for the prototype.

4.3.2 Temperature Control System Modelling

The general idea was to heat the 96-well plate with samples inside by placing it on a heat-conducting platform. This platform would be required to be a good conductor, easily machined, and simple to interface with a 96-well plate. The first step in this process was selecting material for the heating platform. Two of the most common heat-conducting materials are aluminum and copper.

Therefore, it was important to carry out a rough analysis on the heat conduction characteristics, namely, how fast the material can heat up 96-well plate from room temperature (24° C) to the final desired assay temperature of 37 °C and 65 °C as well as how fast can it cool the 96-well plate from the desired assay temperature back to room temperature. Lastly, given the selected material, it was necessary to decide on how to machine the metal block so that it could facilitate heat conduction between the Peltier TEC module and the block, and between the block and the 96-well plate. Given our short time range at TRT, we cannot conduct all testing to determine which part to choose or which material to choose. Therefore, this modelling section would provide theoretical calculation that can help us select an option without experimental testing. This gave us an educated starting point and provided more insight for future improvement.

4.3.2.1 Transient Model for Heating: Aluminum vs. Copper

First, a modelling for transient response of how temperature versus time behavior between copper and aluminum was conducted. In this model, we used the transient equation as follows:

$$\Theta = \frac{E_{in}}{h * A} + \left(\Theta_i - \frac{E_{in}}{h * A} \right) * e^{-t/Tau}$$

Θ is the temperature difference between current temperature and ambient temperature, which was chosen to be 25 °C. Θ_i is the initial temperature difference which we assumed was 0 °C because the metal block had remained at room temperature for some time. E_{in} is power delivered to the Peltier TEC module. Since we used 8 V from power supply and we had 1.5 A current draw on average, the energy value was calculated as:

$$Energy = V * I = 8 * 1.5 = 12 \text{ Watts}$$

For the purpose of proof-of-concept, we only used three rows of wells, each row having eight wells, for each assay. Therefore, to reduce the time and effort in machining metal block, we chose the size of block that could fit three rows of wells. The dimension found by rough estimation gave the area of metal block as 0.006954 m². The value h is a heat transfer coefficient, which were advised by a mechanical engineer in TRT to be 30 $\frac{W}{K*m^2}$. Tau value in here represents time versus temperature relationship of different metals. The equation we used for tau calculation was:

$$Tau = \frac{m * c}{h * A}$$

Tau calculated for aluminum was 196.29 seconds and for copper was 278 seconds. The variable m is the mass of the metal block. The mass of the aluminum block was chosen to be 0.045 kg and the mass of copper block was chosen to be 0.15 kg. These mass values were calculated using the same area of 0.006954 m² as above. C is the specific heat capacity value for copper and aluminum, which are 390

$\frac{J}{Kg \cdot K}$ and $910 \frac{J}{Kg \cdot K}$ respectively. Putting those values into above Θ transient equation, we could find the temperature of metal block by:

$$Metal\ Temperature = \Theta + Initial\ Metal\ Temperature = \Theta + 25$$

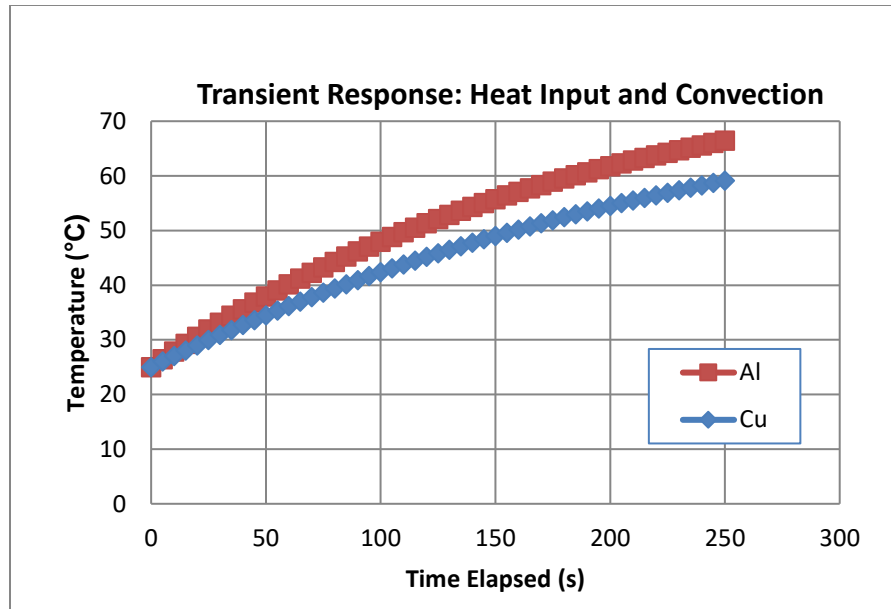


Figure 18 Transient Response: Heat Input and Convection of Aluminum vs. Copper

As we can see from Figure 18 above, aluminum in red takes less time to heat up than copper in blue. From this graph, we predicted that aluminum can bring the heat station from room temperature (24 °C) to assay temperature faster than copper. However, it was also required to make sure that the system is capable of returning to room temperature since there are assay steps incubating samples at room temperature. As a result, the following section will study the cooling capability between the two materials before making decision.

4.3.2.2 Transient Model for Cooling: Aluminum vs. Copper

In this model, we used the transient equation based on Newton's law of cooling as follows:

$$T(t) = T_{env} + (T(0) - T_{env}) * e^{-\frac{t}{\tau_0}}$$

The ambient temperature (T_{env}) was chosen to be 22 °C based on room temperature in TRT station at that time. The block was assumed to be near 54 °C at the beginning ($T(0)$). All other values, such as heat coefficient and tau values were kept the same as the previous modelling. Putting these numbers into $T(t)$ equation, we had cooling characteristics of aluminum and copper as seen in the graph below.

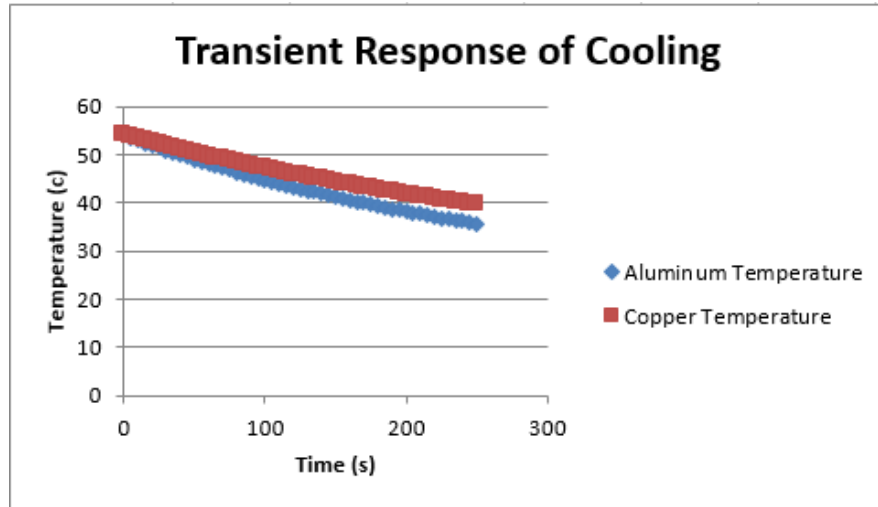


Figure 19 Transient Cooling Response of aluminum versus copper

As we can see from Figure 19 above, aluminum in blue cools down faster than copper in red from 54° C. From these cooling and heating experiments, testing with both aluminum and copper blocks with the same surface area and thickness, we concluded that aluminum can both heat up and cool down faster than copper. Therefore, aluminum was chosen as the material for heating station.

4.3.2.3 Thermal Conductance Circuit

After selecting aluminum as the material for the heating block, it was important to decide how we should machine the metal block to facilitate the best heat conduction between the metal block and the 96-well plate. The first idea was to use a thin aluminum sheet as can be seen from the diagram below. In this method, we would attach the Peltier TEC module to one end of the block surface so it can transfer the heat to the aluminum sheet and then place the polystyrene well plate onto the sheet, near the Peltier TEC. We will justify this configuration's thermal resistance in a generalized system. It should be noted that for the purpose of simplicity of the model, air resistance was disregarded and thermal contact conductance was assumed to have one constant value of $20000 \frac{W}{K \cdot m^2}$, which was advised by a TRT mechanical engineer. Moreover, since the internal design of Peltier TEC is a p-n junction, which is complicated to model, we also disregarded the Peltier TEC internal heat resistance.

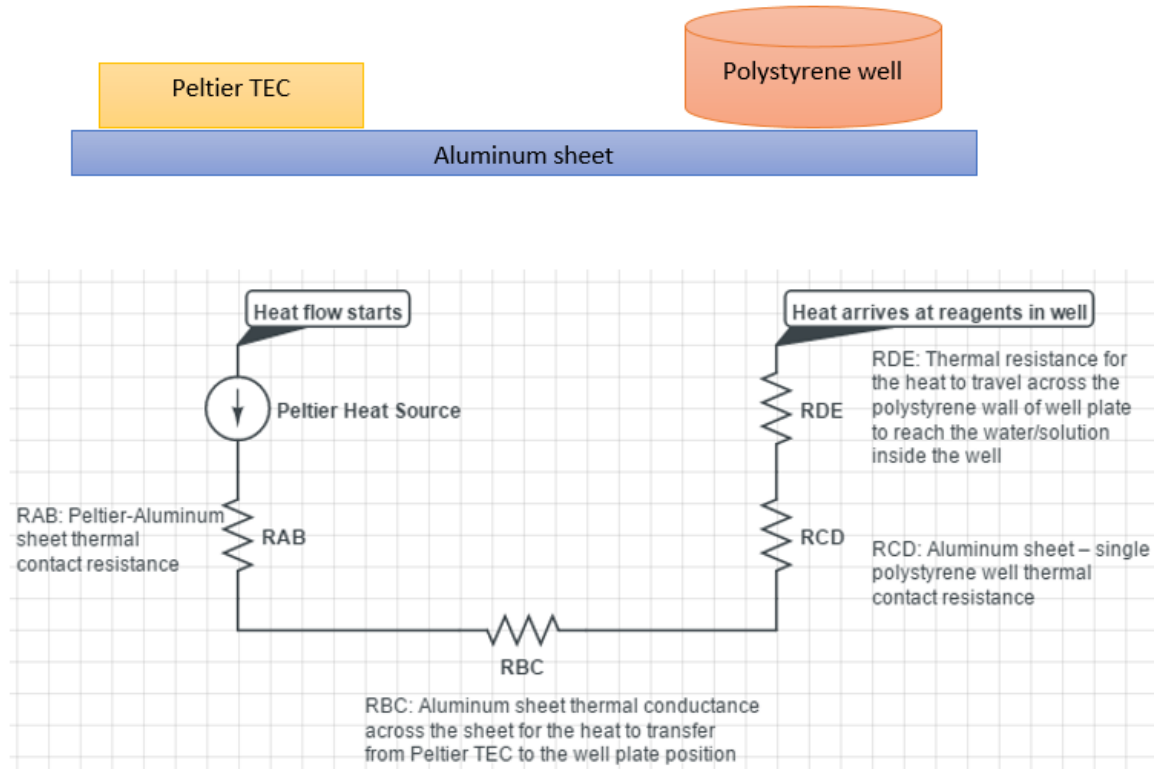


Figure 20 Thermal circuit of aluminum sheet with polystyrene well

A typical thermal system usually breaks down into a resistance circuit similar to an electrical resistor circuit and can be used to study thermal behavior. The heat source, similar to a power source, delivers energy through several blocks of resistances. In our system, the thermal resistance circuit represents how much of the original heat will remain after going through the Peltier-metal block contact resistance, internal metal block resistance, and so on until it reaches the output. The output of this system is the temperature inside the polystyrene wall. As we can see from Figure 20 above, we have four resistors in series. We can calculate the value of each resistance as following:

- RAB: Peltier-Aluminum sheet thermal contact resistance. h_c is the thermal contact conductance is: $20000 \frac{W}{K \cdot m^2}$. A is the surface area of Peltier TEC module. From that, we can find the thermal contact resistance with our Peltier TEC module area as:

$$R_{PeltierContact} = \frac{1}{h_c * A} = \frac{1}{20000 * 0.0016} = 0.03125 \frac{K}{W}$$

- RBC: Aluminum sheet thermal conductance across the sheet for the heat to transfer from Peltier TEC to the well plate position. This can be calculated using following equation:

$$R_{Sheet} = \frac{x}{A * k} = 6.9686 \frac{K}{W}$$

In this equation, x is length of material that is parallel to heat flow, which we found to be 0.035 m. K is thermal conductivity of material. For aluminum, this number is $205 \frac{W}{K \cdot m}$. A is the cross-sectional area that is perpendicular to heat transfer flow, which in our case is, 0.0000245 m^2 .

- RCD: Aluminum sheet – single polystyrene well thermal contact resistance. In here we have the similar equation as above:

$$R_{Contact} = \frac{1}{hc * A} = \frac{1}{20000 * 1.01203 * e^{-5}} = 4.94055 \frac{K}{W}$$

- RDE: This is the thermal resistance for the heat to travel across the polystyrene wall of well plate to reach the water/solution inside the well.

$$R_{Polystyrene} = \frac{x}{A * k} = 933.083 \frac{K}{W}$$

Here we assumed that the temperature right at the inner layer of the polystyrene well will be the same as that of the fluid contained in the well in order to simplify our calculation. The system, starting from RAB and ending at RDE, is a series of thermal resistors with the end of each resistor as the start of next resistor. With this series resistance circuit, we can calculate the total thermal resistance by adding up RAB, RBC, RCD and RDE to be $945.023 \frac{K}{W}$ for the first set up of heat block.

In the second setup, instead of a thin aluminum sheet, we used a thicker metal block in which we drilled holes that could hold the wells and reach halfway up the well wall. The same simplification for the thermal system analysis was kept similar to the above setup.

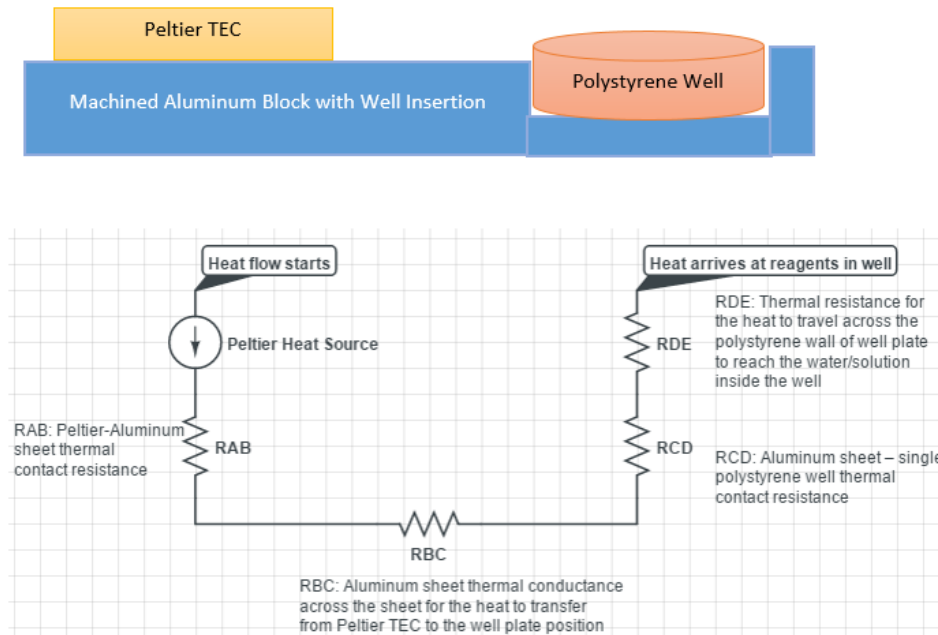


Figure 21 Thermal circuit of a machined aluminum bar and polystyrene well

As we can see from Figure 21 above, we have four resistors in series with each other. We can calculate the value of each resistance value as follow:

- RAB: Peltier-Aluminum block thermal contact resistance. We can find the thermal contact resistance with our Peltier TEC module area as:

$$R_{PeltierContact} = \frac{1}{hc * A} = \frac{1}{20000 * 0.0016} = 0.03125 \frac{K}{W}$$

- RBC: Aluminum sheet thermal conductance across the sheet for the heat to transfer from the Peltier TEC to the well plate. This can be calculated using following equation:

$$R_{Sheet} = \frac{x}{A * k} = 0.813 \frac{K}{W}$$

- RCD: Aluminum block – single polystyrene well thermal contact resistance. Here we have similar equation as above:

$$R_{Contact} = \frac{1}{hc * A} = \frac{1}{20000 * 0.00021} = 0.41 \frac{K}{W}$$

- RDE: This is the thermal resistance for the heat to travel across the polystyrene wall of well plate to reach the water/solution inside the well.

$$R_{Polystyrene} = \frac{x}{A * k} = 409.96 \frac{K}{W}$$

The second system is also a series of thermal resistors. We can calculate the total thermal resistance by adding up RAB, RBC, RCD and RDE, whose sum ends up with the total thermal resistance of 411.216 $\frac{K}{W}$ for the second set up of the heat block.

As we can see after calculating the value for each heat block setup, even though we have a thicker metal block for second setup, it only results in 411.216 $\frac{K}{W}$ compared to 945.023 $\frac{K}{W}$ from the first setup. The second configuration is only 43.5% resistance compared to the first one. This difference is because when we introduce more contact area between the aluminum block and polystyrene well by insertion, we facilitate more heat transfer between them. Therefore, the contact area increases, thereby decreasing the thermal resistance value. Moreover, by fitting each well into metal block, each polystyrene row can be kept more tightly rather than taping into aluminum sheet like in setup one. As a result, we decided to select the second setup for the heat station.

4.4 Final Design Approach

4.4.1 Prototype Architecture

After creating an ideal system architecture, the team also created a basic architecture drawing of the prototype system itself to have a simplified view of the various subsystems that made up the device. This representation can be seen in Figure 22 below.

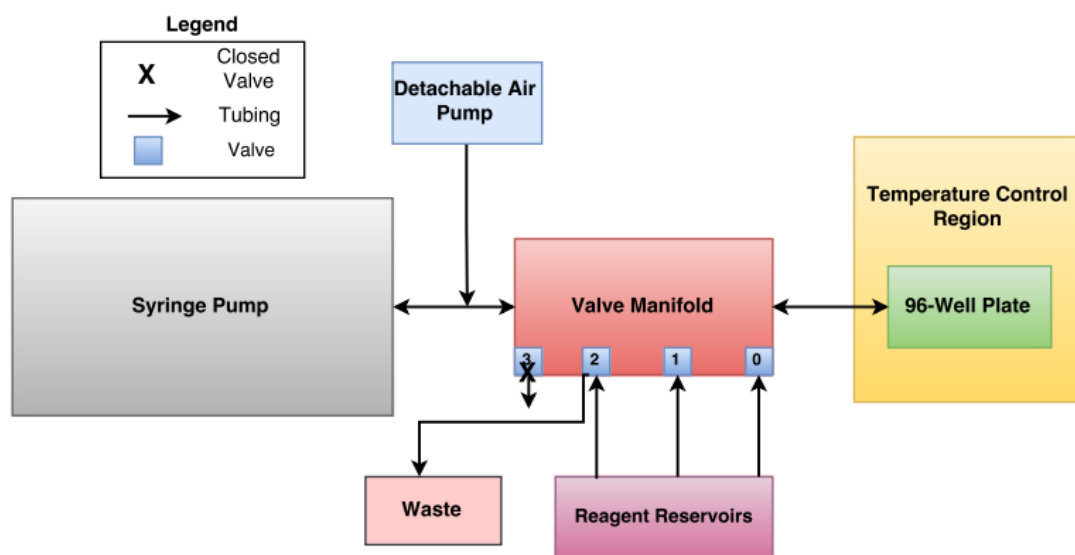


Figure 22 Prototype Architecture

4.4.2 Assay Selection

In order to meet our objective to create a prototype device, which could perform multiplexed assay for the cells, our team looked into different potential substances (contaminants) affecting MSCs during quality control. To accomplish this goal, the team researched various OTS assay kits for mycoplasma, trypsin, endotoxin and BSA. Due to the time constraints of the seven week term and for the sake of proof-of-concept, only mycoplasma and BSA Assay kits were chosen, with the thought that other assays could be implemented in the future. Though a number of manufacturers sell assay kits to detect these contaminants, they differ in terms of sensitivity, time to run the assay, cost, read-outs, temperature, and procedure steps for the assay. After comparing these parameters, the most similar assay kits were chosen based on parameters like read-outs and procedure steps. The comparison tables for both OTS shelf assays can be seen in Table 2 and Table 3 below; the team's choices for each assay are indicated by italics.

Table 2 OTS BSA Assay Tradeoff Analysis

Parameter	Cygnus Technologies	MyBioSource
Sensitivity	0.124 ng/mL	85.5 ng/mL
Time	2 hours	2 hours
Cost	\$525	\$430
Principle	ELISA	ELISA
Read-out	Absorbance	Absorbance
Sample Preparation	Sample dilution	Supernate preparation

Table 3 OTS Mycoplasma Tradeoff Analysis

Parameter	Roche	Thermo Fisher	ATCC	R&D Systems
Sensitivity	10 CFU/mL	4 CFU/mL	Unavailable	15 CFU/mL
Time	5 hours	5 hours	Unavailable	4.5 hours
Cost	\$1000	\$3000	Unavailable	\$380
Principle	Polymerase Chain Reaction (PCR)	PCR	PCR	DNA hybridization/ELISA
Read-Out	Fluorescence, impedance	Fluorescence	Fluorescence, impedance	Absorbance
Sample Preparation	Lysis solution	Lysis solution	Lysis solution	Lysis solution

Additionally, the chosen kits came with precoated assay plates, appropriate for each assay. These assay plates were in stripwell form so the team could continue with the goal of using only the necessary amount of wells for each assay run. It also allowed for easy transfer to a standard absorbance microplate reader.

4.4.3 Fluid Control

After extensive iterations and analysis of potential components, the team chose appropriate components to make up the final fluid control subsystem. The system can be seen in Figure 23 below.

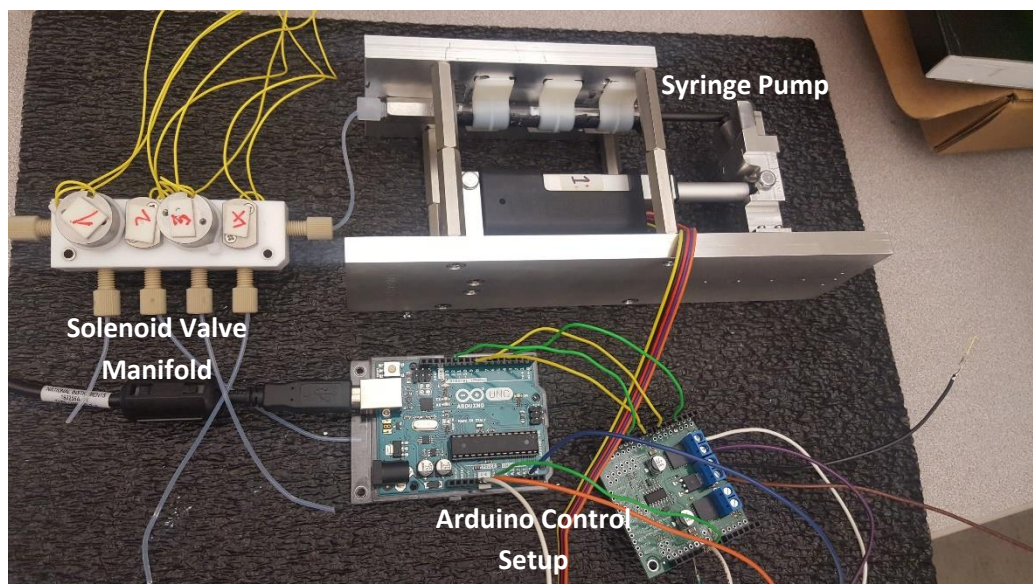


Figure 23 Fluid control system consisting of syringe pump and solenoid valve manifold

After the previously discussed iterations and research, the team decided to utilize a simple syringe pump system that was created in house at TRT. This syringe pump consisted of a machined aluminum platform that supported a Hamilton gas tight 1 mL syringe. The glass syringe plunger is attached to a P16 Actuatorix linear actuator. At the syringe tip, we connected 1/32 in outer diameter tubing into the NResearch solenoid valve manifold, which was controlled by the CoolDrive One Single Valve Driver. The whole system was controlled through the MC33926 motor driver shield from Pololu and an Arduino microcontroller board. This option for fluid control was chosen because of its immediate availability and simple design that would lead to minimizing testing time and more thoroughly showing proof-of-concept for the device. An in-house pump was used because of the cost and time it would require to purchase an OTS pump; however, if a syringe pump was used in the future for the final design of the device, a much more precise and well-manufactured pump would be used instead.

The fluid control system also consisted of a removable vacuum pump that was used to flush the system between additions of reagents. This pump remained removable and was only attached to the system when needed because of difficulty had with attaching the pump without adding large amounts of excess tubing pathways. This pump was retrieved from a TRT lab and was controlled by a direct connection to a 12 V power source.

4.4.3.1 Fluid Control System Schematic

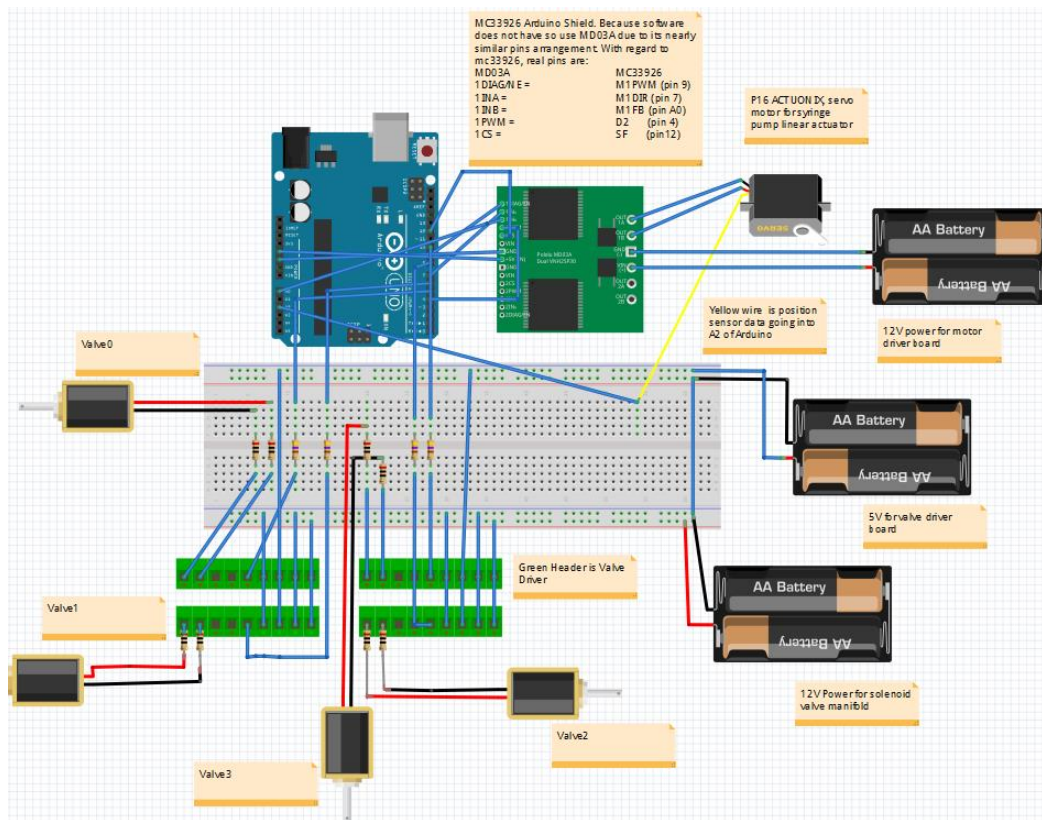


Figure 24 Schematic showing control of syringe pump and valve manifold system

The schematic, seen in Figure 24, was drawn using Fritzing software, which is an open-source tool online that allows the user to draw schematics for the Arduino and the most popular Arduino components. From the above figure, we show a more detailed representation about how each component communicates with each other. Here the MC33926 Motor controller Arduino Shield is replaced with a MD03A Motor Driver since there is not schematics library for the MC33926 version and the MD03A is the closest match inside software library. Therefore, we replaced the MD03A as our motor driver and specified the correct name in the picture. As we can see on the motor driver board, the two ports in middle are connected to a 12 V power source so as to drive the P16 Actuator through two top terminals. By sending commands from the Arduino to the motor driver to the M1PWM pin, we can control how fast or slow, reverse or forward mode the linear actuator should travel. Since the valve manifold we use has four single valves inside it, we tried to replicate with four motors, naming them valve1, valve2, valve3 and valve4. The motor and valve driver have the same design of two connections into positive and negative rails of power supply, as we observe the black and red wires in the picture. These four valves will be turned on and off through four separate 8-pin CoolDrive One valve driver as represented in four green 8-pin headers. The input to pin 1 and pin 2 will be 12 V of power to

power the valve when on through pin 8 and 9. This power delivery is turned on and off through the 5 V digital signal from Arduino feeding into pin 5 of the valve driver. A more detailed schematic of the resistances and voltages at each step during this process can be seen in Figure 25.

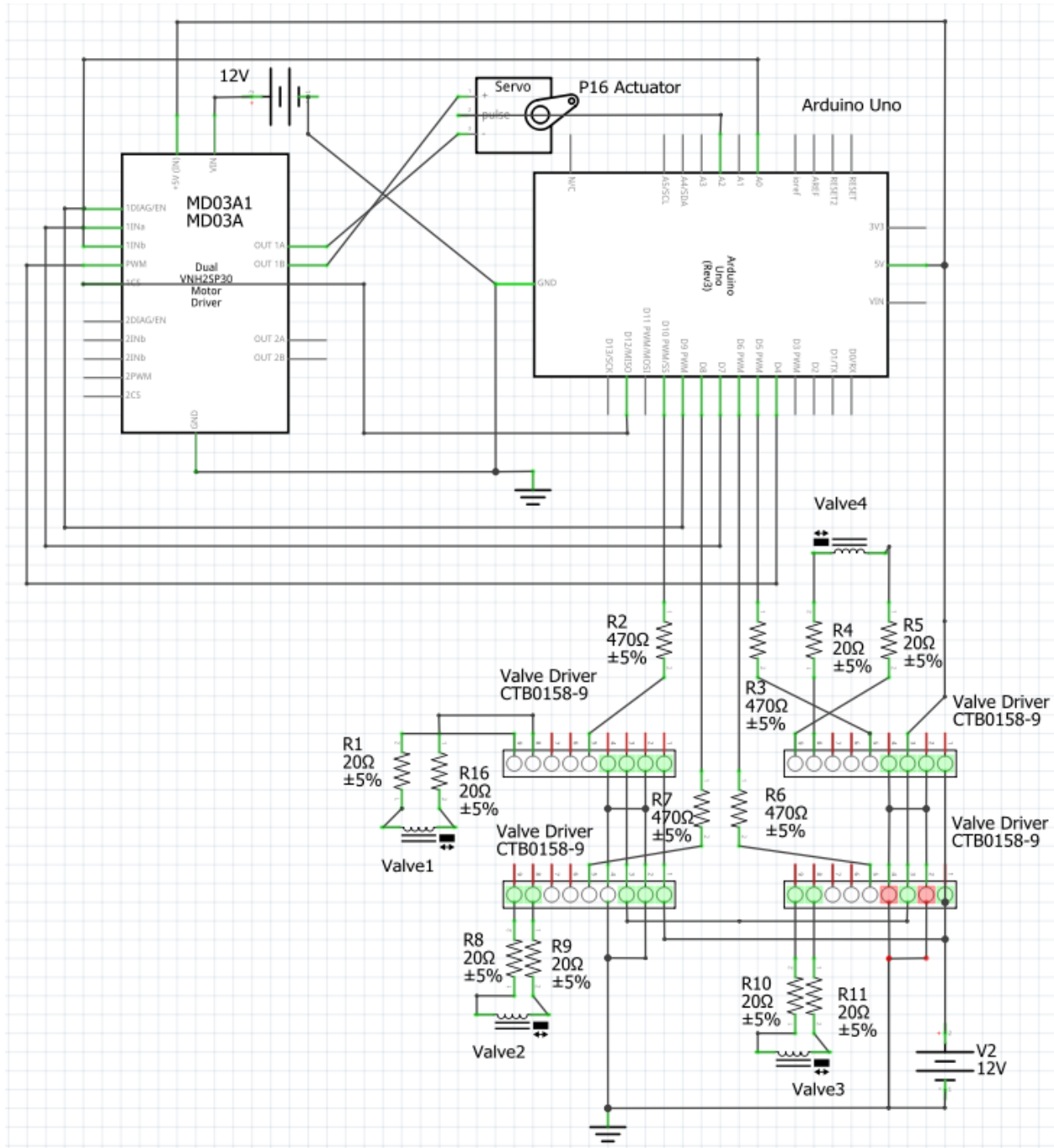


Figure 25 Fluidic control subsystem detailed schematic

4.4.4 Temperature Control

4.4.4.1 Temperature Control System Architecture

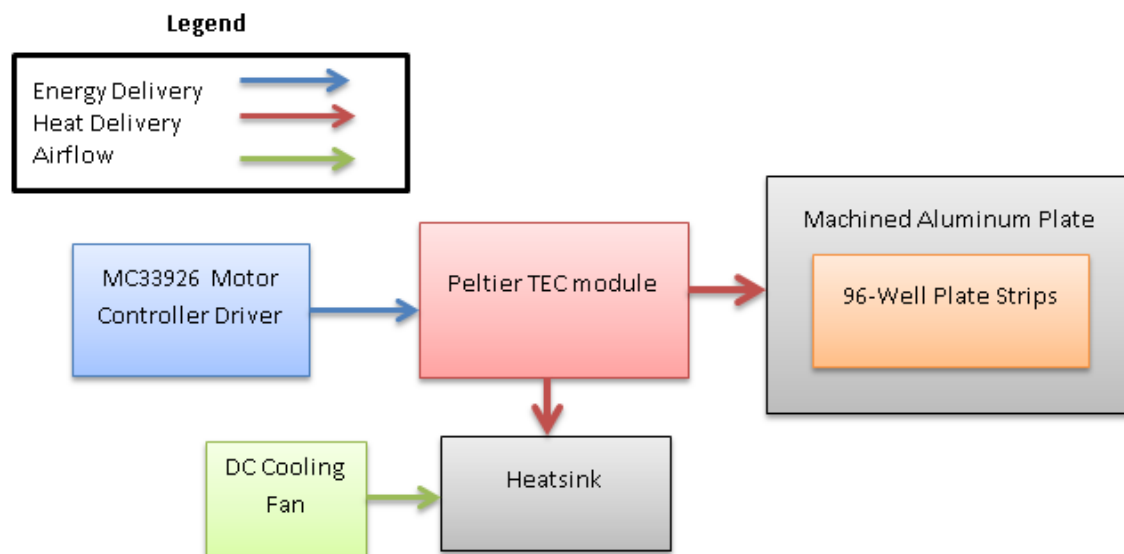


Figure 26 Prototype temperature control system architecture drawing

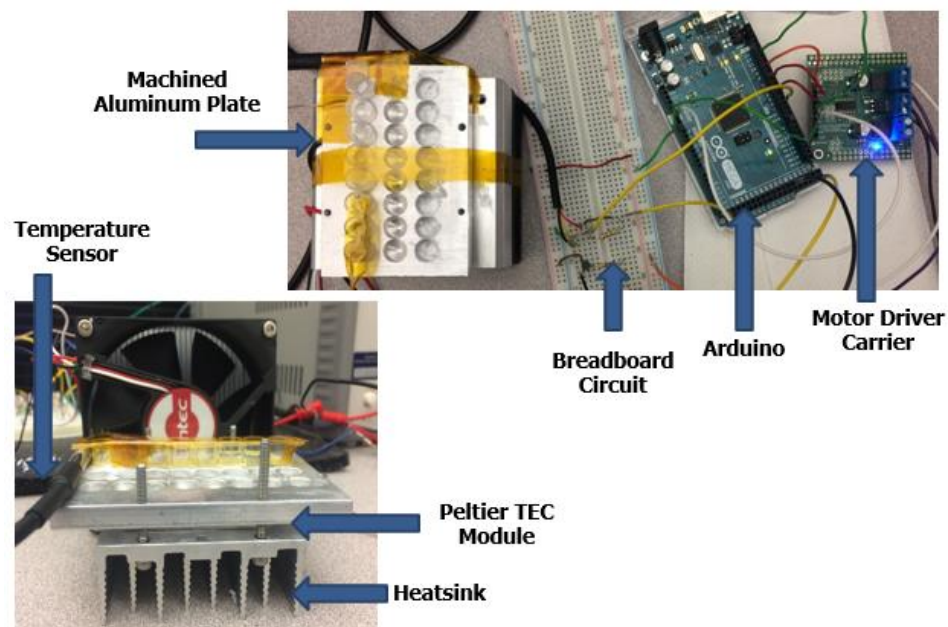


Figure 27 Image of entire temperature control system

Figure 26 presents a block diagram for the heat control system flow and Figure 27 shows the experimental setup of the temperature control system. As we can see, the MC33926 motor controller driver will receive Arduino command for how much power should be drawn from the power supply and fed into the Peltier TEC module. This amount of power in blue then flows into the Peltier TEC, triggering

the Peltier effect across the p-n junction and generating heat flow in red to the machined aluminum plate. The plate temperature will be reported back to the Arduino in order to readjust power magnitude so as to make the metal plate stays consistently near the desired assay temperature. The heat/cold flow in red on the other side will be absorbed through the heatsink and then blown away by air flow in green from a DC cooling fan. This method is to prevent change in temperature on the opposite site facing heatsink from disturbing heating process at aluminum plate.

4.4.4.2 Temperature Control System Schematic

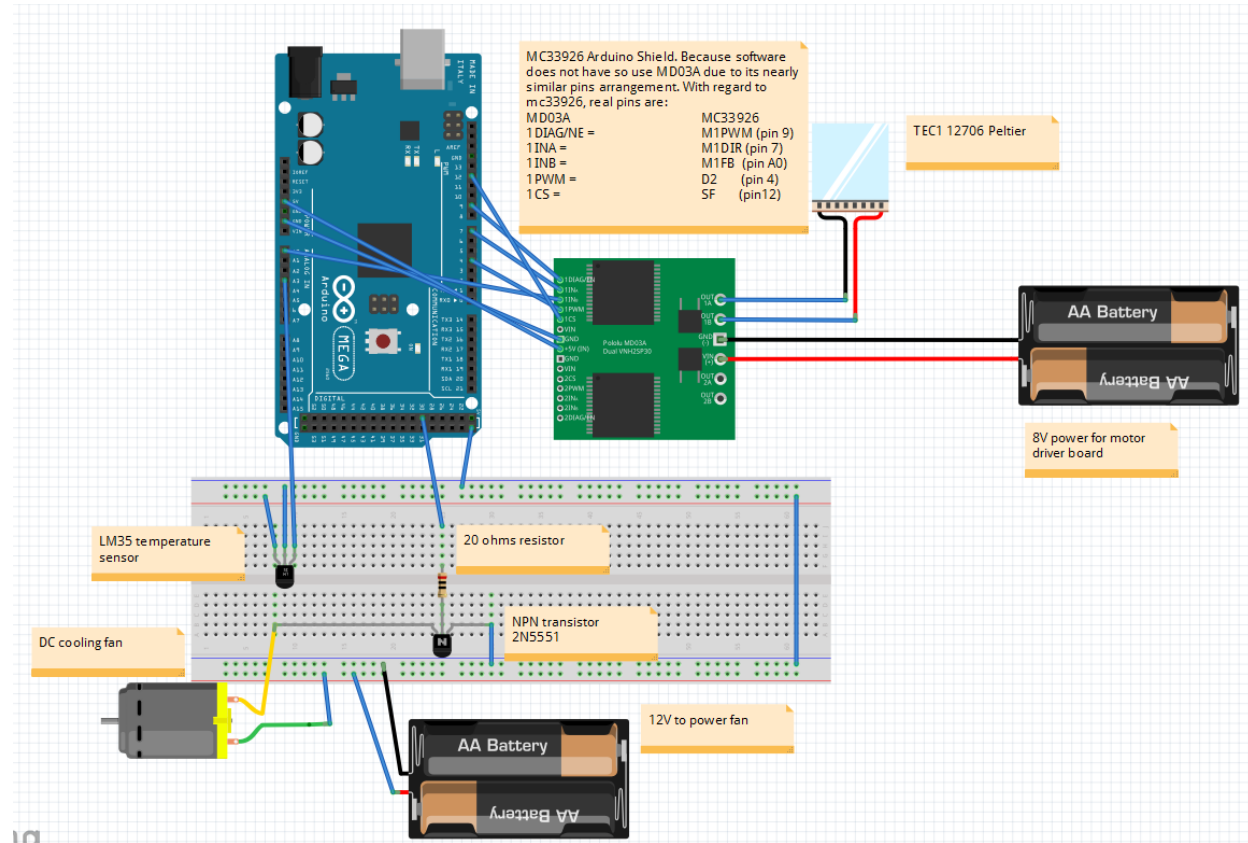


Figure 28 Temperature Control System Schematic

Similar to the previous shown schematics for fluidic control, the MC33926 Motor controller Arduino Shield is replaced with a MD03A Motor Driver since there is not a schematics library for MC33926 version. As we can see on the motor driver board, the two ports in middle are connected to an 8 V battery to drive the Peltier TEC module through the two top terminals. Power magnitude and polarity are also controlled through Arduino commands. Additionally, the LM35 temperature sensor reports data through analog input pin 3 on the Arduino. Moreover, the DC cooling fan is controlled through a switch-like NPN transistor. When digital pin 31 writes a high signal to the middle terminal of NPN transistor, the cooling fan yellow negative terminal is connected to both ground and turn on. On the other site, if the digital

signal is low, the negative terminal is connected to the open circuit and no power can flow across the DC fan. The entire schematic for the temperature control system can be seen in Figure 28 and a more detailed schematic of the resistances and voltages at each junction can be seen below in Figure 29.

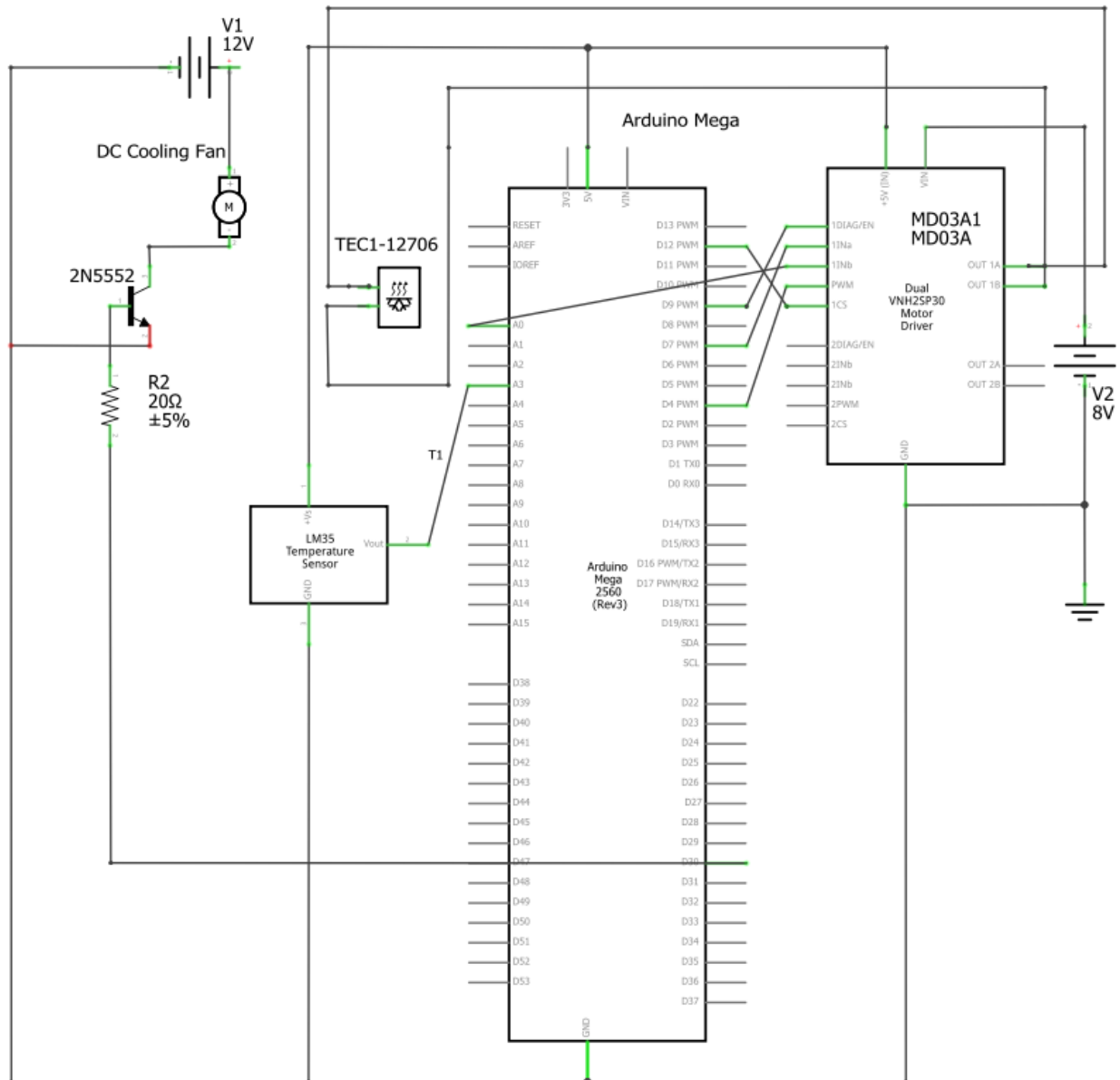


Figure 29 Temperature control subsystem detailed schematic

4.5 Pretotype Design

The team's client statement included creating both a prototype of the proof-of-concept device and a pretotype for the potential future product. A pretotype is a future concept describing the completed product as it could be in the future, upon completion of the project, with all goal product objectives met. The objectives for this device include that the device be automatable, multiplexed, time

efficient, cost efficient, scalable, regulation compliant, and used for autologous transplant of MSCs. The pretotype describes the ideal sub-sections of the device, consisting of a sample preparation area, reagent distribution system, temperature control regions, proper reagent storage, waste storage and removal system, and finally the assay plate itself where the assays will be performed. A SolidWorks mock-up of a potential design for this device can be seen in Figure 33 below.

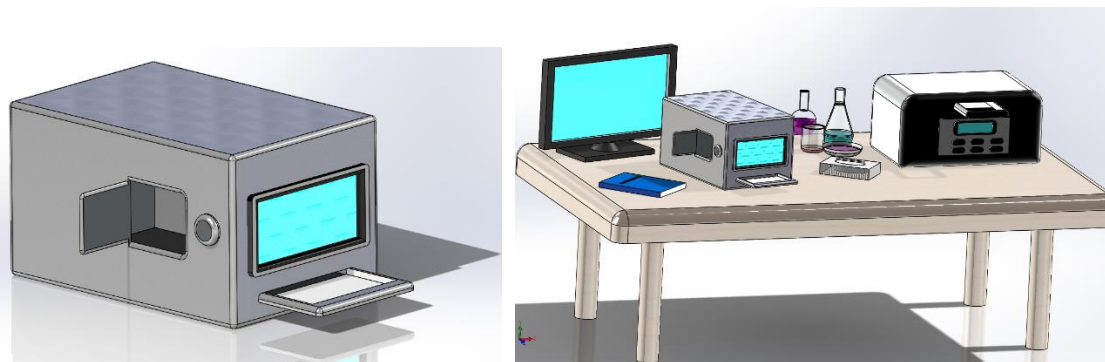


Figure 30 SolidWorks drawing of potential assay device (left) and potential assay device integrated into a lab bench setting (right)

In this device, the cell sample to be tested would be pipetted into the designated reservoir in the sample preparation section. After pipetting, the compartment door would be closed using the “open/close” button on the device. The sample preparation section would contain a centrifuging and supernatant collection region and a cell lysis solution creation region in order to transfer the correct cell solution into the assay plate. This section will also be capable of creating standard dilutions or control solutions as needed for the assays. After sample preparation, the reagents will be transferred automatically from the sample preparation section to the assay completion system, using fluid controls that are completely contained within the unit. This section would be temperature controlled as per the assay requirements. The assay reagents are stored in temperature regulated reservoirs that adhere to the appropriate storage conditions. The system is also equipped with pumping and valve controls to transfer the reagents from the storage reservoirs to the assay plate with controlled flowrate and pressure. A waste region would also be contained in the device for the collection of any waste or residual reagents from the assay. The assays would be completed on a 96-well disposable plate, which will be pre-coated with the necessary surface chemistry required to run each assay. The plate has a separate section for each assay to be completed, namely BSA, mycoplasma, endotoxin and trypsin. Finally, the device would be equipped with a user-interface screen indicating the conditions within the device, including pressure and temperature, and the status of the assay completion. Upon completion

the device will indicate “complete” on the UI screen. The assay plate would be removed and placed in a standard absorbance microplate reader to obtain the results.

The team also created a potential brochure (Appendix A) for advertising the device and its advantages over the current methods of quality control. There would many advantages of using the device by automating the device to multiplex these four assays simultaneously. Multiplexing the assays would largely reduce the labor, time, and cost involved during the assay process, especially since each cell sample for autologous transplant must be tested separately. The device would be affordable as well as easy to use and conveniently sized in order to fit on a standard lab bench. By automating the assays, the results will have increased accuracy and will greatly reduce the chance of errors and false results from the tests because human error would be almost entirely removed. The device would be very efficient and would not require any additional equipment.

5 Design Verification

This chapter will discuss the experiments that the team conducted to test various parts of the device to ensure functionality of each subsystem. These experiments were planned and conducted with proof-of-concept in mind and were designed to show that this design was feasible and can be pushed forward in the future. These experiments were created specifically for this project but in the future when the device has been refined further, the group would recommend adhering to standard methods of testing for this type of device, based on the engineering standards referenced in section 3.2.2. As a medical device, the system must meet these standards in order to be introduced onto the market and into testing laboratories in the future.

5.1 Assay Experimentation

5.1.1 Mycoplasma Baseline Assay Experiment

During the assay experimentation process, the team decided that it would be necessary to run a baseline assay test for each of the chosen assays using the manufacturer's procedure and standard laboratory equipment. There were no automated steps used in the baseline assay experiments and all fluid handling was completed by hand with standard pipettes. Temperature control was accomplished with a water bath and a standard incubator, as specified by the manufacturer instructions. The results from these baseline assays could later be used as a comparison against the results of the assay run using the system to show the system's level of effectiveness. These assays were run solely with the controls included with the kits because no cells were used in the duration of the project.

5.1.1.1 Initial Mycoplasma Assay Run

The team first ran the R&D Systems Mycoprobe Mycoplasma Detection assay using the manufacturer insert procedure (Appendix B) as well as standard methods and lab equipment for volume dispensing, incubation, and transfer. The kit that was used for this baseline test was already available in the lab, as a leftover from the previous TRT that had already been completed. The team used this kit because of its availability. A new kit was ordered from the manufacturer but had not yet arrived at that time.

During this experiment, the team encountered a number of setbacks which led to inconclusive and unusable results. The experimental plan called for three wells of the positive control and three wells of the negative control. However, there was only enough positive control left in the kit for one full well to be run. Additionally, this assay kit had been stored for about six months in the lab, which was three months longer than the manufacturer insert claimed the kit would be usable for. The assay was run as

described despite these problems in order to become more familiar with the process for the next experiment.

After completion of the assay, the wells were read in a standard microplate reader at 450nm wavelength and a color change should have occurred but was not visible, as can be seen in Figure 31 below. A successful assay run would have resulted in the positive control wells turning a dark red color and the negative control wells remaining clear. Use of the microplate reader yields the optical density (OD) of each well, which was required to be above or below a certain threshold, as described by the manufacturer, to be deemed acceptable. At the completion of this experiment, the team decided that the data was not accurate enough to be used as a baseline and that the experiment would need to be run again.

Table 4 Manufacturer included OD result comparison (left) Experimental OD and results (right)

OD Values	Result	Experimental Condition	Optical Density	Result
<0.05	Mycoplasma Negative	Positive Control	0.0106	Negative
0.05-0.1	Inconclusive	Positive Control	0.00934	Negative
>0.1	Mycoplasma Positive	Negative Control	0.0102	Negative
		Negative Control	0.00648	Negative
		Negative Control	0.00934	Negative



Figure 31 Mycoplasma Assay Initial Run Result Wells.

Right two wells: positive control; left three wells: negative control

5.1.1.2 Secondary Mycoplasma Assay Run

In this experiment, the team used a new R&D Systems mycoplasma detection kit to ensure that the baseline data was accurate. The manufacturer insert was again followed and standard laboratory procedures were used to conduct the assay. At the conclusion of the experiment, the wells were again read in a microplate reader to determine the optical densities of the solutions. The assay was successful during this experiment and the positive and negative controls reacted as expected with the appropriate optical densities present, as seen in Figure 32 below.

It is important to note that for both baseline mycoplasma assay runs, there was a slight misinterpretation of data due to human error. The plates are meant to be read at 490nm and then again at 600nm, with the second value being subtracted from the first value to get the final optical density of the value. This difference is meant to account for the optical imperfections in the well plate and is recommended by the manufacturer. Upon further inquiry with the manufacturer after this mistake was made, the team decided that these results were acceptable because had the difference been taken, the negative controls would have been in the correct range to represent a negative value. This decision was also necessary because of the time and material constraints that the team was under.

Table 5 Manufacturer included O.D. result comparison (left) Experimental O.D. and results

O.D. Values	Result
<0.05	Mycoplasma Negative
0.05-0.1	Inconclusive
>0.1	Mycoplasma Positive

Experimental Condition	Optical Density	Result
Positive Control	2.05	Positive
Positive Control	2.02	Positive
Positive Control	2.16	Positive
Negative Control	0.161	Inconclusive
Negative Control	0.1	Inconclusive
Negative Control	0.113	Inconclusive



Figure 32 Mycoplasma Assay Secondary Run Result Wells.

Left three wells: positive control; right three wells: negative control

5.1.2 BSA Baseline Assay Experiment

The team also ran a baseline assay experiment for the BSA assay to have results to compare to once the project was successfully completed. The team used the MyBioSource BSA Detection Kit in this experiment and the manufacturer insert instructions (Appendix C) were followed accordingly. This assay, different than the previous, used a standard dilution curve as a control. The experiment was run only with the standard curve and again with no cells.

5.1.2.1 Initial BSA Assay Run

The first assay run was conducted with a previously used kit obtained from the TRT prior work and therefore again presented potential errors because of the length of storage time. Despite this excess of time, the experiment was conducted as planned with the standard BSA dilution curve run in duplicate. The assay kit included a graph of an expected BSA standard curve that could be used as a reference for the curve created from the experimental assay and can be seen in green in Figure 33.

At the completion of this experiment, the wells were read at 490nm wavelength and the results were analyzed according to the manufacturer, graphing the optical density versus the log of BSA concentration. The resulting standard curves, shown compared to the manufacturer example in Figure 34 below, were intended to have a gradient from virtually clear to dark yellow but this result was not present. The standard curves were both inaccurate and could not be considered as appropriate baseline data to compare to in the future. Therefore, the team again decided to rerun the experiment to achieve better results.

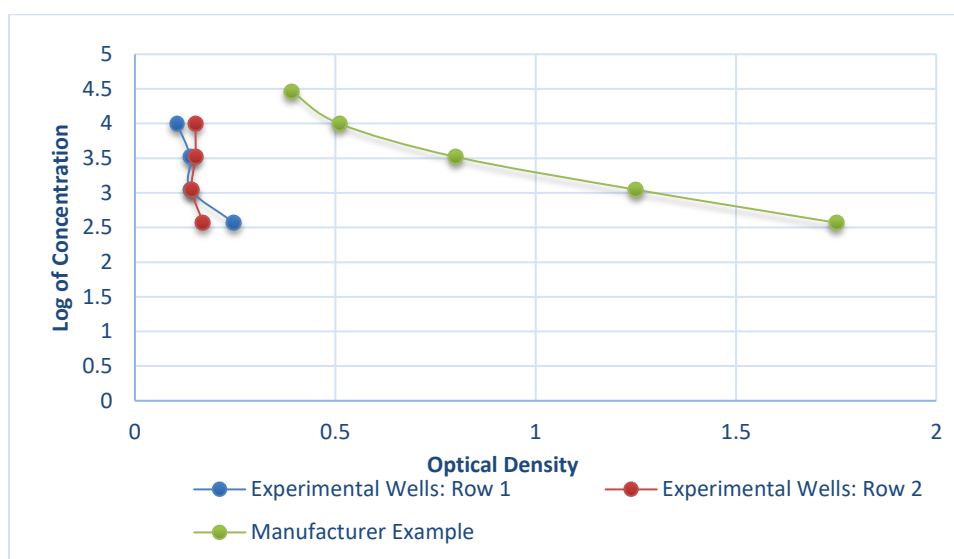


Figure 33 Initial BSA Assay Standard Dilution Curve compare to manufacturer example

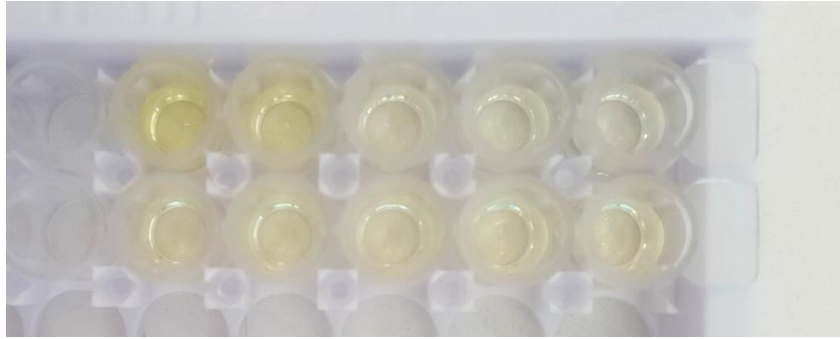


Figure 34 Initial BSA assay result wells. Descending concentration from left-most well (30,000 ng/mL) to right-most well (0ng/mL)

5.1.2.2 Secondary BSA Assay Run

The second iteration of the BSA detection assay was successful and able to be used as baseline data for future comparison. The team used a new MyBioSource BSA detection kit for this experiment and followed standard laboratory procedures and the manufacturer instructions. At the completion of the assay, a decided gradient could be seen in the wells. However, there was a limited amount of the dilution reagent which only allowed for one standard curve to be run rather than two. The absorbance readings were again analyzed and graphed and the results can be seen in Figure 35 below. The wells at the conclusion of the experiment can also be seen in Figure 39.

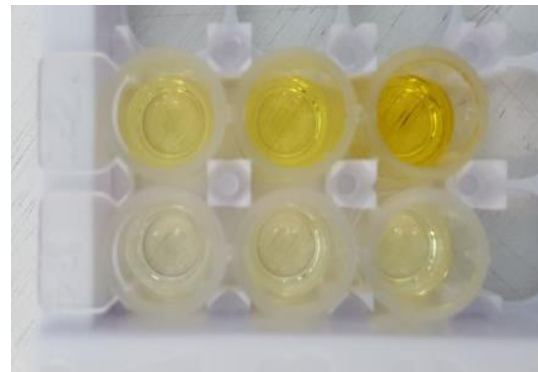
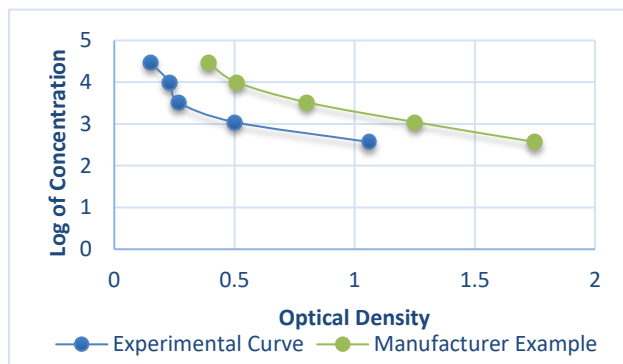


Figure 35 Baseline BSA Assay Standard Dilution Curve (left) and BSA resultant wells (right) with concentration descending from top right well (30,000 ng/mL) to bottom right (0ng/mL)

5.2 Fluidic Control Experimentation

5.2.1 Syringe Pump Calibration Curve Determination Experiment

5.2.1.1 Purpose

The purpose of this experiment was to find correlation between linear actuator distance and volume of water dispensed by the automated syringe pump. Using this correlation, a calibration curve could be generated that related this distance and volume and integrated into the Arduino code. After

integrating this calibration into the Arduino code, ideally the system would be much more accurate in dispensing the desired amount of volume.

5.2.1.2 Experimental Procedure

This experiment was performed using the pre-existing syringe pump assembly consisting of a 1mL glass syringe and linear actuator in a machined aluminum frame. The assembly was connected to a programmed Arduino Uno controller board to initiate and terminate movement of the linear actuator. The Arduino code was programmed to prompt the user for a position value that the linear actuator would then travel to.

The first step in this experiment was to determine the maximum volume that the syringe could intake. Though it was a 1 mL syringe, the aluminum frame restricted full movement of the syringe so it was unable to reach capacity. The group achieved this by taking water into the system to the linear actuator's limit and measuring the mass difference of the reservoir the water was taken from. The average intake was measured at 768 μL .

To measure the calibration between linear actuator distance and volume output the team filled the syringe to capacity, input randomly chosen linear actuator positions, and measured the output volume of fluid dispensed. A total of 12 linear actuator positions were tested and the entire experiment was repeated three times with these volumes to ensure accurate data. A full description of the experimental procedure can be found in Appendix D.

5.2.1.3 Experimental Results and Analysis

At the conclusion of the experiment, the group transferred the collected data to Excel for analysis. To create the calibration curve, the distance travelled by the linear actuator was plotted against the volume output at that position. To achieve the most accurate curve, data points from all three experimental iterations were included in this plot but major outliers were removed. These outliers were removed because they were most likely due to human error and did not reflect on the effectiveness of the system. The graph in Figure 36 below shows the calibration curve between the linear actuator distance and the volume dispensed with outliers removed. The full data set and graph including outliers can be seen in Appendix D. The calibration curve created in this experiment was then integrated into the Arduino code so the team could input a value into the code and know with relative certainty what volume would be dispensed.

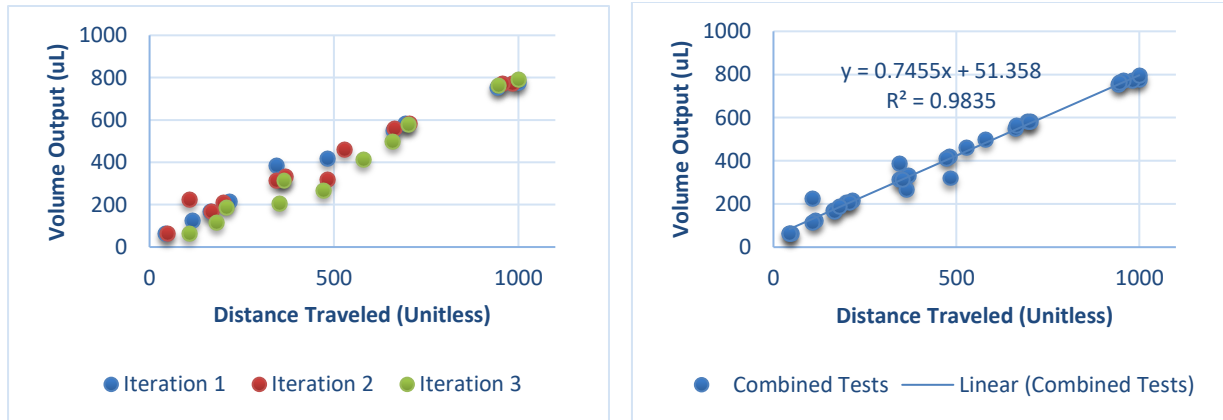


Figure 36 Graph of output volume vs. linear actuator distance data from all experimental iterations without outliers (left).
Generated calibration curve from all iteration data with outliers removed (right).

5.2.2 Syringe Pump with Manifold: Dead Volumes Experiment

5.2.2.1 Purpose

The purpose of this experiment was to empirically determine the volume lost in the solenoid valve manifold when various volumes of fluid were dispensed by the syringe pump system. This information would be used to factor in to the volume entered into the Arduino code to be dispensed by the system.

5.2.2.2 Experimental Procedure

The procedure for this experiment was similar to that of the previous experiment, with the main difference being the integration of the solenoid valve manifold into the syringe pump system. The system was filled to capacity and randomly chosen output volumes were entered into the Arduino code. The subsequent output volume was compared to the goal output volume to create another curve for the system with the integrated manifold. This experiment was performed with the 12 chosen volumes from the previous experiment to output and the entire experiment was performed three times. A fully detailed description of the experimental procedure can be found in Appendix E.

5.2.2.3 Experimental Results and Analysis

The data was collected and analyzed in Excel. The goal volume output is compared graphically to the actual volume output of the system. This curve was then compared to the previously created calibration curve to identify any discrepancies or offsets. This comparison can be seen in Figure 37. The team observed that the offset between the curve created without the manifold and the curve created with the manifold was not uniform. It was initially hypothesized that the valve manifold would have a constant volume lost within it. However, the data showed that the amount of volume lost in the

system slightly increased as the volumes dispensed increased. The full data set from this experiment can be found in Appendix E.

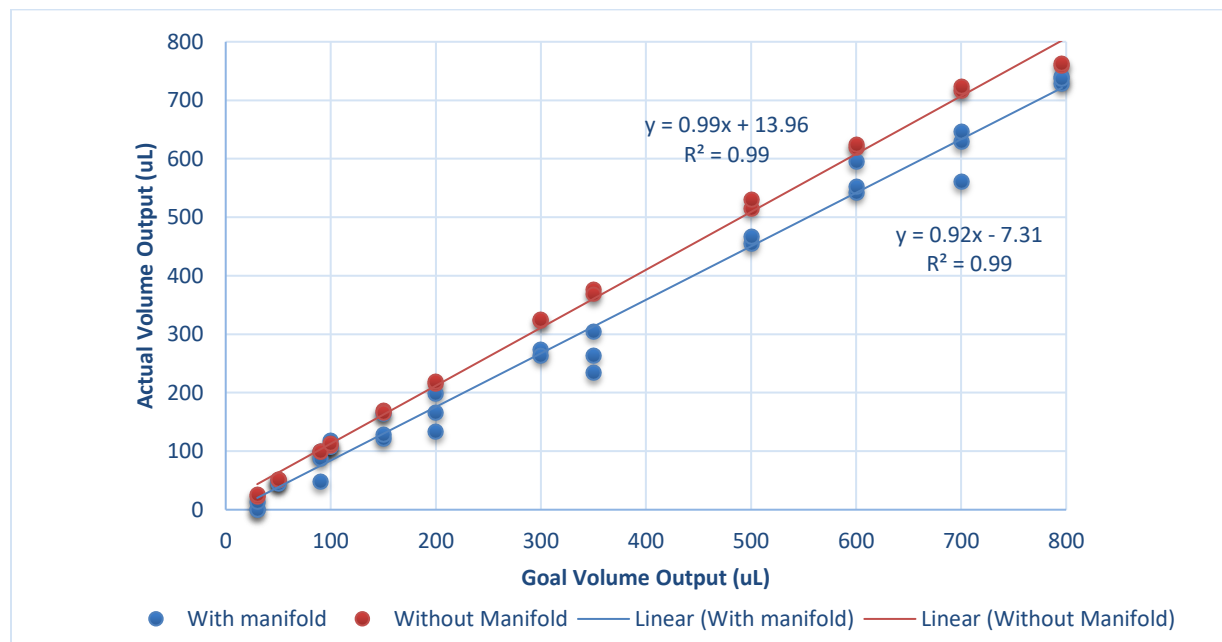


Figure 37 Volume output comparison between system with and without manifold

5.2.3 Syringe Pump with Manifold: Intake Accuracies Experiment

5.2.3.1 Purpose

The goal of this experiment was to determine the accuracy of the fluid intake of the syringe pump and valve manifold system. This information would show the team if the system was capable of taking in the goal amount of volume or if there was volume not taken in by the system.

5.2.3.2 Experimental Procedure

To perform this experiment, the team used the syringe pump system with the integrated valve manifold as described in previous sections. A fluid reservoir was then filled with water and weighed. A range of randomly selected volumes between 0 and 700 μL were chosen as intake volumes and entered into the Arduino code. After the syringe pump, which began fully empty, had taken in the entered volume of fluid, the mass difference of the reservoir was measured to determine the actual intake of the system. 12 volumes were tested and the experiment was repeated three times. A fully detailed description of the experimental procedure can be found in Appendix F.

5.2.3.3 Experimental Results and Analysis

Once the data was collected, it was transferred to Excel for analysis. The team compared the goal volume input values to the actual volume taken in by the system, as seen in Figure 42. However, this graph is not an accurate representation of the experimental results because its relatively linear

relationship is misleading. The team then plotted the goal input volumes against the change in volume that corresponded to each data point. This graph signified the difference between the goal intake volume and the actual intake volume to show how much volume was not taken in by the system, as seen in Figure 38. This graph shows that the intake loss was not uniform but was consistent over the three iterations of the experiment. These results were disappointing as there was such a large difference between the goal intake and actual intake of the system. The full data set from this experiment can be found in Appendix F.

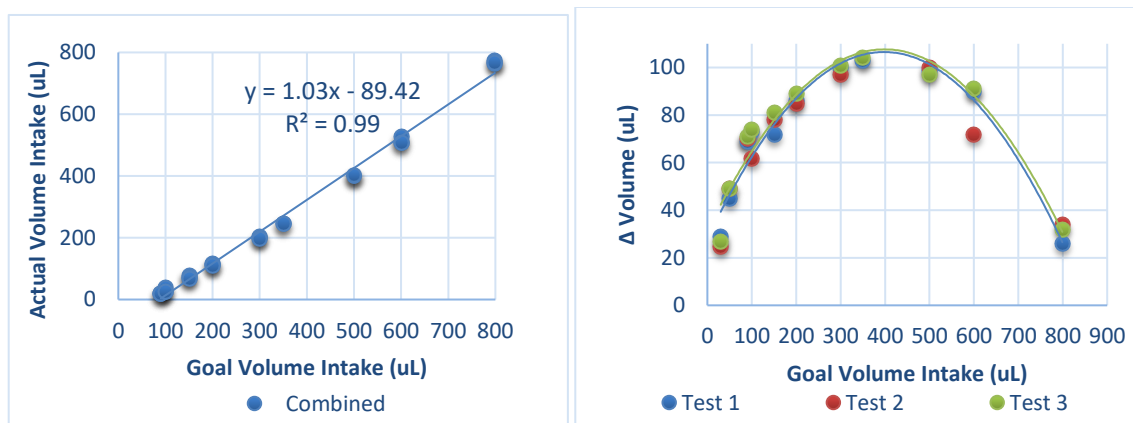


Figure 38 Results of system intake experiment: goal intake vs. actual intake (left). Change in intake volume vs. goal volume intake (right)

5.2.4 Syringe Pump with Manifold and Air Pump: Output Volume Loss Experiment

5.2.4.1 Purpose

The purpose of this experiment was to determine the effectiveness of an attached air pump used to flush the valve manifold of volumes left behind after dispensing. If seen as effective, this attached air pump could be used to more accurately dispense volumes and ensure that all fluid was removed from the manifold.

5.2.4.2 Experimental Procedure

In this experiment, an air pump was integrated into the system between the valve manifold and syringe pump. The procedure for this experiment was similar to previously described experiments, beginning with a full syringe and dispensing to a range of randomly chosen volume values. After dispensing the volume of fluid, as in previous experiments, the air pump was turned on for 1-2 seconds to allow all residual fluids to be flushed from the system and into the collection reservoir. The reservoir was then weighed to identify the mass difference and final output volume from the system. This experiment consisted of 12 volume data points and the entire experiment was performed three times. A detailed description of the procedure can be found in Appendix G.

5.2.4.3 Experimental Results and Analysis

Upon completion of the experiment, the data was collected and transferred to Excel for analysis. Upon further analysis of the data, it was seen that the air pump did assist with increasing the amount of volume that was dispensed from the system. When comparing the amount of volume lost in the system when using the air pump to the amount of volumes lost in the system when the air pump was not integrated, as seen in Figure 39 below, the group saw that the volumes lost became less varied upon integration of the pump. However, the team decided against integrating the pump into the system because of the excess amount of tubing required to attach the air pump. Because the previous intake experiment proved to be rather unsuccessful, the team did not want to integrate any more unnecessary tubing that could decrease the intake accuracy even more. Therefore, it was decided to implement the a vacuum air pump instead, only as needed, in order to fully flush out the system between reagent additions. Therefore, it would not introduce additional tubing during intake but could still assist with ridding the system of the left behind volumes.

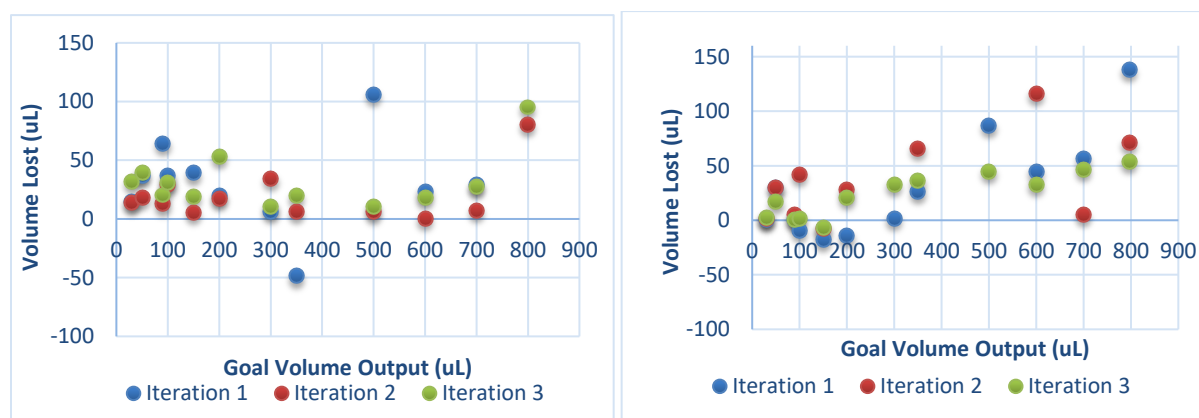


Figure 39 Distribution of volume lost with air pump integration (left) and distribution of volume lost with no air pump (right)

5.2.5 Cross Contamination Experiment

5.2.5.1 Purpose

One of the final experiments that the team conducted was a qualitative cross contamination test to determine if the system was being fully cleared out by the integrated vacuum. This was necessary in order to lessen the chance of mixing between the reagents and compromising of the assay.

5.2.5.2 Experimental Procedure

During this experiment, the team used yellow dyed water to fully fill the system and then dispense all volume into a 96-well plate, as can be seen in the bottom row of Figure 40 below. This water was not contaminated because it was the first color through the system. We then disconnected the manifold from the syringe pump and fully vacuumed it out, opening all valves and leaving the

vacuum on until no liquid was seen leaving the manifold. The syringe pump itself, still separate from the manifold was filled and emptied with uncolored water 3 times to ensure that any residual color was eradicated. The system was then filled with red colored water and the emptying process was repeated. Finally, yellow water was taken in and pumped out of the system again and the resultant wells were observed for any color change that might have occurred from residual red colored water. We repeated the whole process again with yellow colored water as the base again but then followed with green colored water as the secondary color.

5.2.5.3 Experimental Results and Analysis

The team saw that the residual volume removal did not fully clear out the system as we had hoped. Even after extensive vacuuming of the valve manifold, we saw that both red and green colored water affected the yellow colored water that followed it. However, the concentration of the contaminated color did lessen in later wells but the color was still present. The results from this experiment can be seen in Figure 40, where the top/left wells were the result of the green colored water contamination, the middle wells were the result of the red colored water contamination, and the right/bottom wells are the result of no contamination for comparison. This was a qualitative experiment due to lack of time. However, though the results were only obtained visually, the team believed the outcome was still helpful for the project.

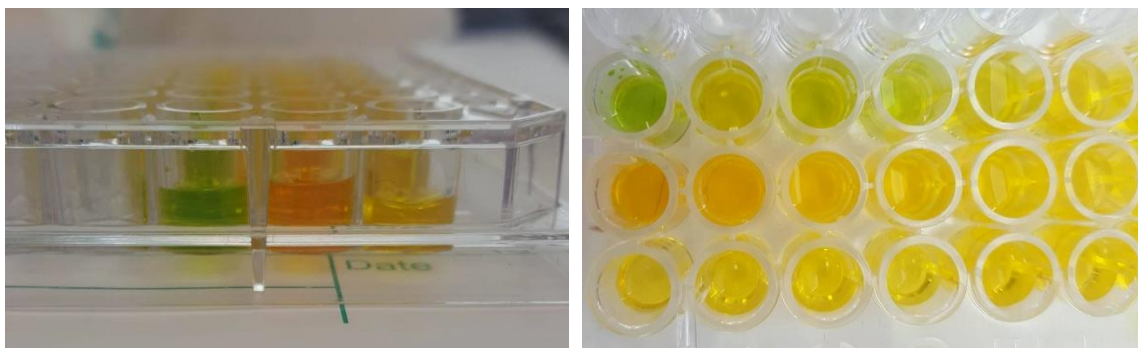


Figure 40 Top view of contaminated wells (left). Side view of contaminated wells (right)

5.2.6 BSA Assay Run: Water Trial Experiment

5.2.6.1 Purpose

The purpose of this experiment was to determine if the system was able to correctly intake and dispense the specific volumes needed to run the BSA detection assay. This experiment was run as a mock assay trial using water instead of reagents to ensure that materials did not go to waste if there was a flaw in the system. For this experiment, the system that was used was our final prototype system, containing the syringe pump, solenoid valve manifold, and detachable vacuum.

5.2.6.2 Experimental Procedure

To complete this experiment, the team followed the MyBioSource kit insert instructions to determine what volumes would be necessary for the BSA assay. The system was then used to intake and output water in the same way that would be used in the actual assay run, namely using the automated pumping system to intake and output fluid but with manual control over tubing to ensure accuracy in delivering the fluid. The desired intake volume was entered into the Arduino code and after the intake was completed, the system would be returned to position zero to empty the contents into the desired well. The intake and output was performed on four volumes dispensing into six wells and the entire experiment was completed three times. A full description of this experimental procedure and a table of the volumes used in this experiment can be found in Appendix H.

5.2.6.3 Experimental Results and Analysis

At the completion of the experiment, the team saw that the system was consistently dispensing less volume than had been requested. However, a relatively consistent amount of water was lost at each of these volumes, as seen in Figure 41 below, which allowed the team to be able to account for the volume loss at each point. Based on the data collected, the team decided to integrate a volume buffer into the volume value that was entered into the Arduino software. After averaging the output losses and differences in volume intake at volume point, the volume buffer was determined to be 15 μL . The full data set can be found in Appendix H.

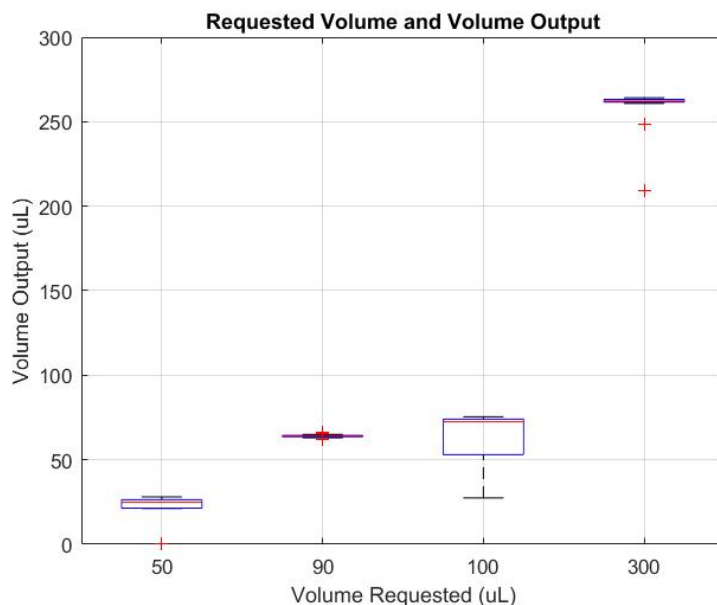


Figure 41 Distribution of volumes requested vs. actual volume output for four volumes

5.3 Temperature Control Experimentation

5.3.1 Heating from Room Temperature to 65 °C Experiment

5.3.1.1 Purpose

The purpose of this experiment was to determine the time it took to heat the control system from 24 °C to the maximum incubation temperature, 65 °C, and vice versa. It was also necessary to determine if there was a major difference in heating times when the system was connected to an 80x80 mm heatsink or a 60x60 mm heat sink.

5.3.1.2 Experimental Procedure

To complete this experiment, the temperature control system was set up with a temperature sensor attached to the aluminum assay strip well platform for monitoring its surface temperature. The Peltier module was connected to the aluminum plate on the side that would be generating heat and to a heat sink on the other, which would be diffusing heat and cooling. Either side of the Peltier module can be used to heat or cool depending on the voltage and polarity applied to it. There were two size options for the heat sink: 80x80 mm and 60x60 mm and the system was tested with both in order to identify any major differences between the two. In addition, other specifications such as block mass, block area, Peltier module area, and polystyrene well was kept the same as discussed in the modelling section.

This experiment was completed by controlling the system with a motor driver board and an Arduino Mega microcontroller board. Energy was delivered to the Peltier module to heat up the aluminum plate by controlling the “speed” parameter of motor driver board. This speed is the output of the PID control system, which is implemented inside the Arduino. The input of the PID control loop is the temperature data from the temperature sensor. In general, the Arduino PID control loop continuously keeps track of how far the plate is from the goal temperature. For example, to go from RT (~24 °C) to 65 °C, the PID control will tell the motor controller to allow full current draw from the Peltier at 8 V. As the aluminum gets closer to the desired temperature, the current draw to the Peltier module decreases until the temperature is reached.

It is important to note that this test was carried out by filling 75% volume of each well with water. Each well volume is 360 µL maximum. The well strip was placed in the aluminum block for heating and was open to room temperature air with a temperature of about 24 °C. The temperature sensor LM35 was used to measure the metal block temperature, data of which was then recorded into Arduino serial monitor. For parallel monitoring, we dipped a Fluke thermocouple into the water of one well and double checked that when the metal block stabilizes at the assay temperature, the water should be at the same temperature too.

5.3.1.3 Experimental Results and Analysis

The data collected from the Arduino during the experiment showed that the temperature control system reached its goal temperature and remained there after about four minutes. The goal for the system was that it should be able to heat to the desired temperature in less than five minutes.

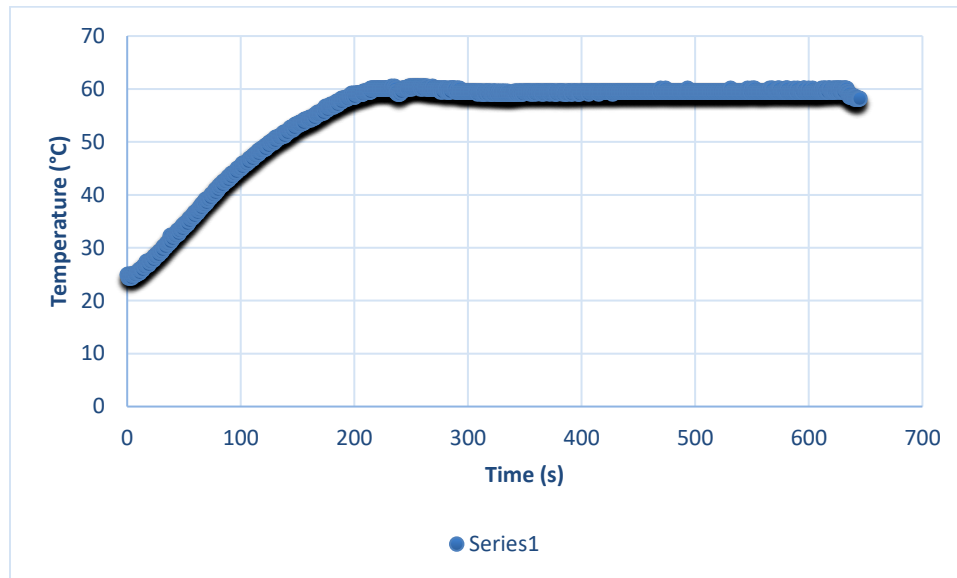


Figure 42 Heating from room temperature (24 °C) to 65 °C with 80 x 80 mm attached heat sink

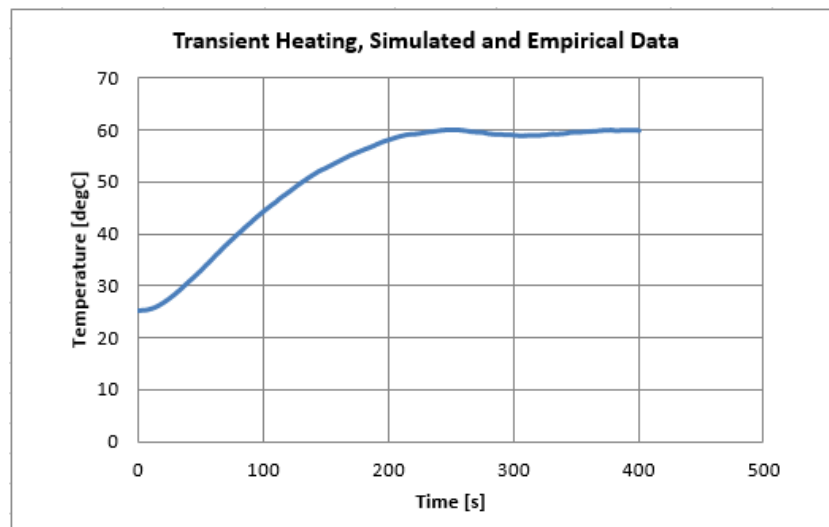


Figure 43 Heating from room temperature (24 °C) to 65 °C with 60 x 60 mm attached heat sink

As we can see from Figure 42 and Figure 43 above, the heating characteristics of both graphs are similar. From room temperature of 25 °C heating to 55 °C, we have a nearly linear increment. This is due to the PID controller seeing that aluminum block is still far from the desired heat goal so it allows full current draw from Peltier TEC module. From 55 °C to 60 °C, the PID starts decreasing current draw

allowance, which results in a non-linear curve of temperature that stabilizes upon reaching goal temperature. In general, the heat system can go from room temperature to 65 °C in less than five minutes, which meets the temperature transition goal.

Because the heating behavior of system with two different heat sinks, 60x60 mm and 80x80 mm, is very similar, we can assume that the size of the heatsink does not affect significantly the heating performance of the system. Therefore, to determine which heatsink to use, more experiments needed to be conducted.

5.3.2 Cooling from 65 °C to Room Temperature (24 °C) Experiment

5.3.2.1 Purpose

The purpose of this experiment was to ensure that the system was capable of cooling the aluminum block from the highest incubation temperature, 65 °C, to 24 °C within the specified amount of time, five minutes. It also provided more data on which heat sink was a better option for the system.

5.3.2.2 Experimental Procedure

After reaching 60 °C, we turned off the power delivered to Peltier module and turned on the cooling fan. However, as mentioned earlier, one of the problem with this is that Peltier's job is to maintain a heat difference across two plates. For example, if the allowed temperature difference between the two surfaces is 70 °C and the hot side temperature is currently 30 °C, it allows the cold side to be -40 °C. However, this is not always true. Since the heating effect on cold side is significant that it will keep increasing the heat much faster than the cold side, the cold side need to go back to -20 °C, -10 °C, 0 °C and start going above 0 °C again. Even though we already implemented a heatsink and cooling fan for this problem it does not go away entirely. As a result, the longer we reverse energy delivered, the more heat we may get later instead of cold, which can slow down our cooling process. Therefore, triggering this reverse action at lower temperature definitely saves more power usage than at 60 °C. As a result, we decided to only turn off the Peltier module and use DC cooling fan for the first few minutes of cooling. We observed that with this approach, the cooling process still dropped fast until reaching 29 °C. At 29 °C, since the temperature is close to room temperature, the cooling process slows down. At that point, we then start reversing the energy delivered to Peltier module, while the DC cooling fan remains on the whole time.

5.3.2.3 Experimental Results and Analysis

Below is the experimental data of this method for the two sizes of available heatsinks. As we can see from Figure 44, the small heatsink can get the system to cool down faster. Take a point at 200

seconds, the small heatsink decrease the system to 27 °C while at 200 seconds, the larger heatsink cools the system down to 30 °C only. From this result, we chose the 60x60 mm heatsink as the better option.

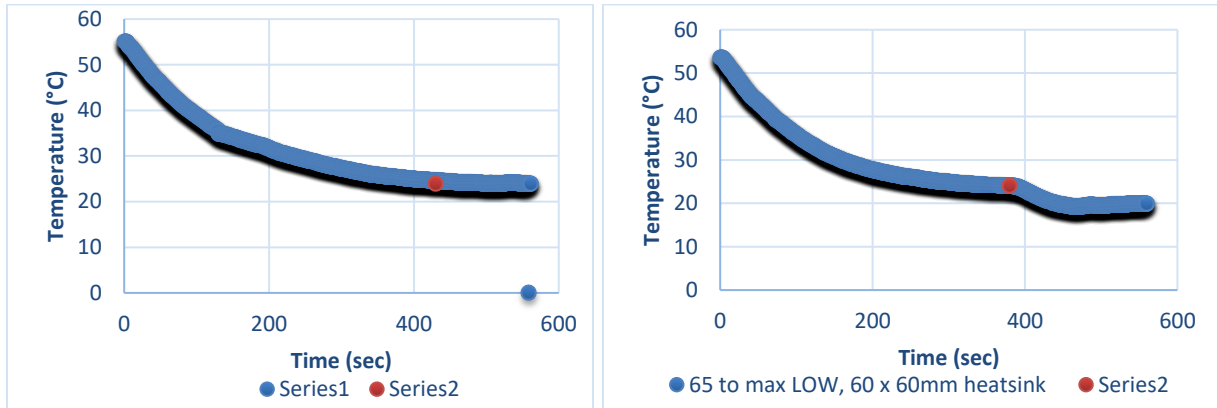


Figure 44 Cooling from 65 °C to room temperature with 80x80 mm heat sink (left) and system cool from 65 °C to room temperature with 60x60 mm heat sink (right)

5.3.3 Temperature Control System Cooling Experiment

After doing testing on all options that we have: aluminum versus copper, aluminum sheet versus machined aluminum block, and 60 x 60 mm versus 80 x 80 mm heatsink, we finalized the components in each of the conclusions discussed in the Final Design section. We also knew that the system can remain stable around 65 °C, which is the max temperature needed for the assays Therefore, the team performed an experiment with this final design to test if it can stay stable at room temperature after cooling down from 65 °C.

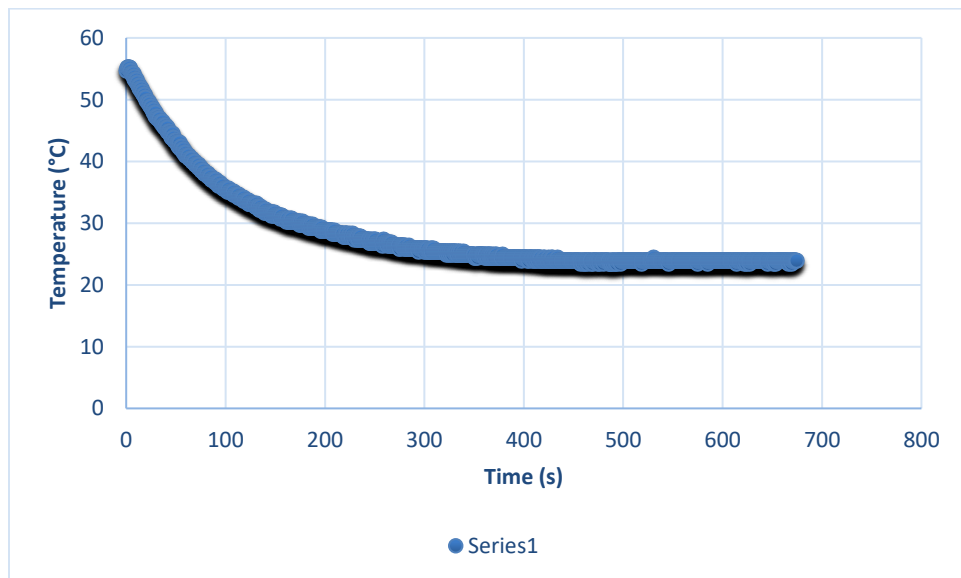


Figure 45 Cooling stability graph of cooling the system from 60 °C to 24 °C

As we can see from Figure 45, the heat block went down from 55 °C to room temperature of 24 °C and stayed there from time 400 seconds to time 690 seconds, which showed that the system was capable of keeping the metal block stable at room temperature.

It was important to note that in these experiments, we had 60 °C instead of 65 °C because of the offset between the temperature sensor feeding data to the Arduino versus the true temperature of metal block. The true temperature was measured through a more sensitive sensor, which was a Fluke thermistor. By placing both sensor in the same location, we observed that when the Fluke thermistor claims 65 °C, the LM35 sensor sees 60 °C. Moreover, some of the cooling graphs start from 55 °C instead of 60 °C. This change was because when we turned off the power supply and changed the desired temperature in the Arduino to room temperature, it took around five seconds for the data collecting monitor to start recording. These 5 seconds resulted in the previous 5 °C drop from 60 °C that we cannot monitor.

6 Design Validation

Device validation is necessary to show that the design created is effective and meets the goals that were originally set out at the outset of the project. Typically, validation for a medical device would take place in a clinical setting where it would be put to use as a replacement for the system being improved. However, for this project, the designed device was not able to be used in a clinical setting because the final goal was proof-of-concept rather than immediate clinical application. Therefore, the team validated the system as much as possible by showing that the system was capable of accurately running the assays that the final device would automatically run in a clinical setting. Running these assays with the system shows that the device is capable of the fluid and temperature control necessary for the assays and therefore proves that this idea is feasible and can be moved forward in the future.

6.1 Prototype Validation: BSA Assay Run with System

The first assay run to show validation of the designed system was the BSA detection assay. The manufacturer procedure was followed using the system instead of typical laboratory equipment, including pipettes and incubators. During this experiment, the team ran the included BSA standard dilution curve to show completion of the assay. No cell solution was tested in the experiment, as the main goal was only proof-of-concept. The standard dilution curve was created by hand, using standard laboratory tools. We chose this method of creating the standard curve because in the future device, a separate sample preparation station will be responsible for this task. Because we were only demonstrating proof-of-concept for the reagent distribution system, the team decided that the curve should be created by hand to ensure that it was as accurate as possible before the system was used. Once the dilutions were created, the subsequent steps of the assay were completed in duplicate using the system with manual control of tubing as necessary. This device is only semi-automated and therefore all fluidic output and intake was automated but it was necessary to move the intake/output tubes into the subsequent wells and reagent reservoirs by hand. This step would be automated in the future but the project was unable to reach that stage during the seven week time period.

Once the assay was successfully completed, the plate was read in an absorbance plate reader at 450 nm and the values were plotted against the log of the BSA concentration in each well, as seen in Figure 46 below and the full data set can be found in Appendix I. The resulting curves showed a descending concentration, as necessary, but offset from the baseline assay run data. Iteration 1 was significantly more uniform and more accurately showed the desired results. The curve representing Iteration 2 was offset and unpredictable, showing that the device had the ability to correctly control fluids dispensed but was not consistent in doing so. The team believed the explanation for the offset of

the curves was due to the system consistently dispensing about 15 μL more than required. This volume offset would also increase the concentration of the reagents added to the various wells, which would cause the entire curve to be slightly offset. However, for the sake of consistency, the group did not modify the system to account for this 15 μL offset during this or the next experiment.

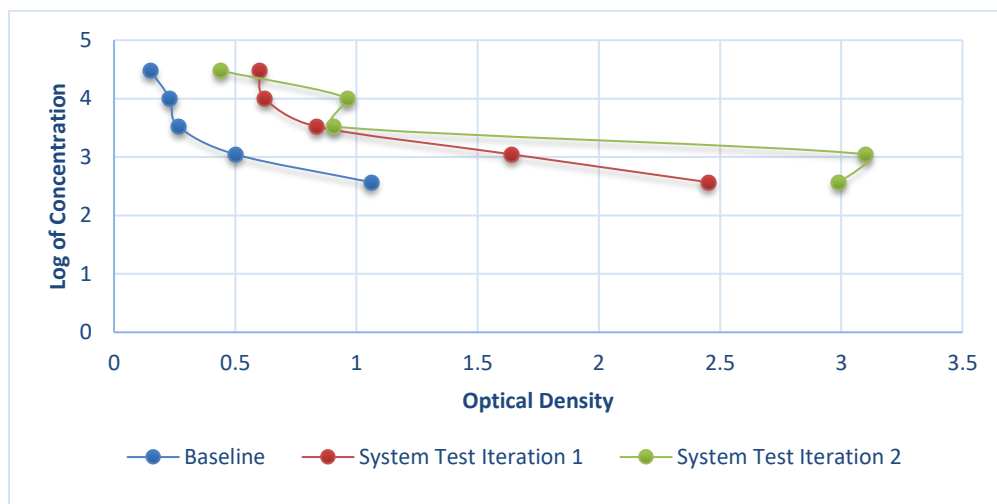


Figure 46 Comparison of baseline assay test results and system assay test results

6.2 Prototype Validation: Mycoplasma Assay Run with System

The team also completed the mycoplasma detection assay using the system instead of the usual laboratory tools. To complete this assay, again no cell solutions were used and only the positive/negative controls were run to show proof-of-concept. The manufacturer kit instructions were closely followed. Three wells of each positive and negative control were run and the results were compared to those of the baseline mycoplasma assay results. The results of the system assay run showed that the 15 μL volume offset again increased the concentration of the wells. The colorimetric differences between the baseline assay wells and the system assay wells can be seen in Figure 47 below.

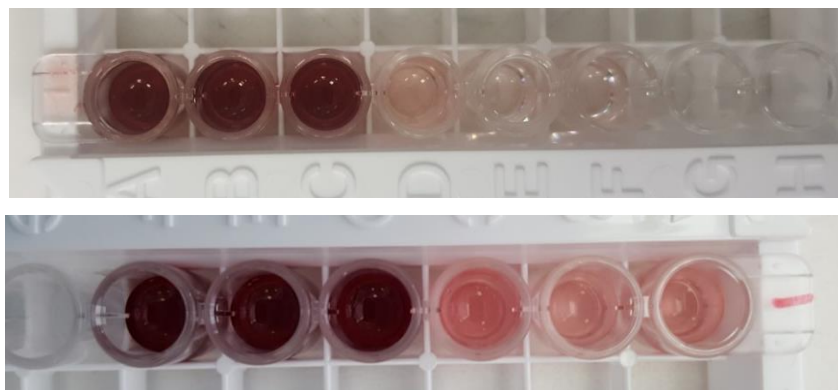


Figure 47 Comparison of baseline mycoplasma assay results (top) to system mycoplasma assay results (bottom). Positive controls indicated by darker red color: left wells. Negative controls indicated by transparent color: right wells.

The resulting assay wells were read in an absorbance plate reader at both 490nm and 600nm and this data set can be found in Appendix J. The optical densities measured at 600nm were then subtracted from the readings at 490nm to account for the optical imperfections in the assay plate, as instructed by the assay manufacturer. These final optical densities were then compared to a table provided by the manufacturer that specified what optical densities corresponded to a positive, negative, or inconclusive result. The results and the manufacturer information can be seen in Table 5 below.

**Table 6 Manufacturer specifications for assay results (left).
Optical density comparison between baseline and system assay results (right)**

O.D. Values (490 nm – 600 nm)	Result	Experimental Condition	Average Optical Density (490 nm –600 nm)	Result
<0.05	Mycoplasma Positive	Baseline Assay Run: Positive Control	1.14	Positive
0.05-0.1	Inconclusive	Baseline Assay Run: Negative Control	-0.127	Negative
>0.1	Mycoplasma Positive	System Assay Run: Positive Control	3.02	Positive
		System Assay Run: Negative Control	0.269	Positive

7 Discussion

The results of this project were positive overall and showed that the device created is a legitimate first step in designing a fully automated, multiplexed assay machine but would need significant improvement in the future. Because the team's main goal was basic proof-of-concept, the created prototype reached this goal but could not meet all expectations because of the limited span of time in which the project was completed. The biggest obstacle that the team faced was the time constraint of the seven week onsite portion of the project. Because of this short span of time in which to complete the project, it was vital that the team waste no time and use as many available resources as possible. As such, it was necessary to use components that were not ideal but were necessary because of their immediate availability. If the project were to be continued in the future, the ideas and knowledge gained by this proof-of-concept device could be applied to better, more appropriate components to make the device significantly more reliable and successful.

Another important aspect of this project was the level of automation of the system. Since it was designed to be a proof-of-concept device, the system was only semi-automated and did require a high level of manual control, including tubing control and Arduino code prompts, in order to perform successfully. However, had time allowed, the team is confident that the system would be able to become significantly more automated.

Additionally, the long term goal for this device is to greatly reduce time and labor costs because of the automated nature of the device. At this stage of project development and because the device was only semi-automated, we were not able to show a reduction of time spent on completing the assays and therefore this area of concern could be improved in the future. However, if work on this project continues, the group is confident that a large reduction in manual involvement time would occur. This time reduction would also greatly lessen labor costs because a laboratory technician's time could be spent working on other areas and not focusing solely on completing the QC tests.

7.1 Fluidic Control System Discussion

The fluidics control portion of the device was only partially successful and therefore would require significant improvement in the future when this project is developed further. The team's extensive testing showed that the system was capable of controlling the volumes of fluids necessary to run the assays but was often inconsistent in doing so accurately. Therefore, different components would have to be integrated into the system in the future in order to increase the accuracy and consistency of the device.

One of the main issues with this design was the solenoid valve manifold, used to intake volumes into the syringe pump and output them into a specific well. When the solenoid valve manifold was integrated into the system, intake and output both became more difficult because of the tortuous inner pathway of the manifold. The design of the manifold was such that the internal path was a zigzag between the valve ports, which led to extensive volume loss and inconsistencies with the measurements. The manifold was particularly problematic in regards to volume intake into the system. Looking at the experimental results, the team saw up to about a 30% volume loss of the volumes taken into the system. A potential reason for these inaccuracies is that the syringe pump was not large enough or powerful enough to generate enough of a vacuum to overcome the tortuous manifold pathway and bring the desired volume into the system. This discrepancy between goal and actual intake and output would not be acceptable in a final design and therefore would have to be addressed.

Additionally, the valve manifold greatly increased the risk of cross contamination because of the number of places in which fluids could remain, even after pumping and vacuuming out the system. It is crucial to the success of the assays that preemptive reagent mixing is very limited or lacking entirely. The system was still able to complete the assays relatively successfully despite this problem, but it would definitely need to be addressed in future iterations of the design.

The system also had significant difficulty accurately dispensing smaller volumes of fluid. Because of the length of the internal manifold pathway, moving from one valve to another often required a higher volume of fluid than was supposed to be dispensed. To address this problem, the system was filled with the reagent of choice and then the smaller volumes were pumped out after a number of “blank” volumes were dispensed. In an ideal system, this internal loss could be accounted for accurately in order to not waste reagents. Since the team was so limited by the time constraints of the project, this problem was not a high priority to address as long as the system could be manipulated to work correctly.

7.2 Temperature Control System Discussion

The temperature control portion of the device remained very successful throughout the duration of the project. The integration of the Peltier heating modules greatly increased speed and efficiency of both heating and cooling of the system and allowed for greater control over the temperatures involved. The system acted as an appropriate replacement for the typical incubator or water bath for heating of the assay plates. It was able to reach necessary temperature, whether by heating or cooling, within five minutes, meeting the goal the team had put in place.

7.3 Potential Project Impacts

This section discusses the potential impacts our project could have on certain aspects of society. These considerations are necessary to ensure that this project will be beneficial in all areas.

7.3.1 Economics

This device would ideally have a positive impact on the economics of the medical device industry. It would lead to collaborations between assay manufacturers and the device manufacturer. Additionally, cost of quality control would greatly decrease because of the limited minimal involvement needed to use this equipment. Therefore, the laboratories in which it was used would save expenses on quality control that could be implemented elsewhere, giving business to more companies and positively impacting this field.

7.3.2 Environmental Impact

This device will have a positive environmental impact because of the reduction of disposable pieces used when the device is fully automated and functional. Because there is a reduction of human error, there will be less waste of any disposable pieces used by the machine. Additionally, the device will be mostly made up of reusable parts that will not be disposed of after every use, which also increases its level of positive environmental impact.

7.3.3 Societal Influence

If stem cell therapy becomes the norm in the future, then this device would have the capacity to have a very positive societal influence by increasing the safety and reliability of this method of treatment.

7.3.4 Political Ramifications

Political ramifications would be a minor issue for this device. There is little about this device that would cause it to cause any political ramifications because of its generally scientific and non-controversial applications. One potential concern that could be raised is that the automatic nature of this device could remove jobs for those who do these tests manually currently. However, with the introduction of this device, those employees would be able to focus on increasing throughput of cell quality control in the lab and would be able to expand their field of interest.

7.3.5 Ethical Concerns

This device does not have any major associated ethical concerns. Whenever this device would be used, it would be with the direct consent of the patient whose cells were being cultured and transplanted. A potential ethical concern for this device is if it was expanded to the quality control of embryonic stem cells or a similar type of currently controversial cell type. However, the device itself

would only be acting as a method of QC and therefore should not be associated with the ethical concerns of the cells themselves.

7.3.6 Health and Safety Issues

Health and safety were the main concerns of this project because of the effects these cells can have on the patients they are reintroduced into. The goal of this device was to decrease human error and increase reproducibility to ensure that the cells were healthy and acceptable to be used as a treatment. If the cells have a false negative result, the patient's safety can be at risk because of the effects these contaminants can have in an *in vivo* environment. Therefore, with the reduction of human error, this device will help to decrease the number of false negative results and better assure the usability of the stem cells for transplant.

7.3.7 Manufacturability

Because this device will be utilizing a number of currently existing technologies and subsystems combined into one device, manufacturability should be a minor concern. Because many pieces of the device are already manufactured separately, it would be relatively simple to assemble these parts into the final device.

7.3.8 Sustainability

The system would be made up of reusable and durable parts that would allow for long-term use. The final device subsystems would ideally utilize materials that would not degrade over time with regular use. Because of the expensive nature of the device, it would be necessary that it be a one-time purchase for laboratories because of the likely high cost involved.

8 Conclusions and Recommendations

The goal of this project was to create a semi-automated proof-of-concept device that could demonstrate the ability to control the fluidic and temperature environment requirements for specific biological assays to be run correctly. In the future, this project will hopefully be advanced to a fully automated, multiplexed device that is capable of running the four key quality control assays, to detect mycoplasma, trypsin, endotoxin, and BSA, with high quality, reproducible results.

Overall, we were able to create a proof-of-concept prototype that was capable of controlling fluids and temperature in such a way that allowed for successful completion of these biological assays. The fluidic control system would be required to be improved in the future because it was only relatively consistent with taking in and dispensing fluids from the system into the assay plate. A more accurate and consistent pumping system would have to be implemented. There was minimal cross contamination in the system, though some was present. Additionally, the correct temperature environment was provided by the temperature control system and the system was able to heat from room temperature to a maximum of 65 °C in less than five minutes and remain stable at this temperature for as long as required. It was also able to cool back down to room temperature in the same amount of time. Using these systems along with some manual involvement, the mycoplasma and BSA detection assays were able to be completed with acceptable results using only the system.

Though we completed the goals set out at the beginning of the project, there is still a large area for improvement in the future. In regards to the fluid control system, it would be beneficial for the device to have a much more capable and accurate pumping and valve separation system. One potential option would be to integrate a peristaltic pumping droplet mechanism system. This type of system could greatly increase the level of control over the volumes released and decrease the chance of volume offsets. Another potential replacement for the syringe pump is a network of pinch valves connected to T-valves, each corresponding to a specific and separate reagent. Using built up pressure in the system, opening one valve for a specific amount of time would release a known amount of volume into the system. This idea would again yield higher control and less chance for inaccuracies with the volumes dispensed.

The temperature control system could also be advanced in the future by integrating a storage system with the proper environment for reagents, which require specific freezing or refrigeration conditions if they are intended to be contained in the device itself. The device is designed to be as self-sufficient as possible so including the reagents in the system would be a beneficial addition to the device.

In the future, the system would also benefit from being much more automated than the current prototype device. Because of the time constraints of the project, it was higher priority for the team to ensure that the processes themselves were working rather than concentrating on automating a system that might not be functional. Therefore, now that the system has proved functional, it would be beneficial to integrate additional steps into the Arduino code to greatly lessen the amount of manual involvement necessary for the system to function correctly.

In conclusion, our MQP was relatively successful in showing proof-of-concept of the created system. However, there were some complications and many areas have room for improvement in the future. Therefore, further development of this device could potentially result in a fully automated, multiplexed assay system that minimizes cost and manual involvement while also increasing reliability and reproducibility.

9 References

- Alliance for Regenerative Medicine. (2014). Regenerative Medicine Annual Industry Report.
- Anderson, N. (n.d.). Biotin Streptavidin | Innova Biosciences. Retrieved January 23, 2017, from (<https://www.innovabiosciences.com/innova/biotin-streptavidin.html>)
- Bender, Eric. (2016). Cell-based therapy: Cells on trial. *Nature*. 540:106-108. (http://www.nature.com/nature/journal/v540/n7634_suppl/full/540S106a.html)
- Bioreliance. Raw Material Testing. (2017). (<http://www.bioreliance.com/us/services/biopharmaceutical-services/raw-material-testing>)
- Boston Children's Hospital. (2017). About Stem Cells: Pluripotent Stem Cells 101. (<http://stemcell.childrenshospital.org/about-stem-cells/pluripotent-stem-cells-101/>)
- BSA ELISA kit; All Bovine Serum Albumin (BSA) ELISA Kit. (n.d.). (https://www.mybiosource.com/prods/ELISA-Kit/All/Bovine-Serum-Albumin-BSA/BSA/datasheet.php?products_id=2000242#QLINFO)
- Cancer Treatment Centers of America. (2017). How We Treat Cancer: Find Treatments at our Hospitals. (<http://www.cancercenter.com/treatments/>)
- Chan, H. N., et al. (2016). Simple, Cost-Effective 3D Printed Microfluidic Components for Disposable, Point-of-Care Colorimetric Analysis. *ACS Sensors*, 1(3), 227-234. doi:10.1021/acssensors.5b00100
- Chandana, T., Gunasingh, G. P., Cherian, K.M., Sankaranarayanan, K.(2011). "Humanized" Stem Cell Culture Techniques: The Animal Serum Controversy. *Stem Cells International*. 504723. (<https://www.ncbi.nlm.nih.gov/pmc/articles/PMC3096451/>)
- Drummond, G. & Ludlam, C. (1999). Is Albumin Harmful?. *British Journal of Haematology*. 106(2). 266-9 (https://www.researchgate.net/publication/12838543_Is_albumin_harmful)
- Francis, G. L. (2010). Albumin and mammalian cell culture: implications for biotechnology applications. *Cytotechnology*, 62(1), 1-16. (<https://www.ncbi.nlm.nih.gov/pmc/articles/PMC2860567/>)
- ImmunoChemistry Technologies. (2017). Back to Basics: What is an immunoassay?. (<https://immunochemistry.com/2016/07/07/back-basics-immunoassay/>)
- International Organization for Standardization. (2009). ISO 11737 Sterilization of Medical Devices. (http://www.iso.org/iso/iso_catalogue/catalogue_tc/catalogue_detail.htm?csnumber=44955)
- International Organization for Standardization. (2017). ISO-9000 Quality Management. (<https://www.iso.org/iso-9001-quality-management.html>)
- International Organization for Standardization. (2016). ISO-13485 Medical Device- Quality Management Systems. (<https://www.iso.org/standard/59752.html>)

International Organization for Standardization. (2015). ISO-14000 Environmental Management. (<https://www.iso.org/iso-14001-environmental-management.html>)

International Organization for Standardization. (2015). IEC 60601-1-11:2015 Medical Electrical Equipment. (<https://www.iso.org/standard/65529.html>)

Kim, N., & Cho, S. G. (2013). Clinical applications of mesenchymal stem cells. *The Korean journal of internal medicine*, 28(4), 387-402.

Leukemia & Lymphoma Society. (2017). Autologous Stem Cell Transplantation. (<https://www.lls.org/treatment/types-of-treatment/stem-cell-transplantation/autologous-stem-cell-transplantation>)

Memorial Sloan Kettering Cancer Center. (2017). Autologous Stem Cell Transplant: A Guide for Patients & Caregivers. (<https://www.mskcc.org/cancer-care/patient-education/autologous-stem-cell-transplant-guide-patients-caregivers>)

MyBioSource. (2016). Enzyme-linked Immunosorbent Assay for Bovine Serum Albumin (BSA). (https://www.mybiosource.com/prods/ELISA-Kit/General/Bovine-Serum-Albumin-BSA/BSA/datasheet.php?products_id=2000242)

National Cell Manufacturing Consortium. (2016). Achieving Large-Scale, Cost-Effective, Reproducible Manufacturing of High Quality Cells: A Technology Roadmap to 2025.

National Institutes of Health (NIH). (2016). Stem Cell Basics IV. U.S. Department of Health and Human Services. (<https://stemcells.nih.gov/info/basics/4.htm>)

Perkel, J. (2011). Multiplexed Protein Assays. Biocompare. (<http://www.biocompare.com/Editorial-Articles/41806-Multiplexed-Protein-Assays/>)

R&D Systems. (2016). Mycoprobe Mycoplasma Detection Kit. (<https://resources.rndsystems.com/pdfs/datasheets/cul001b.pdf>)

Ryan, J. (2008). Understanding and Managing Cell Culture Contamination. *Corning Incorporated Life Sciences*. (<http://www.level.com.tw/html/ezcatfiles/vipweb20/img/img/20297/contamination-COR.pdf>)

Sigma Aldrich. (2017). What is Endotoxin? (<http://www.sigmaaldrich.com/life-science/stem-cell-biology/3d-stem-cell-culture/learning-center/what-is-endotoxin.html>)

Sigma Aldrich. (2017). Trypsin: Physical Properties and In Vivo Processing. (<http://www.sigmaaldrich.com/technical-documents/articles/biology/trypsin.html>)

Smith, C. (2012). Get the Blight Out: 5 Common Methods of Mycoplasma Detection. *Biocompare*. (<http://www.biocompare.com/Editorial-Articles/122209-Mycoplasma-Detection/>)

Stacey, G. N. (2011). Cell culture contamination. *Cancer cell culture: methods and protocols*, 79-91. (<https://www.ncbi.nlm.nih.gov/pubmed/21516399>)

Thermonamic. Specification of Thermoelectric Module. (<http://www.thermonamic.com/TEC1-12706-English.PDF>)

Ullah, I., Subbarao, R. B., & Rho, G. J. (2015). Human mesenchymal stem cells-current trends and future prospective. *Bioscience reports*, 35(2), e00191.
(<https://www.ncbi.nlm.nih.gov/pmc/articles/PMC4413017/>)

U.S. Food & Drug Administration. (2017). Marketed Products. Office of Cellular, Tissue and Gene Therapies.
(<https://www.fda.gov/biologicsbloodvaccines/cellulargenetherapyproducts/approvedproducts/default.Htm>)

United State Government Accountability Office. (2015). Regenerative Medicine: Federal Investment, Information Sharing, and Challenges in an Evolving Field. Report to Congressional Requesters.

Volokhov, D. V., Graham, L. J., Brorson, K. A., & Chizhikov, V. E. (2011). Mycoplasma testing of cell substrates and biologics: review of alternative non-microbiological techniques. *Molecular and cellular probes*, 25(2), 69-77. (<http://europepmc.org/abstract/MED/21232597>)

Worthington Biochemical Corporation. (2017). Trypsin. (<http://www.worthington-biochem.com/try/>)

Zhang, X., Chen, Z., & Huang, Y. (2015). A valve-less microfluidic peristaltic pumping method. *Biomicrofluidics*, 9(1), 014118. doi:10.1063/1.4907982

Appendices

Appendix A: Potential Pretotype Brochure

Company

Automated System Running
Major Four Quality Control
Assays

Company Name



MULTIPLEXING ASSAY DEVICE

The automated multiplexing device is capable of doing everything from the start to finish. The user just puts the cell sample in the machine and moves the cartridge to microplate reader after completion of multiplexing of the Mycoplasma, Endotoxin, BSA and Trypsin assay.

MULTIPLEXING ASSAY DEVICE

AUTOMATED SYSTEM RUNNING MAJOR FOUR QUALITY CONTROL ASSAYS

ABOUT THIS DEVICE

Ensuring the quality of MSCs for Autologous Transplant

The device is an automated system that is capable of running simultaneously four key quality control assays for the detection of Mycoplasma, Endotoxin, Bovine Serum Albumin (BSA), and Trypsin for ensuring the quality of mesenchymal stem cells for autologous transplant. The device consists of 3 major sections: Sample Preparation Station, System, and the Cartridge.

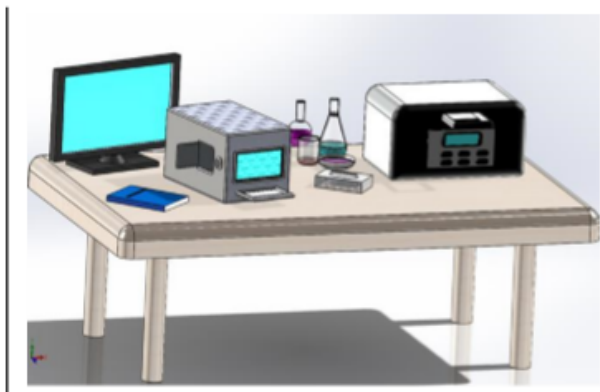
The sample preparation section of the device consists of reservoirs where the cell samples can be placed. The station will centrifuge and collect supernate, create a cell lysis solution, or create standard dilutions for a standard curve as required for each assay.

Internal fluid controls will transfer the appropriate volumes of the prepared samples to assay specific sections of a disposable, 96-well plate sized cartridge placed into the device. The various sections of the cartridge are

pre-coated to ensure that the assay is successful. Additionally, the system is independently temperature regulated for accurate incubation for each test.

The reagents, washes, and buffers required for the assays are stored in separate reservoirs with appropriate temperature controls. The system's pumping mechanisms control volume, pressure, and flowrate of the stored reagents into the appropriate cartridge sections using microfluidic tubing.

The device is equipped with a user interface screen for starting and stopping the assay process and observing the internal temperature and pressure conditions. When the assays have been completed, the convenient dimensions of the cartridge allow for simple and easy data retrieval from a standard microplate reader. This device will greatly decrease labor and equipment costs in quality control.

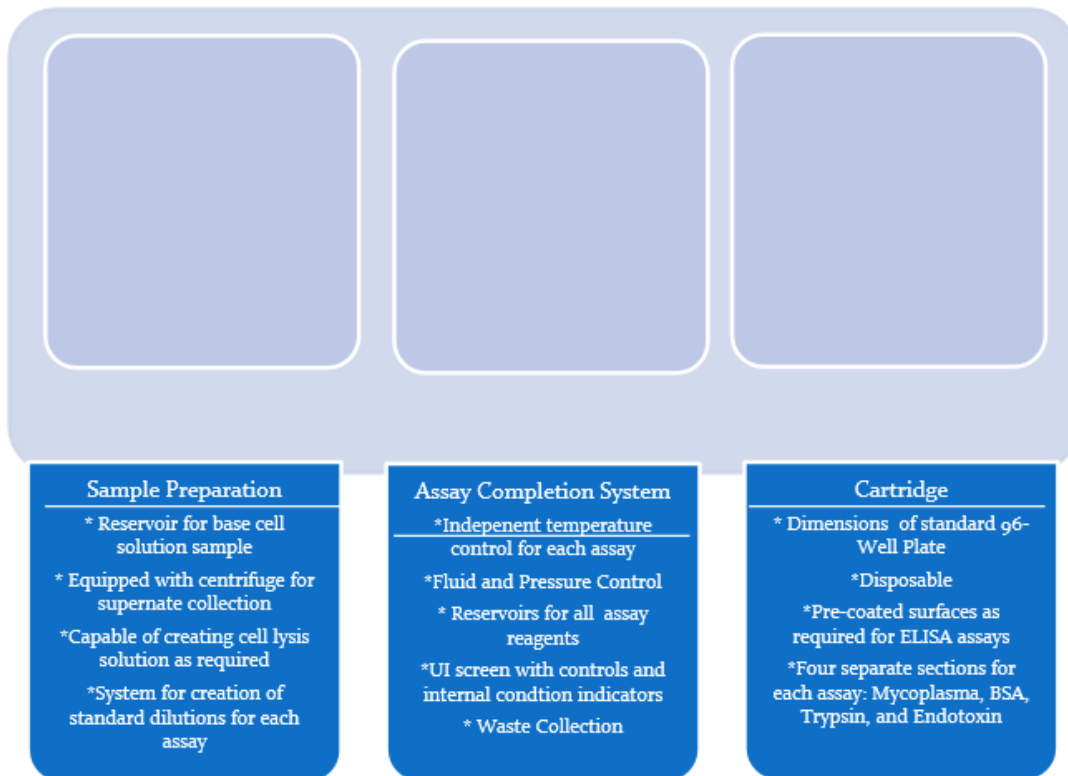


7 EASY STEPS:

1. Prepare cell sample to be tested and pipette – mL into the designated reservoir.
2. Press "Open/Close" button on screen to insert cartridge and close the cartridge compartment.
3. Observe internal conditions readings on screen to ensure the machine has reached proper conditions. If so, hit the "Start" button.
4. The machine will commence with sample preparation and assay completion. Upon completion, machine will alert and display "Complete" on the screen.
5. Remove the cartridge and transfer to standard microplate reader to obtain data at required wavelengths.
6. When required, press "Open Waste" button on screen to remove and empty waste reservoir as needed.
7. When required, remove back panel of device to access reagent storage. Device will alert when volumes are low.

THREE MAJOR SECTIONS IN THE MULTIPLEXING ASSAY DEVICE

What makes the Multiplexing Assay Device?



ADVANTAGES

Benefits of using this device

- ❖ Autonomous device performs multiplexing of 4 major assays for detection of Mycoplasma, BSA, Trypsin and Endotoxin
- ❖ Greatly reduces labor and equipment costs of quality control
- ❖ Reduces time required to perform appropriate sample preparations and assays individually
- ❖ Compliant with FDA regulations
- ❖ Affordable and cost efficient
- ❖ Convenient benchtop size
- ❖ Increased accuracy and reliability
- ❖ User friendly control monitor
- ❖ Easy to understand display of internal conditions including temperature and pressure
- ❖ Disposable cartridges
- ❖ Automated temperature, fluid, and pressure control to comply with requirements of each assay
- ❖ Equipped with a monitored waste container
- ❖ No additional equipment required

Appendix B: R&D Systems Mycoprobe Mycoplasma Detection Assay Kit Procedure

MATERIALS PROVIDED & STORAGE CONDITIONS

Store the unopened kit at 2-8 °C. Do not use past kit expiration date.

PART	PART #	DESCRIPTION	STORAGE OF OPENED/ RECONSTITUTED MATERIAL
Streptavidin Coated Microplate	890649	96 well polystyrene microplate (12 strips of 8 wells) coated with streptavidin.	Return unused wells to the foil pouch containing the desiccant pack, reseal along entire edge of zip-seal. May be stored for up to 3 months at 2-8 °C.*
Hybridization Microplate	895494	96 well polystyrene microplate.	May be stored for up to 3 months at 2-8 °C.*
Cell Lysis Diluent Concentrate	895540	2 vials (1.7 mL/vial) of a 10-fold concentrated solution.	
Sample Diluent	895284	2 vials (21 mL/vial) of a buffered protein solution with preservatives.	
Anti-Digoxigenin-AP Conjugate	890650	21 mL of a polyclonal antibody against digoxigenin conjugated to alkaline phosphatase with preservatives.	
Capture Probes	893000	1.1 mL of a six-fold concentrated stock solution.	
Detection Probes	893001	1.1 mL of a six-fold concentrated stock solution.	
Positive Control	892896	1.1 mL of a solution containing a synthetic DNA oligonucleotide.	
Wash Buffer Concentrate	895285	100 mL of a 10-fold concentrated solution with preservatives.	
Stop Solution	895032	6 mL of 2 N sulfuric acid.	
Substrate	895884	1 vial of lyophilized NADPH with stabilizers.	Store in an upright position for up to 3 months at ≤ -80 °C.*
Substrate Diluent	895885	7 mL of a buffered solution with stabilizers.	
Amplifier	895886	1 vial of lyophilized amplifier enzymes with stabilizers.	
Amplifier Diluent	895887	7 mL of a buffered solution containing INT-violet with stabilizers.	
Float Collar	720045	Microplate float collar for water bath.	
Plate Sealers	N/A	12 adhesive strips.	

* Provided this is within the expiration date of the kit.

OTHER SUPPLIES REQUIRED

- Microplate reader capable of measuring absorbance at 490 nm with the correction wavelength set at 650 nm or 690 nm
- Pipettes and pipette tips
- Deionized water, RNase-free
- Squirt bottle or manifold dispenser
- 1000 mL graduated cylinder for preparation of Wash Buffer
- Horizontal orbital microplate shaker (0.12" orbit) capable of maintaining a speed of 500 ± 50 rpm
- 65 ± 1 °C water bath
- Vortex mixer
- Gloves and mask
- Tubes for sample preparation.

REAGENT PREPARATION

Bring all reagents to room temperature before use.

Cell Lysis Diluent (diluted 1:10) - Add 3.4 mL of Cell Lysis Diluent Concentrate to 30.6 mL of Sample Diluent to prepare 34 mL of Cell Lysis Diluent (diluted 1:10).

Probes (1X) - To assay an entire 96 well plate, add 1.0 mL of the Capture Probes and 1.0 mL of the Detection Probes to 4.0 mL of Sample Diluent. Adjust the volumes accordingly if assaying fewer than 96 wells. Make a fresh dilution of probes before running each assay.

Wash Buffer (1X) - If crystals have formed in the concentrate, warm to room temperature and mix gently until the crystals have completely dissolved. Add 100 mL of Wash Buffer Concentrate to 900 mL of RNase-free deionized water to prepare 1000 mL of Wash Buffer (1X).

Substrate Solution - Reconstitute the lyophilized Substrate with 6.0 mL of Substrate Diluent at least 10 minutes before use. Re-stopper and re-cap the vial and mix thoroughly.

Avoid contamination.

Amplifier Solution - Reconstitute the lyophilized Amplifier with 6.0 mL of Amplifier Diluent at least 10 minutes before use. Re-stopper and re-cap the vial and mix thoroughly.

Avoid contamination.

Positive Control - Ready to use; no preparation needed.

Negative Control - Use Sample Diluent as the negative control.

SAMPLE PREPARATION

Cell culture supernates (15 $\mu\text{L}/\text{well}$) or cell pellets (4,700 to 19,000 cells/well) are needed as samples in this assay. Passage of cultured cells in the absence of antibiotics (*i.e.*, penicillin and streptomycin) is not needed.

Cell cultures that are visibly contaminated (*i.e.*, turbidity and/or yellow media) are probably due to *E. coli* or fungal infection and should not be tested. Visibly contaminated cell cultures should be discarded and fresh cultures should be started from frozen stock. Mycoplasma contamination of cell cultures is typically not visible, even at high concentrations of mycoplasma (10^7 - 10^8 mycoplasma/mL).

CELL LYSATE SAMPLES

Cell pellet samples should be stored on ice until lysed with Cell Lysis Diluent (diluted 1:10) or stored at $\leq -20^\circ\text{C}$ for use at a later time. Prepare cell lysate samples using the following procedure:

1. Add 400 μL of Cell Lysis Diluent (diluted 1:10) to a cell pellet containing 5×10^5 cells, adherent or non-adherent, to obtain a final concentration of 1.25×10^6 cells/mL.
2. Pipet the cells up and down several times until they are resuspended.
3. Vortex for 15-20 seconds.
4. Dilute the cell lysate 10- to 40-fold with Cell Lysis Diluent (diluted 1:10) to obtain a final concentration of 3.125×10^4 to 1.25×10^5 cells/mL, respectively. For example, add 33 μL of cell lysate from Step 3 to 297 μL of Cell Lysis Diluent (diluted 1:10) to obtain a final concentration of 1.25×10^5 cells/mL. This sample dilution will provide sufficient volume to perform the assay in duplicate and provide excess for pipetting.
5. Assay immediately, cell lysates can be stored at $\leq -20^\circ\text{C}$ for use at a later time. Frozen cell lysate samples should be thawed on ice prior to use. Avoid multiple freeze-thaw cycles.

CELL CULTURE SUPERNATE SAMPLES

Cell culture supernate samples should be stored on ice prior to use or stored at $\leq -20^\circ\text{C}$ for use at a later time. Prepare cell culture supernate samples using the following procedure.

1. Dilute all cell culture supernate samples 10-fold in Cell Lysis Diluent (diluted 1:10). For example, add 33 μL of sample to 297 μL of Cell Lysis Diluent (diluted 1:10). This sample dilution will provide sufficient volume to perform the assay in duplicate and provide excess for pipetting.
2. Vortex for 15-20 seconds.
3. Assay immediately, or the diluted cell culture supernates can be stored at $\leq -20^\circ\text{C}$ for use at a later time. Frozen cell culture supernates should be thawed on ice prior to use. Avoid multiple freeze-thaw cycles.

ASSAY PROCEDURE

Wear gloves, mask, and a labcoat with tight-fitting cuffs during all assay steps. Bring all reagents to room temperature before use. Assaying all samples and controls in duplicate is recommended.

1. Prepare reagents and samples as instructed.
2. Wash the Hybridization Plate 2 times with Wash Buffer. Remove excess Wash Buffer by decanting or aspirating. Invert the plate and blot it against clean paper towels.
3. Add 50 μ L of diluted Probes to the designated wells.
4. Add 150 μ L of Positive Control, Sample Diluent (Negative Control), or sample to the designated wells. Cover with a plate sealer.
5. Apply the float collar to the Hybridization Plate and incubate the plate for 60 minutes in a 65 °C water bath.
6. Remove unused microplate strips from the Streptavidin Plate frame, return them to the foil pouch containing the desiccant pack, and reseal.
7. Wash the Streptavidin Plate 2 times with Wash Buffer and remove excess Wash Buffer as described in Step 2.
8. Transfer 150 μ L from each well of the Hybridization Plate to the washed Streptavidin Plate and apply a new plate sealer.
9. Incubate for 60 minutes at room temperature on a horizontal orbital shaker set at 500 \pm 50 rpm.
10. Wash the Streptavidin Plate 4 times with Wash Buffer and remove excess Wash Buffer.
11. Add 200 μ L of Anti-digoxigenin Conjugate to each well and cover with a new plate sealer.
12. Incubate for 60 minutes on the shaker at room temperature.
13. Wash the Streptavidin Plate 6 times with Wash Buffer and remove excess Wash Buffer.
14. Add 50 μ L of Substrate Solution to each well and cover with a new plate sealer.
15. Incubate for 60 minutes on the shaker at room temperature. **Do not wash.**
16. Add 50 μ L of Amplifier Solution to each well and cover with a new plate sealer.
17. Incubate for 30 minutes on the shaker at room temperature. **Do not wash.**
18. Add 50 μ L of Stop Solution to each well.
19. Determine the optical density (OD) of each well within 30 minutes, using a microplate reader set to 490 nm. If wavelength correction is available, set to 650 nm or 690 nm. If wavelength correction is not available, subtract readings at 650 nm or 690 nm from the readings at 490 nm. This subtraction will correct for optical imperfections in the plate. Readings made directly at 490 nm without correction may be higher and less accurate.

CALCULATION OF RESULTS

Determine the average of the duplicate optical density (O.D.) readings for each control and sample. Subtract the average negative control O.D. value from all average O.D. values. Negative results may have O.D. values below 0.0 after subtraction of the background.

The calculated positive control O.D. value should be ≥ 1.5 . The results from calculated sample O.D. values can be obtained using the following table:

Calculated O.D. Values	Result	Interpretation
< 0.05	Negative	No mycoplasma detected.
0.05-0.10	Inconclusive	Sample is suspect for mycoplasma. Continue to culture for an additional 2-3 days and repeat the test. If sample gives a similar O.D., then no mycoplasma are detected.
> 0.10	Positive	Mycoplasma detected.

TYPICAL DATA

Cell Line	Sample Type	Dilution or Cells/mL	Calculated O.D. Values	Result
CTL-2 mouse cytotoxic T cells	Supernate	1:10	1.025	Positive
BaF3 mouse pro-B cells	Supernate	1:10	0.183	Positive
HepG2 human hepatocellular carcinoma cells	Supernate	1:10	0.000	Negative
A431 human epithelial carcinoma cells	Cell Lysate	1.2×10^5	1.042	Positive
K562 human chronic myelogenous leukemia cells	Cell Lysate	1.2×10^5	1.912	Positive
K562 human chronic myelogenous leukemia cells	Cell Lysate	1.2×10^5	0.005	Negative

SENSITIVITY

This assay detects the following mycoplasma species at the levels shown below. To determine the minimal amount detectable, each species was grown in pure culture, serially diluted, and tested. The first five species listed account for 80-85% of mycoplasma contamination in cultured animal cells. CFU=Colony Forming Units

Mycoplasma Species	Sensitivity (CFU/well)
<i>M. arginini</i>	15
<i>M. orale</i>	65
<i>M. fermentans</i>	75
<i>A. laidlawii</i>	240
<i>M. hyorhinae</i>	560
<i>M. pirum</i>	30
<i>M. hominis</i>	225
<i>M. salivarium</i>	2500

Appendix C: MyBioSource BSA Detection Assay Procedure

MBS2000242 96 Tests
Enzyme-linked Immunosorbent Assay Kit
For Bovine Serum Albumin (BSA)
Organism Species: Pan-species (General)
Instruction manual

FOR IN VITRO AND RESEARCH USE ONLY
NOT FOR USE IN CLINICAL DIAGNOSTIC PROCEDURES

12th Edition (Revised in May, 2016)

[INTENDED USE]

The kit is a competitive inhibition enzyme immunoassay technique for the in vitro quantitative measurement of BSA in serum, plasma, tissue homogenates, cell lysates, cell culture supernates and other biological fluids.

[REAGENTS AND MATERIALS PROVIDED]

Reagents	Quantity	Reagents	Quantity
Pre-coated, ready to use 96-well strip plate	1	Plate sealer for 96 wells	4
Standard	2	Standard Diluent	1×20mL
Detection Reagent A	1×120μL	Assay Diluent A	1×12mL
Detection Reagent B	1×120μL	Assay Diluent B	1×12mL
TMB Substrate	1×9mL	Stop Solution	1×6mL
Wash Buffer (30 × concentrate)	1×20mL	Instruction manual	1

[MATERIALS REQUIRED BUT NOT SUPPLIED]

1. Microplate reader with 450 ± 10 nm filter.
2. Single or multi-channel pipettes with high precision and disposable tips.
3. Microcentrifuge Tubes.
4. Deionized or distilled water.
5. Absorbent paper for blotting the microplate.
6. Container for Wash Solution.
7. 0.01mol/L (or 1×) Phosphate Buffered Saline(PBS), pH7.0-7.2.

[STORAGE OF THE KITS]

1. **For unopened kit:** All the reagents should be kept according to the labels on vials. The **Standard, Detection Reagent A, Detection Reagent B** and the **96-well strip plate** should be stored at -20°C upon receipt while the others should be at 4°C .
2. **For used kit:** When the kit is used, the remaining reagents need to be stored according to the above storage condition. Besides, please return the unused wells to the foil pouch containing the desiccant pack, and zip-seal the foil pouch.

Note:

FOR RESEARCH USE ONLY. NOT FOR USE IN DIAGNOSTIC PROCEDURES

It is highly recommended to use the remaining reagents within 1 month provided this is prior to the expiration date of the kit. For the expiration date of the kit, please refer to the label on the kit box. All components are stable up to the expiration date.

[SAMPLE COLLECTION AND STORAGE]

Serum - Use a serum separator tube and allow samples to clot for two hours at room temperature or overnight at 4°C before centrifugation for 20 minutes at approximately 1,000×g. Assay freshly prepared serum immediately or store samples in aliquot at -20°C or -80°C for later use. Avoid repeated freeze/thaw cycles.

Plasma - Collect plasma using EDTA or heparin as an anticoagulant. Centrifuge samples for 15 minutes at 1,000×g at 2-8°C within 30 minutes of collection. Remove plasma and assay immediately or store samples in aliquot at -20°C or -80°C for later use. Avoid repeated freeze/thaw cycles.

Tissue homogenates - The preparation of tissue homogenates will vary depending upon tissue type.

1. Tissues were rinsed in ice-cold PBS to remove excess blood thoroughly and weighed before homogenization.
2. Minced the tissues to small pieces and homogenized them in fresh lysis buffer (catalog: IS007, different lysis buffer needs to be chosen based on subcellular location of the target protein) (w:v = 1:20-1:50, e.g. 1mL lysis buffer is added in 20-50mg tissue sample) with a glass homogenizer on ice (Micro Tissue Grinders works, too).
3. The resulting suspension was sonicated with an ultrasonic cell disrupter till the solution is clarified.
4. Then, the homogenates were centrifuged for 5 minutes at 10,000×g. Collect the supernatant and assay immediately or aliquot and store at ≤-20°C.

Cell Lysates - Cells need to be lysed before assaying according to the following directions.

1. Adherent cells should be washed by cold PBS gently, and then detached with trypsin, and collected by centrifugation at 1,000×g for 5 minutes (suspension cells can be collected by centrifugation directly).
2. Wash cells three times in cold PBS.
3. Resuspend cells in fresh lysis buffer with concentration of 10⁷ cells/mL. If it is necessary, the cells could be subjected to ultrasonication till the solution is clarified.
4. Centrifuge at 1,500×g for 10 minutes at 2-8°C to remove cellular debris. Assay immediately or aliquot and store at ≤-20°C.

Cell culture supernatants and other biological fluids - Centrifuge samples for 20 minutes at 1,000×g. Collect the supernatant and assay immediately or store samples in aliquot at -20°C or -80°C for later use. Avoid repeated freeze/thaw cycles.

Note:

1. Samples to be used within 5 days may be stored at 4°C, otherwise samples must be stored at -20°C (≤1 month) or -80°C (≤2 months) to avoid loss of bioactivity and contamination.
2. Sample hemolysis will influence the result, so hemolytic specimen should not be used.
3. When performing the assay, bring samples to room temperature.
4. It is highly recommended to use serum instead of plasma for the detection based on quantity of our in-house data.

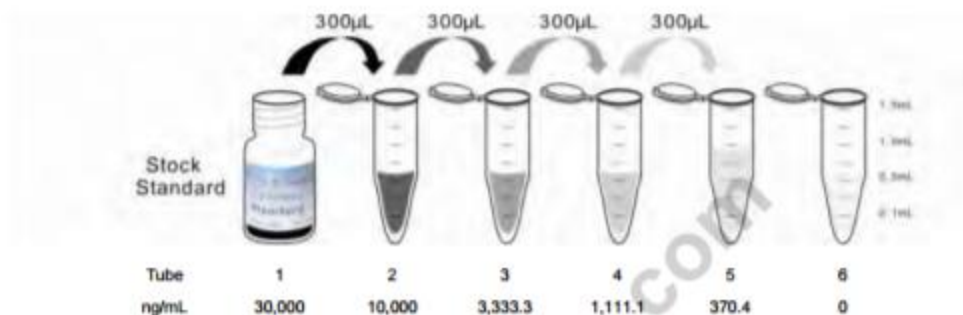
[REAGENT PREPARATION]

1. Bring all kit components and samples to room temperature (18-25°C) before use. If the kit will not be used up in one time, please only take out strips and reagents for present experiment, and leave the remaining strips

FOR RESEARCH USE ONLY. NOT FOR USE IN DIAGNOSTIC PROCEDURES

and reagents in required condition.

2. **Standard** - Reconstitute the **Standard** with 1.0mL of **Standard Diluent**, kept for 10 minutes at room temperature, shake gently(not to foam). The concentration of the standard in the stock solution is 30,000ng/mL. Please prepare 5 tubes containing 0.6mL Standard Diluent and produce a triple dilution series according to the picture shown below. Mix each tube thoroughly before the next transfer. Set up 5 points of diluted standard such as 30,000ng/mL, 10,000ng/mL, 3,333.3ng/mL, 1,111.1ng/mL, 370.4ng/mL, and the last EP tubes with **Standard Diluent** is the blank as 0ng/mL.



3. **Detection Reagent A and Detection Reagent B** - Briefly spin or centrifuge the stock Detection A and Detection B before use. Dilute them to the working concentration 100-fold with **Assay Diluent A** and **B**, respectively.
4. **Wash Solution** - Dilute 20mL of Wash Solution concentrate (30×) with 580mL of deionized or distilled water to prepare 600mL of Wash Solution (1×).
5. **TMB substrate** - Aspirate the needed dosage of the solution with sterilized tips and do not dump the residual solution into the vial again.

Note:

1. Making serial dilution in the wells directly is not permitted.
2. Prepare standard within 15 minutes before assay. Please do not dissolve the reagents at 37°C directly.
3. Detection Reagent A and B are sticky solutions, therefore, slowly pipette them to reduce the volume errors.
4. Please carefully reconstitute Standards or working Detection Reagent A and B according to the instruction, and avoid foaming and mix gently until the crystals are completely dissolved. To minimize imprecision caused by pipetting, use small volumes and ensure that pipettors are calibrated. It is recommended to suck more than 10µL for one pipetting.
5. The reconstituted Standards, Detection Reagent A and Detection Reagent B can be **used only once**.
6. If crystals have formed in the Wash Solution concentrate (30×), warm to room temperature and mix gently until the crystals are completely dissolved.
7. Contaminated water or container for reagent preparation will influence the detection result.

[SAMPLE PREPARATION]

1. We are only responsible for the kit itself, but not for the samples consumed during the assay. The user should calculate the possible amount of the samples used in the whole test. Please reserve sufficient samples in advance.
2. Please predict the concentration before assaying. If values for these are not within the range of the standard curve, users must determine the optimal sample dilutions for their particular experiments.

FOR RESEARCH USE ONLY. NOT FOR USE IN DIAGNOSTIC PROCEDURES

3. Serum/plasma samples require about a 10,000 fold dilution. For example, to prepare a 1:10,000 dilution of sample, transfer 10 μ L of sample to 990 μ L PBS. This yields a 1:100 dilution. Next, dilute the 1:100 sample by transferring 10 μ L to 990 μ L PBS. You now have a 1:10,000 dilution of your sample. Mix thoroughly at each stage. Sample should be diluted by 0.01mol/L PBS(PH=7.0-7.2).
4. If the samples are not indicated in the manual, a preliminary experiment to determine the validity of the kit is necessary.
5. Tissue or cell extraction samples prepared by chemical lysis buffer may cause unexpected ELISA results due to the impacts from certain chemicals.
6. Due to the possibility of mismatching between antigen from other origin and antibody used in our kits (e.g., antibody targets conformational epitope rather than linear epitope), some native or recombinant proteins from other manufacturers may not be recognized by our products.
7. Influenced by the factors including cell viability, cell number or sampling time, samples from cell culture supernatant may not be detected by the kit.
8. Fresh samples without long time storage is recommended for the test. Otherwise, protein degradation and denaturalization may occur in those samples and finally lead to wrong results.

[ASSAY PROCEDURE]

1. Determine wells for diluted standard, blank and sample. Prepare 5 wells for standard points, 1 well for blank. Add 50 μ L each of dilutions of standard (read Reagent Preparation), blank and samples into the appropriate wells, respectively. And then add 50 μ L of Detection Reagent A to each well immediately. Shake the plate gently (using a microplate shaker is recommended). Cover with a Plate sealer. Incubate for 1 hour at 37°C. Detection Reagent A may appear cloudy. Warm to room temperature and mix gently until solution appears uniform.
2. Aspirate the solution and wash with 350 μ L of 1X Wash Solution to each well using a squirt bottle, multi-channel pipette, manifold dispenser or autowasher, and let it sit for 1-2 minutes. Remove the remaining liquid from all wells completely by snapping the plate onto absorbent paper. Repeat 3 times. After the last wash, remove any remaining Wash Buffer by aspirating or decanting. Invert the plate and blot it against absorbent paper.
3. Add 100 μ L of Detection Reagent B working solution to each well. Incubate for 30 minutes at 37°C after covering it with the Plate sealer.
4. Repeat the aspiration/wash process for total 5 times as conducted in step 2.
5. Add 90 μ L of Substrate Solution to each well. Cover with a new Plate sealer. Incubate for 10 - 20 minutes at 37°C (Don't exceed 30 minutes). Protect from light. The liquid will turn blue by the addition of Substrate Solution.
6. Add 50 μ L of Stop Solution to each well. The liquid will turn yellow by the addition of Stop solution. Mix the liquid by tapping the side of the plate. If color change does not appear uniform, gently tap the plate to ensure thorough mixing.
7. Remove any drop of water and fingerprint on the bottom of the plate and confirm there is no bubble on the surface of the liquid. Then, run the microplate reader and conduct measurement at 450nm immediately.

Note:

1. **Assay preparation:** Keep appropriate numbers of wells for each experiment and remove extra wells from microplate. Rest wells should be resealed and stored at -20°C.
2. **Samples or reagents addition:** Please use the freshly prepared Standard. Please carefully add samples

FOR RESEARCH USE ONLY. NOT FOR USE IN DIAGNOSTIC PROCEDURES

to wells and mix gently to avoid foaming. Do not touch the well wall. For each step in the procedure, total dispensing time for addition of reagents or samples to the assay plate **should not exceed 10 minutes**. This will ensure equal elapsed time for each pipetting step, without interruption. Duplication of all standards and specimens, although not required, is recommended. To avoid cross-contamination, change pipette tips between additions of standards, samples, and reagents. Also, use separated reservoirs for each reagent.

3. **Incubation:** To ensure accurate results, proper adhesion of plate sealers during incubation steps is necessary. Do not allow wells to sit uncovered for extended periods between incubation steps. Once reagents are added to the well strips, DO NOT let the strips DRY at any time during the assay. Incubation time and temperature must be controlled.
4. **Washing:** The wash procedure is critical. Complete removal of liquid at each step is essential for good performance. After the last wash, remove any remaining Wash Solution by aspirating or decanting and remove any drop of water and fingerprint on the bottom of the plate. Insufficient washing will result in poor precision and false elevated absorbance reading.
5. **Controlling of reaction time:** Observe the change of color after adding **TMB Substrate** (e.g. observation once every 10 minutes), if the color is too deep, add **Stop Solution** in advance to avoid excessively strong reaction which will result in inaccurate absorbance reading.
6. **TMB Substrate** is easily contaminated. Please protect it from light.
7. The environment humidity which is less than 60% might have some effects on the final performance, therefore, a humidifier is recommended to be used at that condition.

[TEST PRINCIPLE]

This assay employs the competitive inhibition enzyme immunoassay technique. A monoclonal antibody specific to BSA has been pre-coated onto a microplate. A competitive inhibition reaction is launched between biotin labeled BSA and unlabeled BSA (Standards or samples) with the pre-coated antibody specific to BSA. After incubation the unbound conjugate is washed off. Next, avidin conjugated to Horseradish Peroxidase (HRP) is added to each microplate well and incubated. The amount of bound HRP conjugate is reverse proportional to the concentration of BSA in the sample. After addition of the substrate solution, the intensity of color developed is reverse proportional to the concentration of BSA in the sample.

[CALCULATION OF RESULTS]

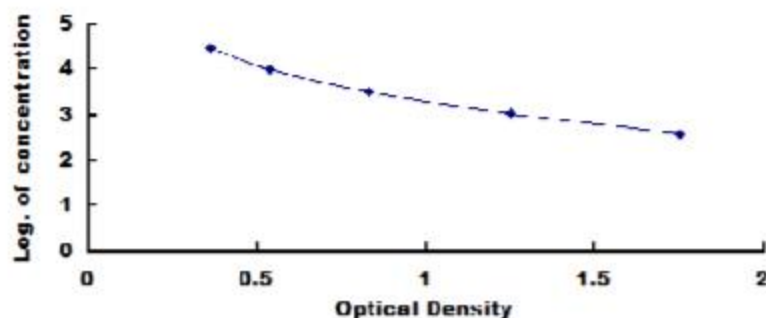
This assay employs the competitive inhibition enzyme immunoassay technique, so there is an inverse correlation between BSA concentration in the sample and the assay signal intensity.

Average the duplicate readings for each standard, control, and samples. Create a standard curve on log-log or semi-log graph paper, with the log of BSA concentration on the y-axis and absorbance on the x-axis. Draw the best fit straight line through the standard points and it can be determined by regression analysis. Using some plot software, for instance, curve expert 1.30, is also recommended. If samples have been diluted, the concentration read from the standard curve must be multiplied by the dilution factor.

[TYPICAL DATA]

In order to make the calculation easier, we plot the O.D. value of the standard (X-axis) against the log of concentration of the standard (Y-axis), although concentration is the independent variable and O.D. value is the dependent variable. The O.D. values of the standard curve may vary according to the conditions of assay performance (e.g. operator, pipetting technique, washing technique or temperature effects). Typical standard curve below is provided for reference only.

FOR RESEARCH USE ONLY. NOT FOR USE IN DIAGNOSTIC PROCEDURES



Typical Standard Curve for BSA ELISA.

[DETECTION RANGE]

370.4-30,000ng/mL. The standard curve concentrations used for the ELISA's were 30,000ng/mL, 10,000ng/mL, 3,333.3ng/mL, 1,111.1ng/mL, 370.4ng/mL.

[SENSITIVITY]

The minimum detectable dose of BSA is typically less than 161.2ng/mL.

The sensitivity of this assay, or Lower Limit of Detection (LLD) was defined as the lowest protein concentration that could be differentiated from zero. It was determined by subtracting two standard deviations to the mean optical density value of twenty zero standard replicates and calculating the corresponding concentration.

[SPECIFICITY]

This assay has high sensitivity and excellent specificity for detection of BSA.

No significant cross-reactivity or interference between BSA and analogues was observed.

Note:

Limited by current skills and knowledge, it is impossible for us to complete the cross- reactivity detection between BSA and all the analogues, therefore, cross reaction may still exist.

[RECOVERY]

Matrices listed below were spiked with certain level of BSA and the recovery rates were calculated by comparing the measured value to the expected amount of BSA in samples.

Matrix	Recovery range (%)	Average(%)
serum(n=5)	85-96	90
EDTA plasma(n=5)	86-98	92
heparin plasma(n=5)	96-105	101

[LINEARITY]

The linearity of the kit was assayed by testing samples spiked with appropriate concentration of BSA and their serial dilutions. The results were demonstrated by the percentage of calculated concentration to the expected.

FOR RESEARCH USE ONLY, NOT FOR USE IN DIAGNOSTIC PROCEDURES

Sample	1: 2	1: 4	1: 8	1: 16
serum(n=5)	81-93%	97-105%	82-97%	84-103%
EDTA plasma(n=5)	90-99%	87-94%	95-102%	87-98%
heparin plasma(n=5)	83-97%	82-92%	80-104%	85-101%

Samples were diluted prior to assay as described in the SAMPLE PREPARATION section.

[PRECISION]

Intra-assay Precision (Precision within an assay): 3 samples with low, middle and high level BSA were tested 20 times on one plate, respectively.

Inter-assay Precision (Precision between assays): 3 samples with low, middle and high level BSA were tested on 3 different plates, 8 replicates in each plate.

$CV(\%) = SD/mean \times 100$

Intra-Assay: $CV < 10\%$

Inter-Assay: $CV < 12\%$

[STABILITY]

The stability of ELISA kit is determined by the loss rate of activity. The loss rate of this kit is less than 5% within the expiration date under appropriate storage condition.

To minimize extra influence on the performance, operation procedures and lab conditions, especially room temperature, air humidity, incubator temperature should be strictly controlled. It is also strongly suggested that the whole assay is performed by the same operator from the beginning to the end.

Appendix D: Syringe Pump Calibration Curve Determination Experiment (Full)

To perform this experiment, the group used the pre-existing syringe pump assembly consisting of a 1ml glass syringe and linear actuator enclosed in a metal assembly. The assembly was connected to a programmed Arduino Uno controller board to initiate and terminate movement of the linear actuator. The Arduino code was programmed to prompt the user for a position value that the linear actuator would then travel to. Open the Arduino software program “*PumpAndValve.ino*” on the computer and enter “0” value for the position of the linear actuator to bring the linear actuator to initial position corresponding to zero volume in the syringe. Then, press “x” to confirm and enter the value. NOTE: Press “x” after entering the desired value. After entering the position, enter the desired speed of the linear actuator to “150” and enter “x” to run the system. NOTE: Always enter each digit of the desired value individually for both position and speed (Example: 150, Enter). Later enter “x” after inputting the desired value for both location and speed (Example: 150, Enter, x). The program will ask for an input for the speed of the linear actuator only at the start of the program (after inputting the first desired location of the position of the linear actuator). The linear actuator will run at the same entered speed (here 150) for different input value positions of the linear actuator until the Arduino program is closed and re-run.

Measuring the maximum volume of the glass syringe in the syringe pump assembly: In order to do so, first tare the mass scale to zero with the doors closed. Place a water filled glass vial (vial A) on the scale (capped). Close the scale doors and record the mass. *NOTE: Record the mass when the “g” symbol appears on the scale.* Uncap the vial A and place the tube connected to the glass syringe into the vial A to pump water from the vial A into the glass syringe within the syringe pump assembly. Within the same Arduino Software Program window input “1000” value for the position of the linear actuator to fill the syringe with water from the vial A. NOTE: The tube from the glass syringe is placed into the filled and weighed glass vial. After entering each digit of “1000” individually (Example: 1000. Enter) enter “x” to run the program (Example: 1000. Enter, x). The pump will start to pull water from the filled vial to the glass syringe. Now take another empty vial (vial B) and empty out water from the glass syringe to the empty vial by entering “0” for the position of the linear actuator. This will pump out all the water from the syringe. Now measure the weight of the vial A with the remaining water using the scale (Ensure to cap the vial and close the doors of the scale before measuring). Calculate the amount of water filled in the glass syringe= total weight of the filled vial A– weight of the vial A with remaining water. Perform the test 3 times and calculate the mean of water filled in the glass syringe.

Calibration Curve Experiment Maximum Syringe Volume Intake Results

Total weight of the filled vial (g)	Vial weight after filling the syringe (g)	Maximum volume intake of the syringe (uL)
13.4468	12.6602	787
12.6602	11.8738	786
11.8738	11.0892	785
11.0892	10.3002	789

Mean Volume Intake: 0.7866g=787uL

Setting up an empty vial to collect the output volume from the Syringe Pump Assembly: In order to do so, we first enter “0” (in the Arduino software program) for the position of the linear actuator to ensure all the water is out of the system. Press “x” and enter to run the program. Take another filled glass vial (vial C). Uncap the water filled vial and place the glass syringe tube into the water filled glass vial. Enter “1000” for the position of the linear actuator to fill the glass syringe within the syringe pump to its maximum capacity. Press “x” and enter to run the program. Now take an empty glass vial (vial D)

and record the mass of the empty vial. *NOTE: Ensure to tare the scale before measuring the mass of the empty vial. Also close the scale doors while measuring the weight of the vial.* Now replace the glass vial C with an empty glass vial (vial D). In the same Arduino software program “Enter position of linear actuator” on the computer, input random positions of the linear actuator. *NOTE: Input random values from “0” (Initial position of the linear actuator) to “1000” (Maximum distance traveled by the linear actuator within the syringe pump assembly).* Collect the pumped water in the vial D. Measure the total mass of the vial D. Calculate the mass of the water dispensed at the input random location= total mass of the vial D - mass of the empty vial D. Repeat the previous steps for twelve random positions for the linear actuator. Repeat the previous step two more times for the same 12 positions of the linear actuator.

Experimental Results and Analysis

Calibration Curve Experiment Iteration 1 Results

Start Position	Input Position	Actual End Position	Distance Traveled	Volume Output (uL)
1000	0	0	1000	775
1000	38	57	943	753
1000	281	306	694	583
1000	324	339	661	552
1000	417 (incorrect)	N/A	N/A	486
1000	500	518	482	418
1000	622	639	361	318
1000	635	655	345	385
1000	773	784	216	218
1000	815	836	164	168
1000	873	884	116	123
1000	950	956	44	66

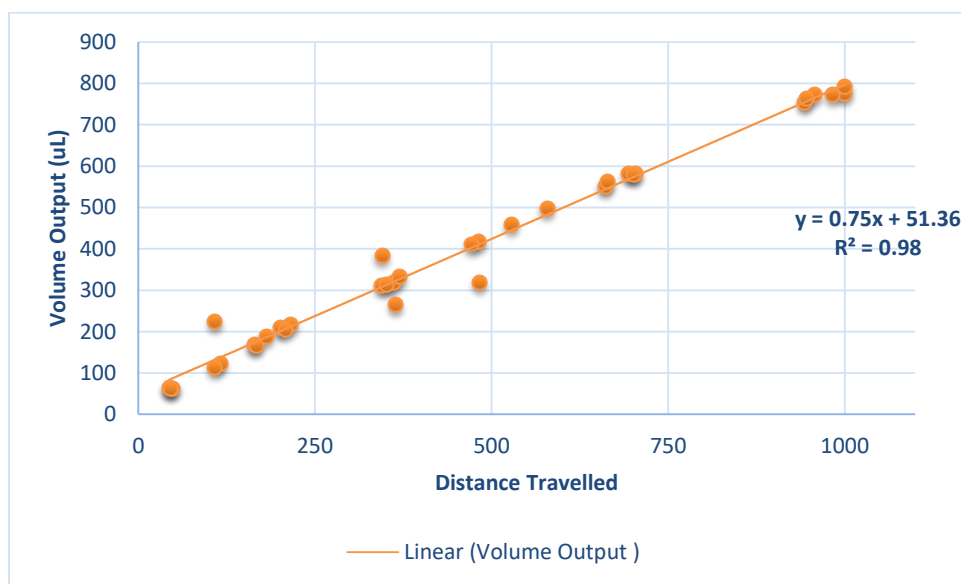
Calibration Curve Experiment Iteration 2 Results

Start Position	Input Position	Actual End Position	Distance Traveled	Volume Output (uL)
1000	0	17	983	772
1000	38	43	957	772
1000	281	296	704	583
1000	324	336	664	562
1000	450	472	528	460
1000	500	517	483	320
1000	622	631	369	332
1000	635	656	344	312
1000	773	799	201	210
1000	815	833	167	167
1000	873	892	108	224
1000	950	951	49	63

Calibration Curve Experiment Iteration 3 Results

Start Position	Input Position	Actual End Position	Distance Traveled	Volume Output (uL)
1000	0	0	1000	793
1000	38	54	946	763
1000	281	299	701	580
1000	324	341	659 (outlier)	101(outlier)
1000	417	421	579	498
1000	500	528	472	412
1000	622	636	364	265
1000	635	648	352	313
1000	773	792	208	205
1000	815	819	181	189
1000	873	892	108	114
1000	950	955	45	63

Volume vs. Distance Traveled for Iterations 1, 2, and 3
Outliers are highlighted in the table above but removed from graph



Calibration curve experiment volume output vs distance traveled for iterations 1-3 with outliers removed

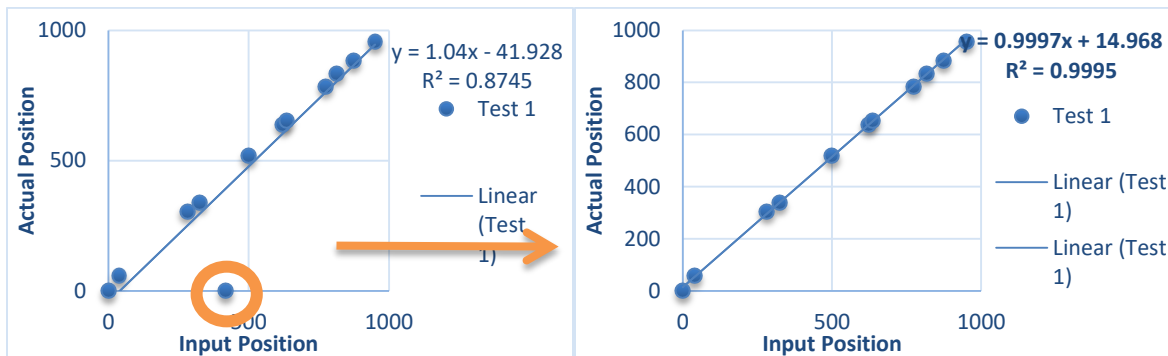
Data	Test 1 (With Outlier)	Test 2	Test 3 (With Outlier)
$y=mx+c$	$y = 0.7429x + 56.842$	$y = 0.7277x + 61.484$	$y = 0.6918x + 34.281$

R square	$R^2 = 0.9883$	$R^2 = 0.9594$	$R^2 = 0.75$
----------	----------------	----------------	--------------

Data	Test 1 (Without Outlier)	Test 2	Test 3 (Without Outlier)
$y=mx+c$	$y = 0.7429x + 56.842$	$y = 0.7277x + 61.484$	$y = 0.7685x + 35.099$
R square	$R^2 = 0.9883$	$R^2 = 0.9594$	$R^2 = 0.9943$

After we removed the outlier from Test 3 the value of m (Slope) in $y=mx+c$ became closer to the m (Slope) values obtained from both Tests 1 and 2. Also, after removing the outliers in Test 3, the R square values of Test 3 became closer to the R square values obtained in Test 1 and 2. These R square values in Test 1,2 and 3 were also closer to approximately 1. The team also thought that possible reasons for outliers could be Human error or Instrument error.

Actual Position vs Input Position
(Outliers are highlighted in the table # above but removed from graph)



ANALYSIS:

Data	Test 1 (With Outlier)	Test 2	Test 3 (With Outlier)
$y=mx+c$	$y = 1.04x - 41.928$	$y = 0.9968x - 13.424$	$y = 0.997x - 11.944$
R square	$R^2 = 0.8745$	$R^2 = 0.9995$	$R^2 = 0.9993$

Data	Test 1 (Without Outlier)	Test 2	Test 3 (Without Outlier)
$y=mx+c$	$y = 0.9997x + 14.968$	$y = 0.9968x - 13.424$	$y = 0.997x - 11.083$

R square	$R^2 = 0.9995$	$R^2 = 0.9995$	$R^2 = 0.9993$
----------	----------------	----------------	----------------

After removing the outlier from Test 1 the value of m (Slope) in $y=mx+c$ are close to the slope values obtained from Test 2 and 3. Also, after removing the outliers, the values of R square for Test 1, 2, and 3 are pretty close and are also close to approximately 1. The reasons for the outliers are Human error possibly, because the outlier's actual position wasn't written down (indication N/A in Test1).

Syringe Pump with Manifold: Dead Volumes Experiment

The previous steps with Manifold attached to the syringe pump. NOTE: While filling the syringe to its complete capacity, remove the manifold and fill the syringe with similar procedure. Connect the manifold right after inputting water. And continue the next steps.

Syringe pump with manifold dead volumes experiment results: Iteration 1

Desired Output Volume(uL)	Actual Output Volume (uL)	Goal Position	Actual Position
30	0	959	959
50	49	932	933
90	99	878	880
100	118	865	n/a*
150	164	798	n/a*
200	198	731	733
300	274	596	600
350	263	529	534
500	455	327	n/a*
600	543	193	194
700	562	59	60
796	741	0	1

**Due to human error, actual position was not recorded*

Syringe pump with manifold dead volumes experiment results: Iteration 2

Desired Output Volume	Actual Output Volume (uL)	Goal Position	Actual Position
30	0	959	957
50	45	932	933
90	48	878	n/a*
100	108	865	866
150	122	798	800
200	134	731	734
300	67	596	n/a*
350	234	529	532
500	722	327	330
600	595	193	194

700	629	59	60
796	729	0	1

**Due to human error, actual position was not recorded*

Syringe pump with manifold dead volumes experiment results: Iteration 3

<i>Desired Output Volume(μl)</i>	<i>Actual Output Volume(μl)</i>	<i>Desired Position</i>	<i>Actual Position</i>
30	13	959	959
50	49	932	933
90	88	878	880
100	107	865	867
150	129	798	799
200	167	731	732
300	264	596	600
350	305	529	533
500	467	327	331
600	553	193	196
700	646	59	<i>n/a*</i>
796	737	0	1

**Due to human error, the actual position was not recorded*



Syringe pump with manifold dead volumes experiment goal vs actual output results for iterations 1-3

Observations:

Data	Test 1	Test 2	Test 3 (With Outlier)
$y=mx+c$	$y = 0.8686x + 9.0011$	$y = \mathbf{1.0158x - 41.19}$	$y = 0.9287x - 5.4455$
R square	$R^2 = 0.983$	$\mathbf{R^2 = 0.8722}$	$R^2 = 0.9982$

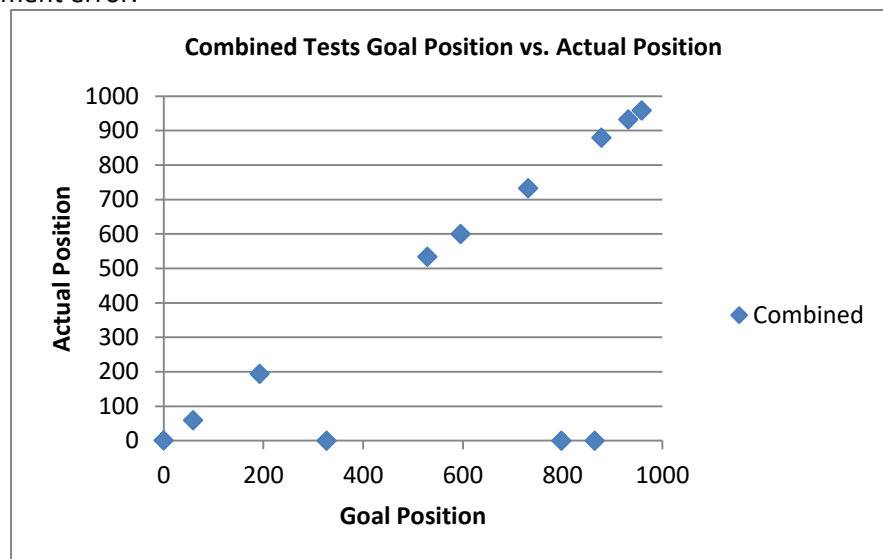
Data	Test 1	Test 2	Test 3 (Without Outlier)
$y=mx+c$	$y = 0.8686x + 9.0011$	$y = 0.9483x - 26.35$	$y = 0.9287x - 5.4455$
R square	$R^2 = 0.983$	$R^2 = 0.9838$	$R^2 = 0.9982$

ANALYSIS:

R²: After removing the outlier the R² value for Test 2 changed from 0.8722 to 0.9838. It can be observed that the values of R² are very close to 1 after removing the outliers in Test 2. Also, the combined tests have R² = 0.9866.

SLOPE: The graphs obtained are pretty linear and the slope values for Test 1 and 3 are relatively close. After removing the outlier from Test 2, the slope values for Test 2 are relatively close to the test values of Test 1 and Test 3. The combined tests have slope (m)= 0.9153.

OUTLIERS: There exist 2 significant outliers in Test 2. The possible reasons for outlier are either human error or instrument error.



Observations:

Data	Test 1	Test 2	Test 3 (With Outlier)
$y=mx+c$	$y = \mathbf{0.7346x - 12.517}$	$y = \mathbf{0.8025x + 30.689}$	$y = \mathbf{1.0221x - 15.657}$
R square	$\mathbf{R^2 = 0.4009}$	$\mathbf{R^2 = 0.5578}$	$\mathbf{R^2 = 0.998}$

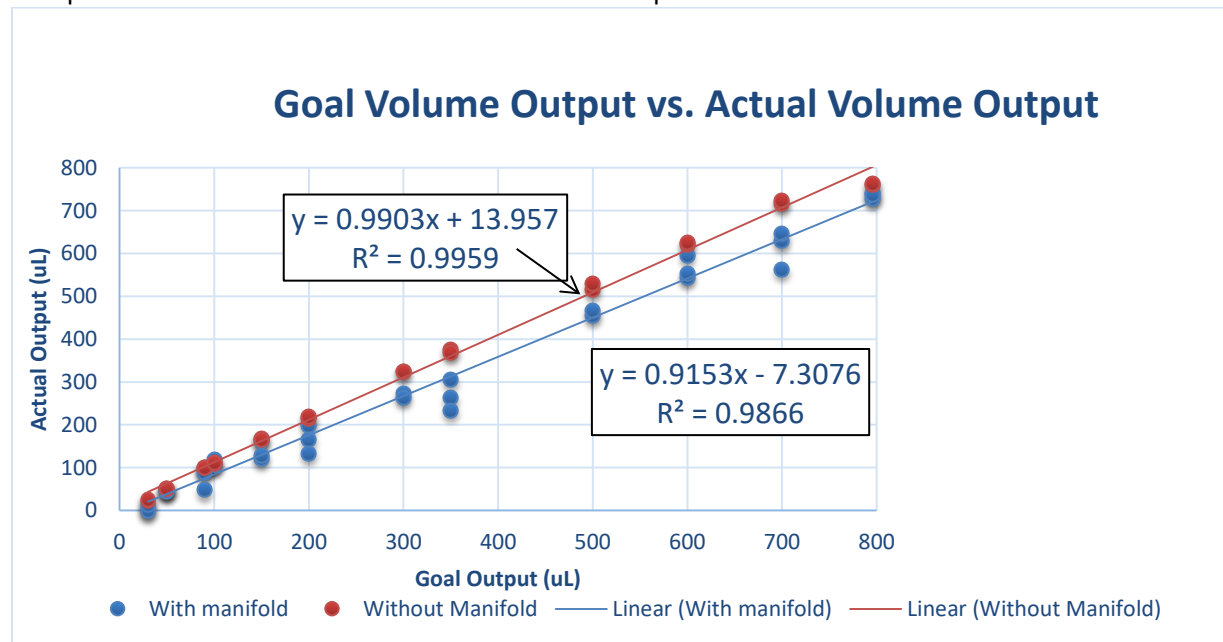
Data	Test 1	Test 2	Test 3 (Without Outlier)
$y=mx+c$	$y = 1.0002x + 1.7836$	$y = 0.9994x + 1.5498$	$y = 0.9982x + 3.2175$
R square	$R^2 = 1$	$R^2 = 1$	$R^2 = 1$

OUTLIERS: There exist 5 significant outliers in Test 1, 2, and 3. The possible reasons for outlier was that the Actual Position wasn't recorded (HUMAN ERROR).

R²: After removing the outliers, the R² value for Test 1, Test 2 and Test 3 = 1.

SLOPE: After removing the outliers, the slope is pretty linear and the values for the Test 1,2 and 3 are close.

Comparison of with and without manifold volume outputs



Volume output comparison between system with and without manifold

Appendix E: Syringe Pump with Manifold: Dead Volumes Experiment (Full)

The purpose of this experiment was to determine volume lost in the valve manifold

Steps: In order to perform this test, we took the already existing Syringe pump assembly consisting of 1ml glass syringe and linear actuator enclosed using metal assembly and connected it to the Solenoid manifold using a 1/32 inch tube. We connected it to the Arduino and the power supply. We also connected a 1/32 inch diameter tube to the manifold assembly to pump water out.

Setting up Arduino Software Program: Open the Arduino software program “*PumpAndValve.ino*” on the computer and enter “0” value to move the syringe to initial position corresponding “0” volume in the syringe. Enter “x” in the Arduino software to confirm. After entering the volume, enter the desired speed of the linear actuator to “150” and enter “x” to run the system. **NOTE:** Always enter each digit of the desired value individually for both volume and speed. (Example: 150, Enter). Always enter “x” after inputting the desired value for both volume and speed. (Example: 150, Enter, x). The program will ask for an input for the speed of the linear actuator only at the start of the program (after inputting the first desired volume). The linear actuator will run at the same entered speed (here 150) for different values of volumes until the Arduino program is closed and re-run.

Setting up an empty vial to collect the output volume from the Syringe Pump Assembly (Without Manifold): Take a filled glass vial (vial A). Uncap the water filled vial A and place the glass syringe tube into the water filled glass vial. Enter “796” in the same Arduino program: “B: Enter volume” to fill the syringe at its maximum capacity. Enter “x” to run. Now take an empty glass vial (vial B) and record the mass of the empty vial. **NOTE: Ensure to tare the scale before measuring the mass of the empty vial (capped).** Also close the scale doors while measuring the weight of the vial. Now replace the glass vial A with an empty glass vial (vial B). (Place the syringe tube into vial B). Subtract a desired volume from 796 (maximum capacity of the syringe). (Example: 50 ul = 796-50=746). Enter the volume value (calculated) to be dispensed in the glass vial B. Enter “x” to run the program. **NOTE:** The test will be performed at the volumes in the following tables:

ASSAY	VOLUME (ml)
BSA/Mycoplasma	0.05ml
BSA	0.09ml
BSA	0.10ml
Mycoplasma	0.15ml
Mycoplasma	0.20ml
BSA/Mycoplasma	0.30ml
BSA	0.35ml
BSA	0.60ml

MINIMUM (mL)	MAXIMUM (mL)
0.03	0.8

Record the total mass of the vial B with the dispensed water. *Calculate the mass of the output water = total mass of the water filled vial B - mass of the empty vial B.* Repeat the previous steps for all the different volumes in the tables above. Repeat the previous step two more times for the same volumes.

(Without Manifold) Re-run the test two times and record the data in the following table:

<i>DESIRED OUTPUT VOLUME(μL)</i>	<i>ACTUAL OUTPUT VOLUME (μL)</i>
30	23
50	52
90	100
100	110
150	169
200	215
300	324
350	376
500	515
600	620
700	716
796	760

Re-run the test the second time and record the data in the following table:

<i>DESIRED OUTPUT VOLUME(μL)</i>	<i>ACTUAL OUTPUT VOLUME (μL)</i>
30	26
50	52
90	100
100	113
150	166
200	220
300	325
350	369
500	530
600	625
700	723
796	763

Steps (With Manifold): Repeat the previous steps with Manifold attached to the syringe pump. NOTE: While filling the syringe to its complete capacity, remove the manifold and fill the syringe with similar procedure. Connect the manifold right after inputting water. And continue the next steps.

Collecting Data (With Manifold)

<i>DESIRED OUTPUT VOLUME(μL)</i>	<i>ACTUAL OUTPUT VOLUME (μL)</i>	<i>DESIRED POSITION</i>	<i>ACTUAL POSITION</i>
30	0	959	959
50	49	932	933
90	99	878	880

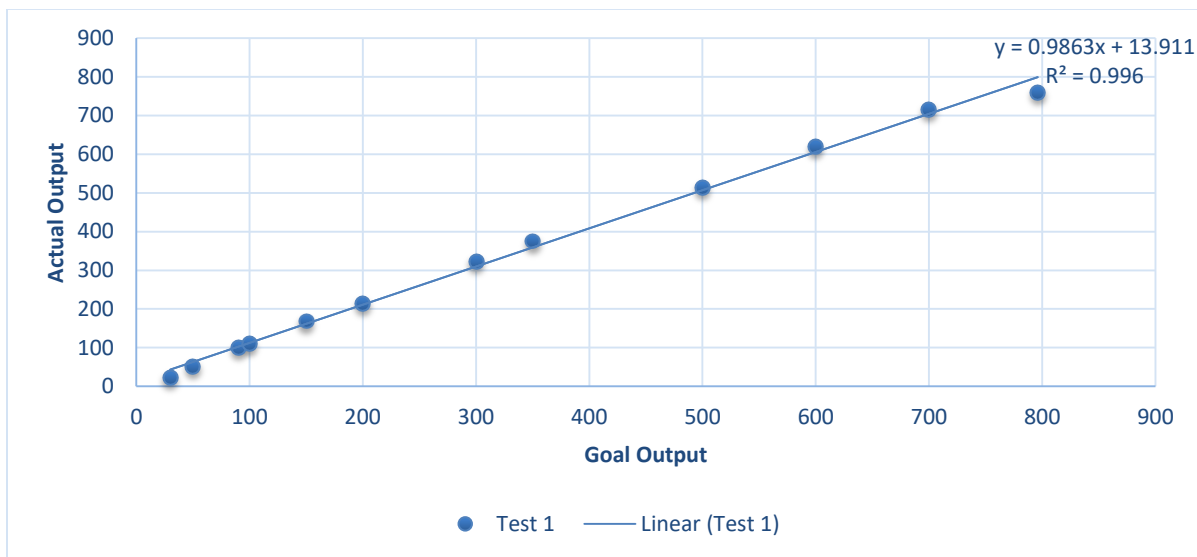
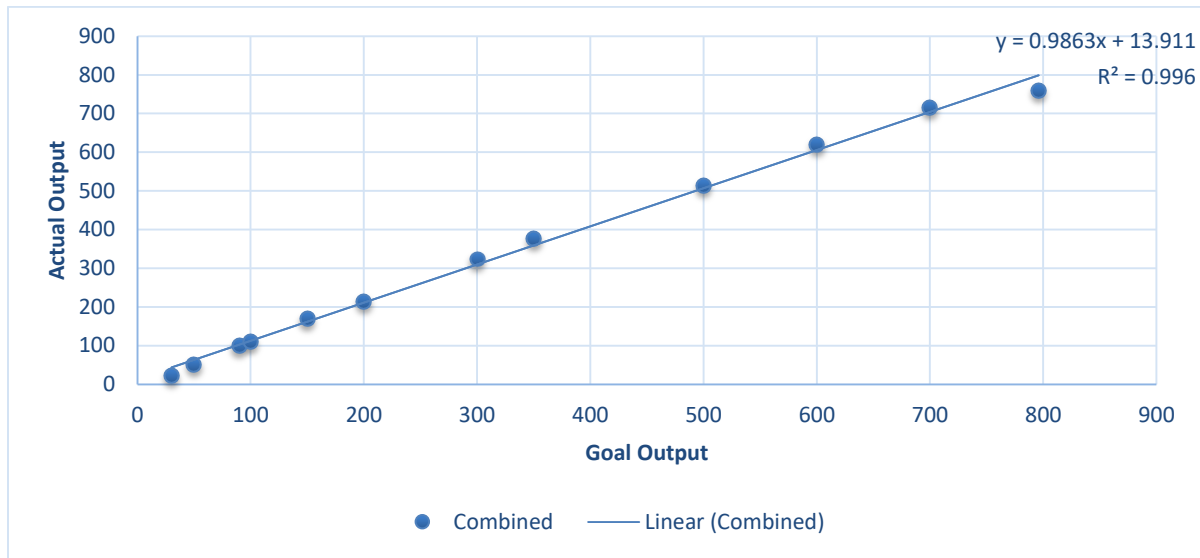
100	118	865	<i>n/a</i>
150	164	798	<i>n/a</i>
200	198	731	733
300	274	596	600
350	263	529	534
500	455	327	<i>n/a</i>
600	543	193	194
700	562	59	60
796	741	0	1

Repeat step two more times.

<i>DESIRED OUTPUT VOLUME(μL)</i>	<i>ACTUAL OUTPUT VOLUME (μL)</i>	<i>DESIRED POSITION</i>	<i>ACTUAL POSITION</i>
30	0	959	957
50	45	932	933
90	48	878	<i>n/a</i>
100	108	865	866
150	122	798	800
200	134	731	734
300	67	596	<i>n/a</i>
350	234	529	532
500	722	327	330
600	595	193	194
700	629	59	60
796	729	0	1

<i>DESIRED OUTPUT VOLUME(μL)</i>	<i>ACTUAL OUTPUT VOLUME (μL)</i>	<i>DESIRED POSITION</i>	<i>ACTUAL POSITION</i>
30	13	959	959
50	49	932	933
90	88	878	880
100	107	865	867
150	129	798	799
200	167	731	732
300	264	596	600
350	305	529	533
500	467	327	331
600	553	193	196
700	646	59	<i>n/a</i>
796	737	0	1

ACTUAL VS GOAL VOLUME OUT- WITHOUT MANIFOLD Test 1 and 2



Observations:

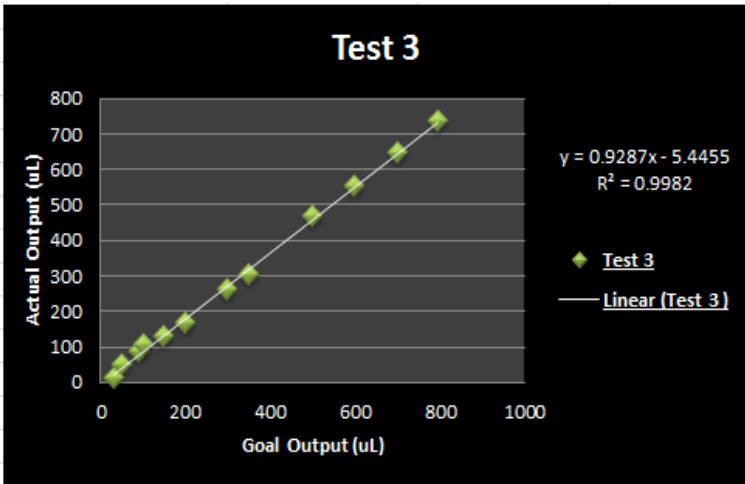
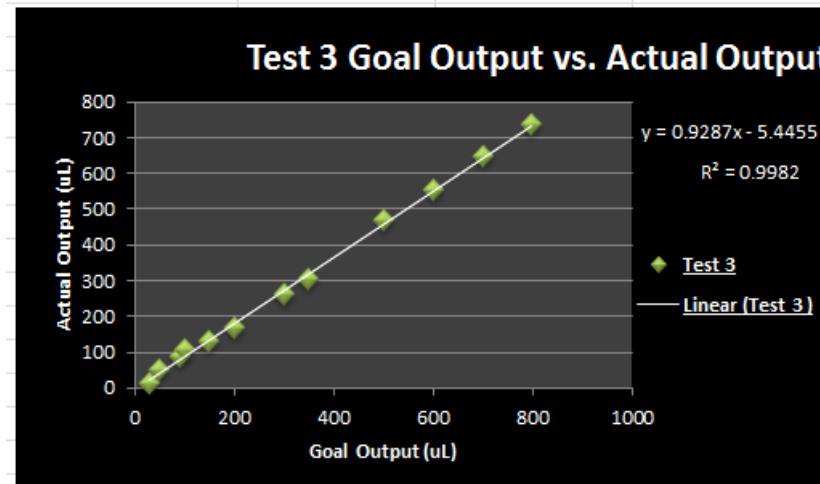
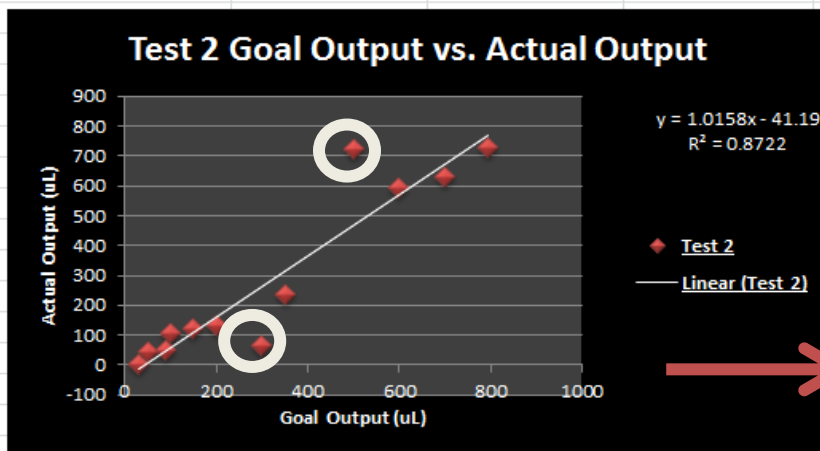
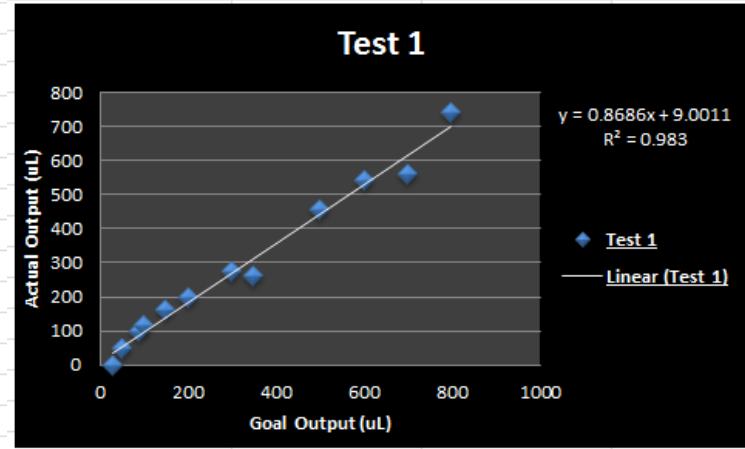
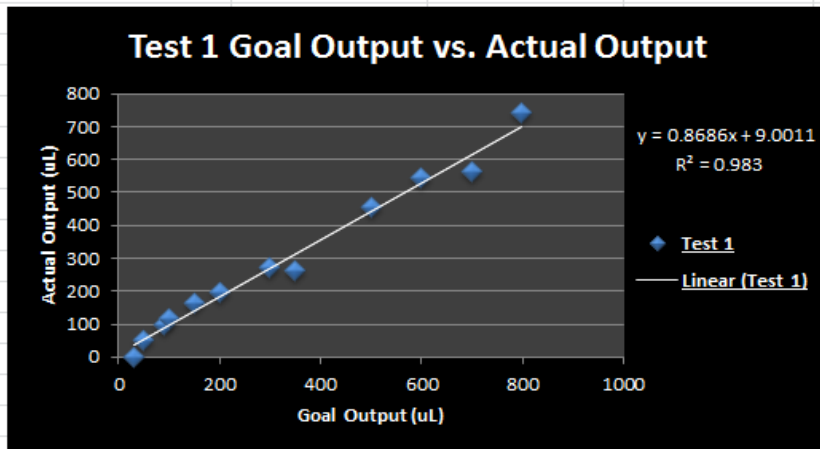
Data	Test 1	Test 2
$y=mx+c$	$y = 0.9863x + 13.911$	$y = 0.9943x + 14.004$
R square	$R^2 = 0.996$	$R^2 = 0.9958$

R^2 : It can be observed that the values of R^2 are very close to 1. **SLOPE**: The graphs obtained are pretty linear and the slope values for Test 1 and 2 are close. **OUTLIERS**: The graphs don't have any significant outliers.

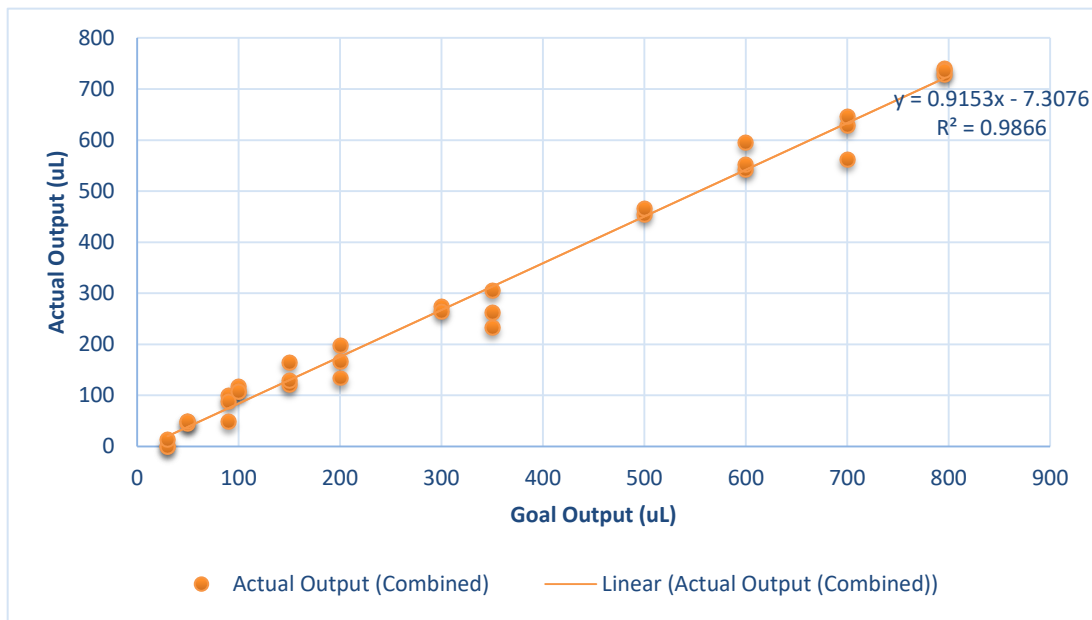
ACTUAL VS GOAL VOLUME OUT- WITH MANIFOLD Test 1, 2 and 3

WITH OUTLIERS

WITHOUT OUTLIERS



Combined Data for Test 1, 2 and 3



Observations:

Data	Test 1	Test 2	Test 3 (With Outlier)
y=mx+c	$y = 0.8686x + 9.0011$	$y = 1.0158x - 41.19$	$y = 0.9287x - 5.4455$
R square	$R^2 = 0.983$	$R^2 = 0.8722$	$R^2 = 0.9982$

Data	Test 1	Test 2	Test 3 (Without Outlier)
y=mx+c	$y = 0.8686x + 9.0011$	$y = 0.9483x - 26.35$	$y = 0.9287x - 5.4455$
R square	$R^2 = 0.983$	$R^2 = 0.9838$	$R^2 = 0.9982$

ANALYSIS:

R²: After removing the outlier the R² value for Test 2 changed from 0.8722 to 0.9838. It can be observed that the values of R² are very close to 1 after removing the outliers in Test 2. Also, the combined tests have R² = 0.9866.

SLOPE: The graphs obtained are pretty linear and the slope values for Test 1 and 3 are relatively close. After removing the outlier from Test 2, the slope values for Test 2 are relatively close to the test values of Test 1 and Test 3. The combined tests have slope (m)= 0.9153.

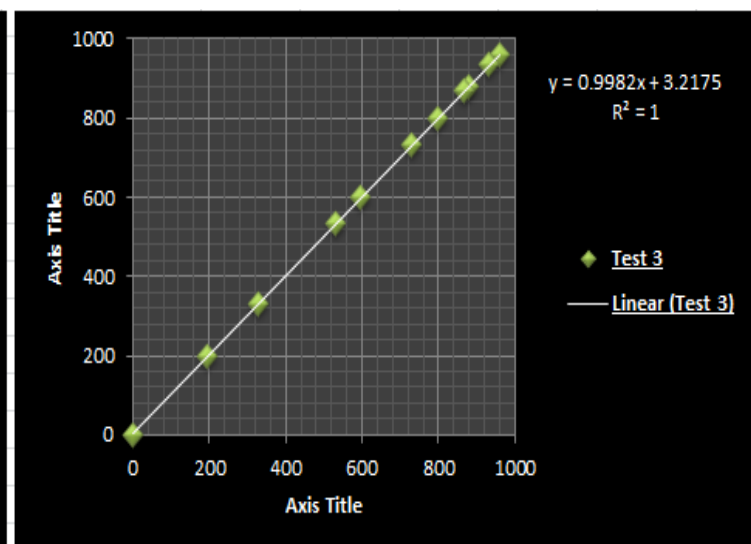
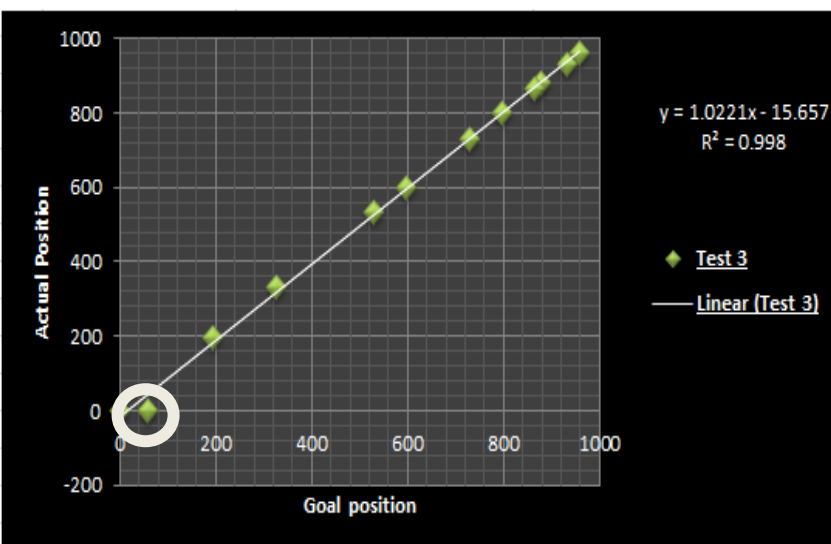
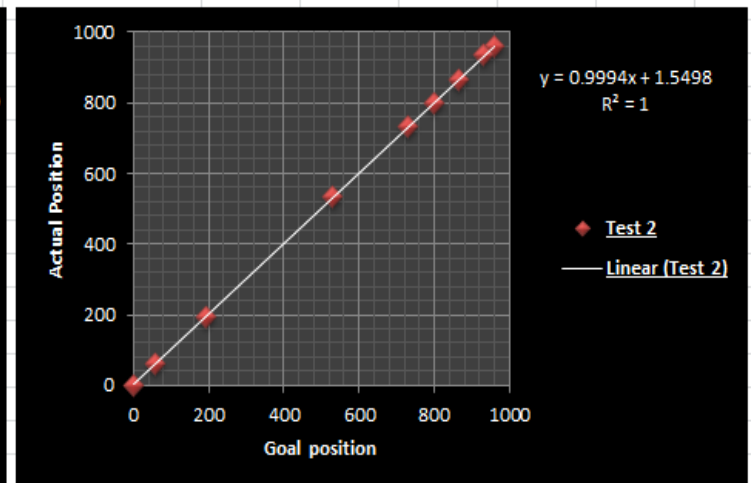
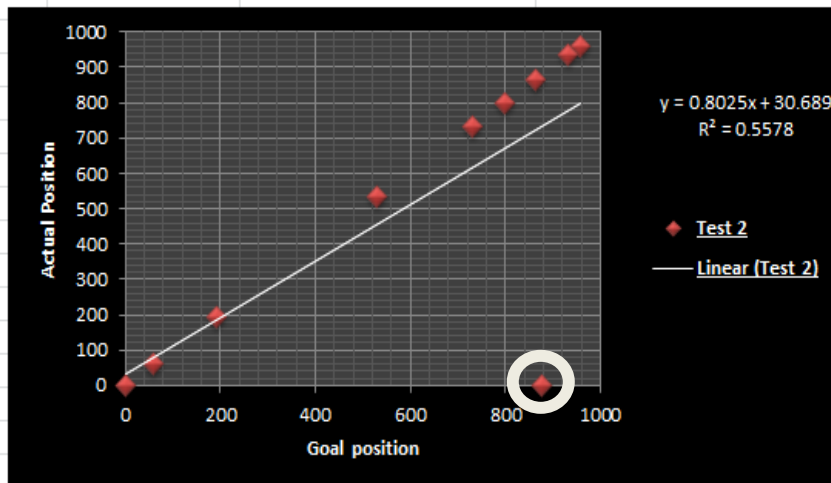
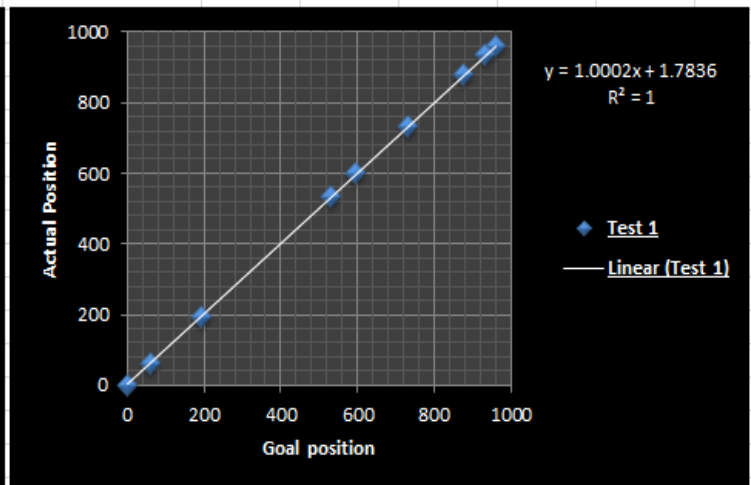
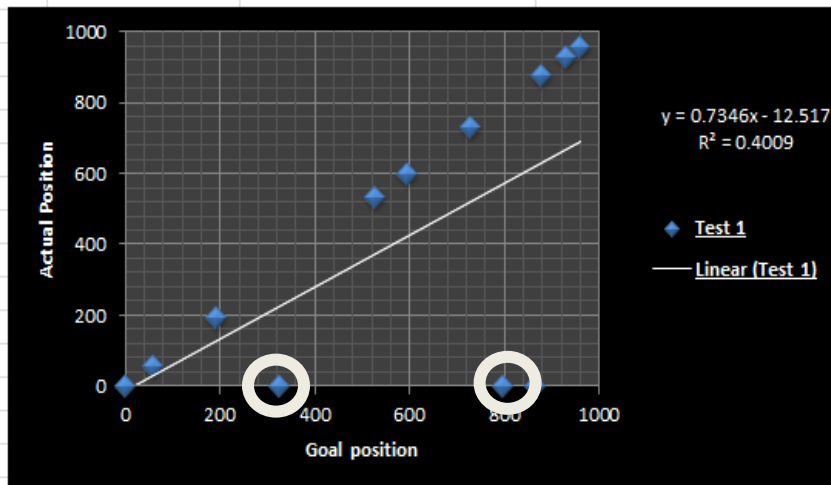
OUTLIERS: There exist 2 significant outliers in Test 2. The possible reasons for outlier are either human error or instrument error.

ACTUAL VS GOAL POSITION- WITH MANIFOLD Test 1, 2 and 3

WITH OUTLIERS

WITH OUTLIERS

NOTE: Removed 2 outliers from the previous volume analysis for Test 2



Observations:

Data	Test 1	Test 2	Test 3 (With Outlier)
$y=mx+c$	$y = 0.7346x - 12.517$	$y = 0.8025x + 30.689$	$y = 1.0221x - 15.657$
<i>R square</i>	$R^2 = 0.4009$	$R^2 = 0.5578$	$R^2 = 0.998$

Data	Test 1	Test 2	Test 3 (Without Outlier)
$y=mx+c$	$y = 1.0002x + 1.7836$	$y = 0.9994x + 1.5498$	$y = 0.9982x + 3.2175$
<i>R square</i>	$R^2 = 1$	$R^2 = 1$	$R^2 = 1$

OUTLIERS: There exist 5 significant outliers in Test 1, 2, and 3. The possible reasons for outlier was that the Actual Position wasn't recorded (HUMAN ERROR).

R²: After removing the outliers, the R² value for Test 1, Test 2 and Test 3 = 1.

SLOPE: After removing the outliers, the slope is pretty linear and the values for the Test 1,2 and 3 are close.

Test3: Air Pump Integration

The purpose of this experiment was to determine if using an air pump helped lessen dead volumes by flushing the remaining dead volumes left behind.

Steps: In order to perform this test, we took the already existing Syringe pump assembly consisting of 1ml glass syringe and linear actuator enclosed using metal assembly and connected it to the Solenoid manifold using a 1/32 inch tube. We connected it to the Arduino and the power supply. We also connected a 1/32 inch diameter tube to the manifold assembly to pump water out. We also connected the air pump to manifold and syringe pump.

Setting up an empty vial to collect the output volume from the Manifold: Take a filled glass vial (vial A). Uncap the water filled vial A and place the glass syringe tube into the water filled glass vial. Enter "799" in the same Arduino program: "B: Enter volume" to fill the syringe at its maximum capacity. Enter "x" to run. Now take an empty glass vial (vial B) and record the mass of the empty vial.

NOTE: Ensure to tare the scale before measuring the mass of the empty vial (capped). Also close the scale doors while measuring the weight of the vial. Connect the manifold to the syringe pump tube.

NOTE: Fill the syringe pump at its full capacity directly using syringe pump tube instead of connecting it to the manifold. Now replace the glass vial A with an empty glass vial (vial B). (Place the manifold tube into vial B). Subtract a desired volume from 799 (*maximum capacity of the syringe*). (Example: 50 ul = 799-50=749). Enter the volume value (calculated) to be dispensed in the glass vial B. Enter "x" to run the program. NOTE: The test will be performed at the volumes in the following tables:

ASSAY	VOLUME (ml)
BSA/Mycoplasma	0.05ml
BSA	0.09ml
BSA	0.10ml
Mycoplasma	0.15ml
Mycoplasma	0.20ml
BSA/Mycoplasma	0.30ml
BSA	0.35ml
BSA	0.60ml

MINIMUM (mL)	MAXIMUM (mL)
0.03	0.8

Enter “y” in the Arduino code to start the air pump. Stop the air pump by entering “s” in the Arduino code. Stop after 1 second. Record the total mass of the vial B with the dispensed water. *Calculate the mass of the output water = total mass of the water filled vial B - mass of the empty vial B.* Repeat the previous steps for all the different volumes in the tables above. Repeat the previous step two more times for the same volumes.

Collecting Data

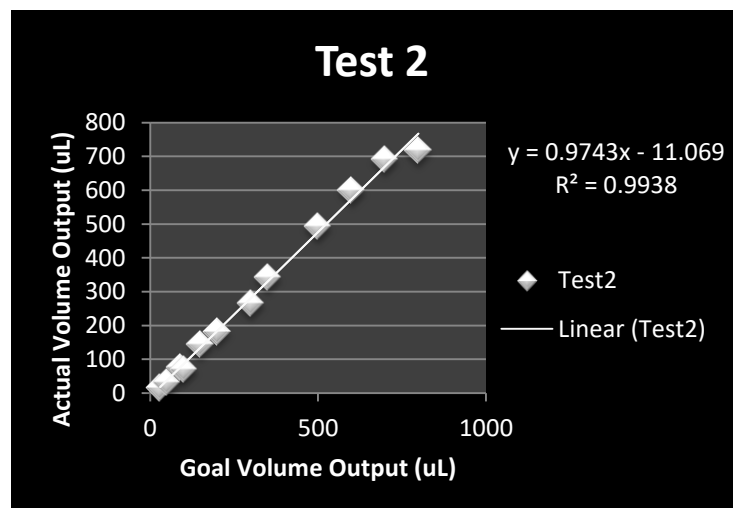
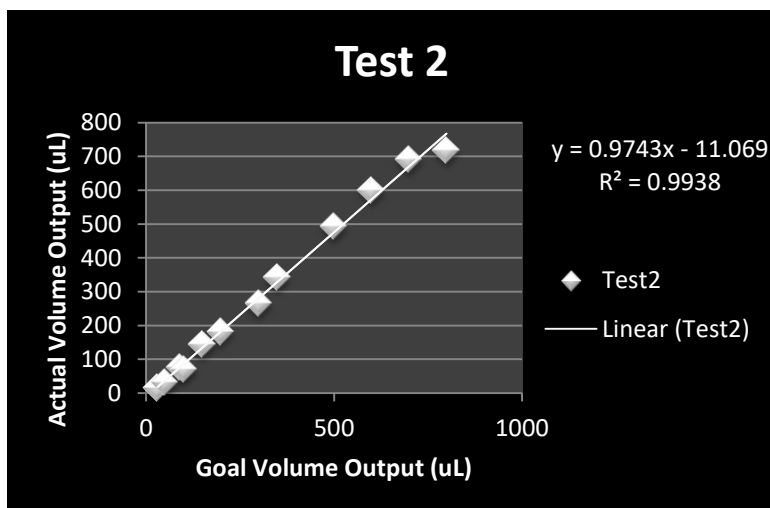
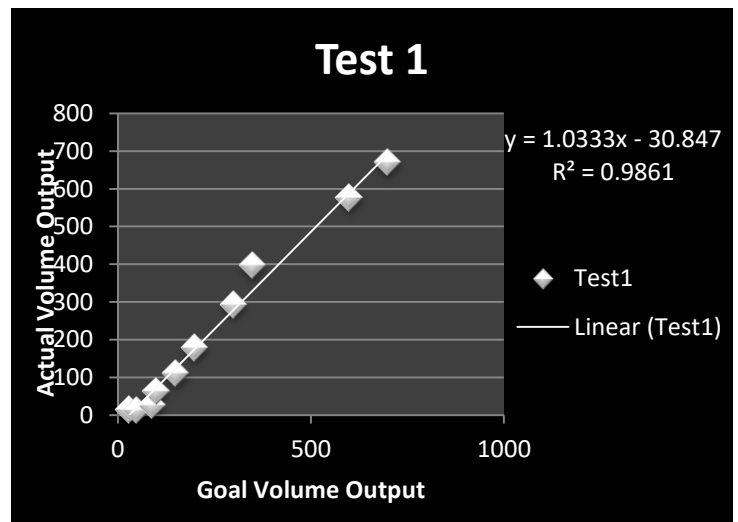
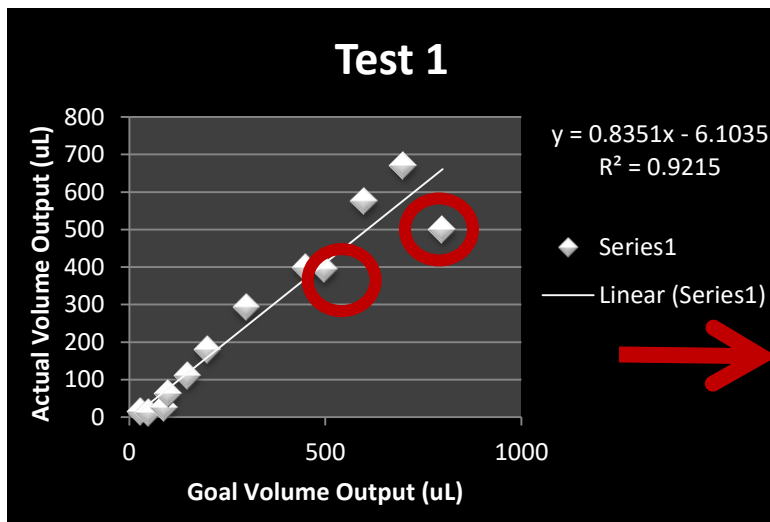
DESIRED OUTPUT VOLUME(μL)	ACTUAL OUTPUT VOLUME (μL)
30	15.1
50	13.1
90	25.6
100	63.3
150	110.8
200	179.8
300	293.4
450 (Instead of 350)	398.6
500	393.7
600	576.6
700	670.9
799	500.3

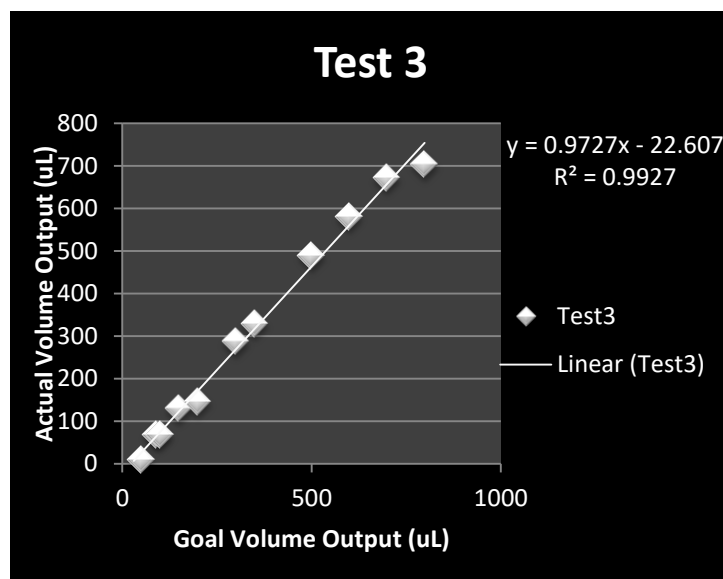
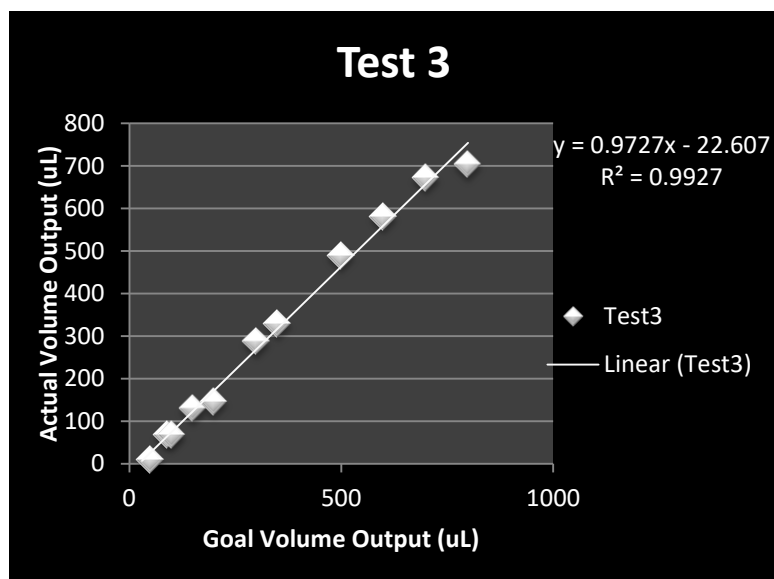
DESIRED OUTPUT VOLUME(μL)	ACTUAL OUTPUT VOLUME (μL)
30	16.1
50	31.8
90	77.1
100	70.8
150	144.4
200	182.7

300	265.7
350	343.8
500	494
600	599.6
700	692.3
799	718.6

DESIRED OUTPUT VOLUME(uL)	ACTUAL OUTPUT VOLUME (uL)
30	-1.8
50	10.9
90	69.6
100	68.6
150	130.7
200	146.9
300	289
350	330.5
500	489.7
600	581.6
700	672.6
799	703.6

Goal Output VS Actual Output
 WITH OUTLIERS IN TEST WITHOUT OUTLIERS IN TEST 1





Data	Test 1 (With Outlier)	Test 2	Test 3
$y=mx+c$	$y = 0.8351x - 6.1035$	$y = 0.9743x - 11.069$	$y = 0.9727x - 22.607$
R square	$R^2 = 0.9215$	$R^2 = 0.9938$	$R^2 = 0.9927$

Data	Test 1 (Without Outlier)	Test 2	Test 3
$y=mx+c$	$y = 1.0333x - 30.847$	$y = 0.9743x - 11.069$	$y = 0.9727x - 22.607$
R square	$R^2 = 0.9861$	$R^2 = 0.9938$	$R^2 = 0.9927$

Observations:

OUTLIERS: There exist 2 significant outliers in Test 1. The possible reasons for outlier are human error or instrument error.

R^2 : After removing the outlier the R^2 value for Test 1 changed from 0.9215 to 0.9861. It can be observed that the values of R^2 are very close to 1 after removing the outliers in Test 2.

SLOPE: The graphs obtained are pretty linear and the slope values for Test 2 and 3 are relatively close. After removing the outlier from Test 1, the slope value for Test 1 is relatively close to the test values of Test 2 and Test 3.

Appendix F: Syringe Pump with Manifold: Intake Inaccuracies Experiment (Full)

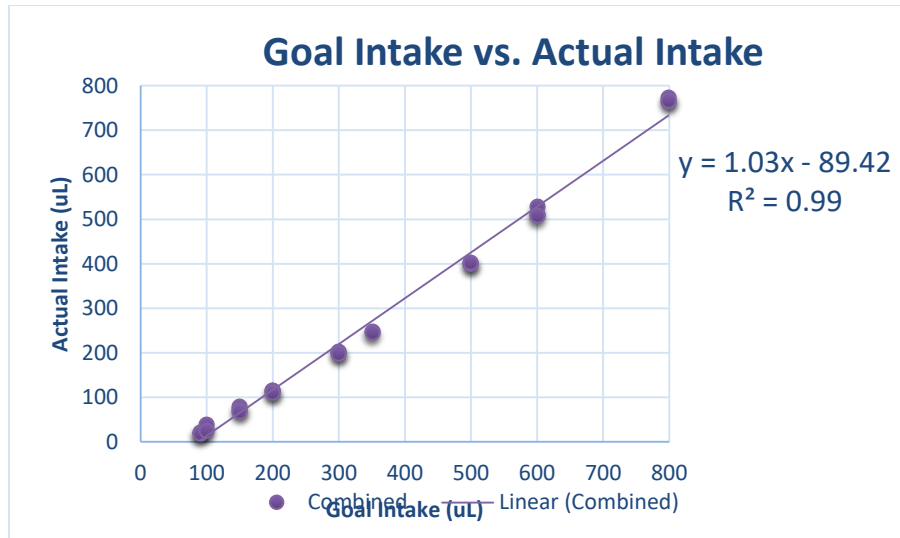
In order to perform this test, we took the already existing Syringe pump assembly consisting of 1ml glass syringe and linear actuator enclosed using metal assembly and connected it to the Solenoid manifold using a 1/32 inch tube. We connected it to the Arduino and the power supply. We also connected a 1/32 inch diameter tube to the manifold assembly to intake water.

Open the Arduino software program “*PumpAndValve.ino*” on the computer and enter “0” value to move the syringe to initial position corresponding “0” volume in the syringe. Enter “x” to confirm. After entering the position, enter the desired speed of the linear actuator to “150” and enter “x” to run the system. *NOTE:* Always enter each digit of the desired value individually for both volume and speed. (Example: 150). Always enter “x” after inputting the desired value for both volume and speed. (Example: 1, Enter, 5, Enter, 0, Enter, x). The program will ask for an input for the speed of the linear actuator only at the start of the program (after inputting the first desired volume). The linear actuator will run at the same entered speed (here 150) for different values of volumes until the Arduino program is closed and re-run.

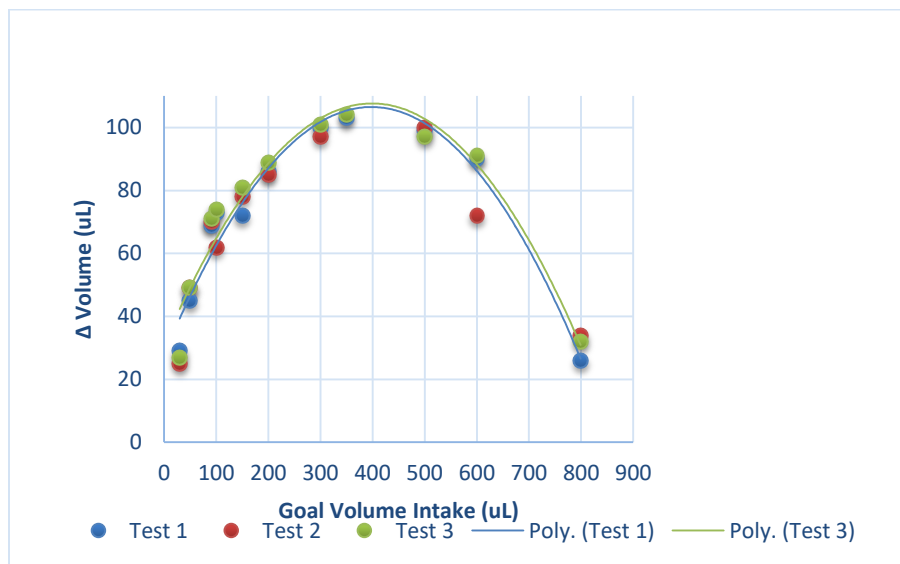
Start with full glass vial of water. Weigh on tared scale to get total mass. *NOTE: Ensure to tare the scale before measuring the mass of the vial (capped). Also close the scale doors while measuring the weight of the vial.* Start syringe at volume 0. Put tubing into glass vial and input desired volume into Arduino interface. Begin program so pump fills syringe. When syringe is full to desired volume position, weigh the vial again to see how much water is actually taken into the syringe

Input volume 0 into the Arduino software to empty out all contents of the syringe into the same vial. Weigh again to see how much volume was dispensed. We chose a range of volumes between 0 and 700 to ensure that the pump is consistent. We also ensured appropriate values to reflect the values we'll need for the assays.

Goal Intake (uL)	Actual Intake (uL) Iteration 1	Actual Intake (uL) Iteration 2	Actual Intake (uL) Iteration 3
30	1	5	3
50	5	1	1
90	21	20	19
100	27	38	26
150	78	72	69
200	114	115	111
300	200	203	199
350	247	402	246
500	401	400	403
600	510	528	509
799	773	765	767



Results of system intake experiment: goal intake vs. actual intake



Results of system intake experiment: Change in intake volume vs. goal volume intake

We obtained a pretty linear relationship for Actual Intake vs. Goal Intake with $y = 1.03x - 89.42$. Also the value of R square equals 0.99, close to 1. After obtaining another graph representing Difference in Volume vs. Goal Volume Intake, we observed that a constant volume difference wasn't observed. Also, after looking at the graph, constant trend of loss of volume wasn't observed.

Appendix G: Syringe Pump with Manifold and Air Pump: Output Volume Loss Experiment (Full)

In order to perform this test, we took the already existing Syringe pump assembly consisting of 1ml glass syringe and linear actuator enclosed using metal assembly and connected it to the Solenoid manifold using a 1/32 inch tube. We connected it to the Arduino and the power supply. We also connected a 1/32 inch diameter tube to the manifold assembly to pump water out. We also connected the air pump to manifold and syringe pump.

Take a filled glass vial (vial A). Uncap the water filled vial and place the glass syringe tube into the water filled glass vial. Enter “799” in the same Arduino program: “PumpAndValve.ino” to fill the syringe at its maximum capacity. Enter “x” to run. Now take an empty glass vial (vial B) and record the mass of the empty vial. *NOTE: Ensure to tare the scale before measuring the mass of the empty vial (capped). Also close the scale doors while measuring the weight of the vial.* Connect the manifold to the syringe pump tube. *NOTE: Fill the syringe pump at its full capacity directly using syringe pump tube instead of connecting it to the manifold.*

Now replace the glass vial A with an empty glass vial (vial B). (Place the manifold tube into vial B). Subtract a desired volume from 799 (*maximum capacity of the syringe*). (Example: 50 μL = 799-50=749). Enter the volume value (calculated) to be dispensed in the glass vial B. Enter “x” to run the program. *NOTE: The test will be performed at the volumes in the following tables:*

Assay	Volume (μL)
Minimum	30
BSA/Mycoplasma	50
BSA	90
BSA	100
Mycoplasma	150
Mycoplasma	200
BSA/Mycoplasma	300
BSA	350
BSA	600
Maximum	800

Enter “y” in the Arduino code to start the air pump. Stop the air pump by entering “s” in the Arduino code. Stop after 1 second. Record the total mass of the vial B with the dispensed water. *Calculate the mass of the output water = total mass of the water filled vial B - mass of the empty vial B.* Repeat the previous steps for all the different volumes in the tables above. Repeat the previous step two more times for the same volumes.

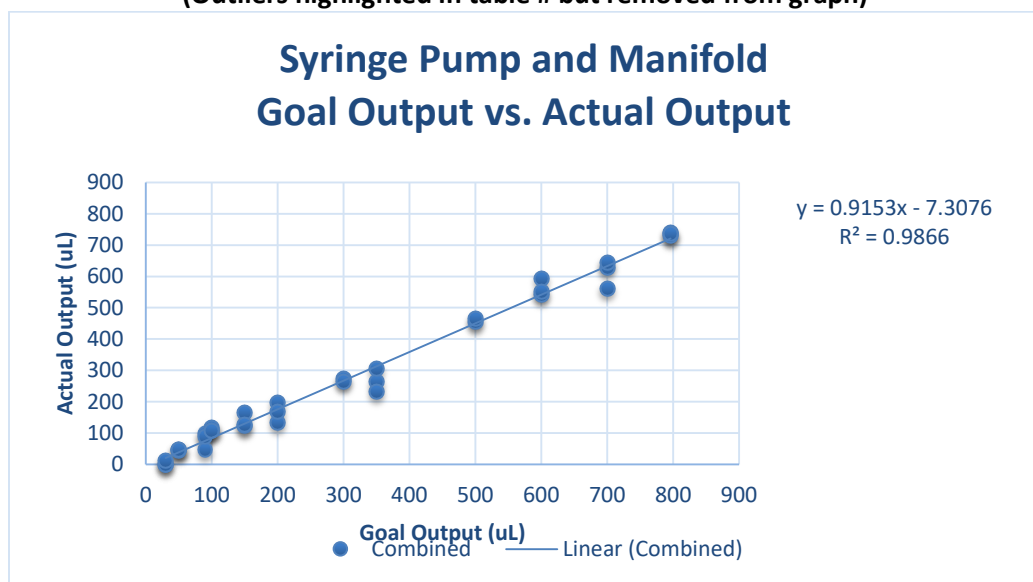
Experimental Results and Analysis

Desired Output Volume (μL)	Actual Output Volume: Iteration 1 (μL)	Actual Output Volume: Iteration 2 (μL)	Actual Output Volume: Iteration 3 (μL)
30	15.1	16.1	-1.8
50	13.1	31.8	10.9
90	25.6	77.1	69.6
100	63.3	70.8	68.6

150	110.8	144.4	130.7
200	179.8	182.7	146.9
300	293.4	265.7	289
350	398.6*	343.8	330.5
500	393.7	494	489.7
600	576.6	599.6	581.6
700	670.9	692.3	672.6
799	500.3	718.6	703.6

**In Iteration 1, value measured at 450 μ L due to human error.*

Goal Output VS Actual Output
(Outliers highlighted in table # but removed from graph)



Data	Test 1 (With Outlier)	Test 2	Test 3
y=mx+c	$y = 0.8351x - 6.1035$	$y = 0.9743x - 11.069$	$y = 0.9727x - 22.607$
R square	$R^2 = 0.9215$	$R^2 = 0.9938$	$R^2 = 0.9927$

Data	Test 1 (Without Outlier)	Test 2	Test 3
y=mx+c	$y = 1.0333x - 30.847$	$y = 0.9743x - 11.069$	$y = 0.9727x - 22.607$
R square	$R^2 = 0.9861$	$R^2 = 0.9938$	$R^2 = 0.9927$

Observations:

OUTLIERS: There exist 2 significant outliers in Test 1. The possible reasons for outlier are human error or instrument error.

R²: After removing the outlier the R² value for Test 1 changed from 0.9215 to 0.9861. It can be observed that the values of R² are very close to 1 after removing the outliers in Test 2.

SLOPE: The graphs obtained are pretty linear and the slope values for Test 2 and 3 are relatively close. After removing the outlier from Test 1, the slope value for Test 1 is relatively close to the test values of Test 2 and Test 3.

Appendix H: BSA Water Trial Experiment: Full

Purpose: Determine if proof-of-concept device has the accuracy and precision to dispense volumes required for BSA assay. The trial was run with water rather than reagents.

Open the Arduino software program “*PumpAndValve.ino*” on the computer and enter “0” value to move the syringe to initial position corresponding “0” volume in the syringe. Enter “x” in the Arduino software to confirm. After entering the volume, enter the desired speed of the linear actuator to “250” and enter “x” to run the system. Enter the goal intake volume into the Arduino code; the goal volumes are listed in the following table: NOTE: 50uL input buffer is used because of variability.

NOTE: Air Pump after pumping each reagent.

Reagent	Volume
Detection Reagent A	50uL
Detection Reagent B	100uL
Wash Buffer	300uL
Substrate Solution	90uL
Stop Solution	50uL

Enter the volumes to intake in the Arduino code as listed in the table above, and begin to fill the syringe from the manifold input/output valve ports (which manifold input ports are designated for which reagent volumes). Now dispense the volume in the same input/output valve port from syringe pump into each well using manual tubing control. Calculate the actual output volumes using mass difference calculations. Repeat each run with 6 wells at each volume three times.

The intake and output w/ buffer volume was calculated as listed in the following table:

Intake w/ buffer volume	100uL	150uL	350uL	140uL
Average Intake Volume (uL)	36	81	270	72
Average Intake Difference (uL)	62	69	80	57
Overall CV of Intake Volume (%)	70	10	2	8

Output w/ buffer Volume	100uL	150uL	350uL	140uL
Average Ouput Volume (uL)	18	54	209	52
Average Output Volume Lost (uL)	15	15	11	8
Overall CV of Output Volume (%)	48	24	6	2

Average Intake Difference (uL)	70uL
Average Output Losst (uL)	15uL

The following volumes were calculated to ensure requested volumes achieve desired output volume:

Goal Output Volume	Actual Arduino Input (uL)	Rounded Arduino Input (uL)
50uL	127	130
90uL	155	170
100uL	174	180
300uL	391	380

Appendix I: System BSA Assay Experiment Data

Log of Concentration	OD: Iteration 1	OD: Iteration 2	OD: Baseline
4.477	0.44	0.599	0.15
4	0.964	0.622	0.23
3.523	0.906	0.834	0.266
3.046	3.1	1.64	0.5
2.569	2.99	2.45	1.06

Appendix J: System Mycoplasma Experiment Data

	Mycoplasma Baseline Assay	System Mycoplasma Assay
Positive Control Readings at 490nm	2.05	4.49
	2.02	4.57
	2.16	4.34
Negative Control Readings at 490nm	0.161	0.354
	0.1	0.334
	0.113	0.516
Positive at 600nm	0.874	1.48
	0.948	1.48
	0.916	1.38
Negative at 600nm	0.0822	0.116
	0.0575	0.113
	0.0736	0.168
Difference Positive	1.123	3.01
	1.109	3.09
	1.191	2.96
Difference Negative	0.0252	0.238
	-0.011	0.221
	-0.141	0.348